



澳門大學  
UNIVERSIDADE DE MACAU  
UNIVERSITY OF MACAU

# Outstanding Academic Papers by Students

## 學生優秀作品



# **Analysis of the Three-stories Unsymmetrical Outrigger-braced Structure**

by

**Zheng ZongJian**

Final Year Project Report submitted in partial fulfillment  
of the requirement of the Degree of

**Bachelor of Science in Civil Engineering**

**2018/2019**



**Faculty of Science and Technology  
University of Macau**







## DECLARATION

I declare that the project report here submitted is original except for the acknowledged source materials, and that the report as a whole, or any part of the report has not been concurrently and previously submitted for any other award or degree at University of Macau or other institutions.

I also recognize that I understand the Rules on Handling Student Academic Dishonesty and the Regulations of the Student Discipline of the University of Macau.

Signature :



Name :

Zheng Zong Jian

Student ID :

D-B5-2673-1

Date :

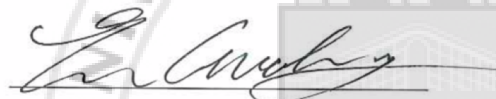
14<sup>th</sup> May, 2019

## APPROVAL FOR SUBMISSION

The project report entitled “Analysis of the three-stories unsymmetrical outrigger-braced structure” was finished by Zheng ZongJian in partial fulfillment of the requirements for the degree of Bachelor of Science in Civil and Environmental Engineering at University of Macau.

Endorsed by,

Signature:



Supervisor: Prof. GuoKang Er



## ACKNOWLEDGEMENTS

I would like to express my great appreciation to my supervisor Prof. Er for his constructive and valuable suggestions during the planning and development of the whole process of the research. He is so generous and kind that he spent a lot of time to instruct my work and check the analyses. The research cannot be proceeded and completed smoothly without Prof. Er. In addition, Mr. HaiEn Du also gives me most suggestions in the calculation of computer program with Matlab.





## ABSTRACT

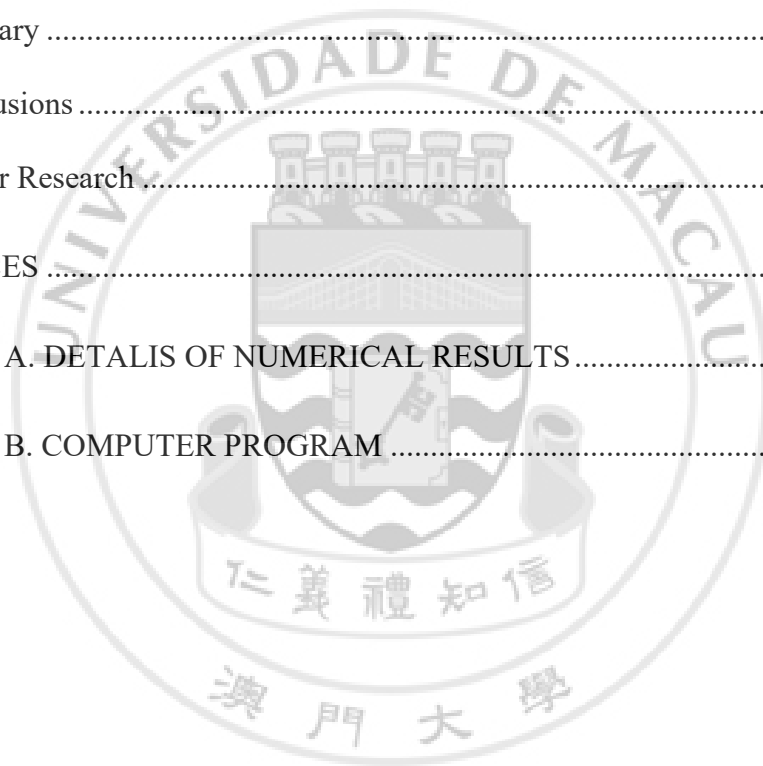
This project is to study the optimum locations of the outriggers of an outrigger-braced structure with unsymmetrical three-stories. In this project, the governing equations about the compatibility of columns' axial deformation for the unsymmetrical three-stories outrigger-braced structure are derived, which is based on the method proposed by Er and Iu (2009). It is an improved version of the method proposed by Smith and Salim (1981) for analyzing the symmetrical outrigger-braced structures. The governing equations about the axial forces in the columns of the three-stories unsymmetrical outrigger-braced structures are formulated. Some non-dimensional parameters are introduced when formulating the governing equations about the axial forces in the columns. They can reduce the complexity of the governing equations and more importantly reflect the behavior of the structures in various cases in general. Based on the objective that the top drift of the structure is minimized, the governing equations of the optimum locations of the outriggers of the three-stories unsymmetrical outrigger-braced structures are formulated. Based on the derived governing equations, a computer program is written for the numerical analysis in software Matlab. The influences of the structural parameters on the optimum locations of the structure are studied numerically. It is found through numerical analyses that the optimum outrigger locations are mainly influenced by the un-symmetry of the structure. The stiffness of the shear wall core, outrigger and column also influences the optimum locations of outriggers. The numerical results are presented with figures under different parameter values and could be referenced in the design of three-stories unsymmetrical outrigger-braced structures.

## TABLE OF CONTENT

DECLARATION .....	i
1. APPROVAL FOR SUBMISSION .....	ii
2. ACKNOWLEDGEMENTS .....	iii
3. ABSTRACT .....	iv
4. LIST OF FIGURES .....	viii
5. LIST OF TABLES .....	xiii
CHAPTER 1 INTRODUCTION .....	1
1.1 History and Classification of Tall Building Structures .....	1
1.1.1 Interior Structural System .....	1
1.1.2 Exterior Structural System .....	2
1.2 Background of Outrigger-braced Structures .....	3
1.3 Objective of the Research .....	4
1.4 Outline of This Thesis .....	4
CHAPTER 2 LITERATURE REVIEW .....	5
2.1 Research History .....	5
2.2 Assumptions for Analysis .....	7
2.3 Theory of Analyzing Outrigger-braced Structures (Adapted from Smith and Coull 1911) .....	7
2.3.1 Compatibility Analysis of a Two-outrigger Structure .....	7
2.3.2 Analysis of Force .....	12
2.3.3 Analysis of Horizontal Deflections .....	13
2.3.4 Restraining Moments .....	14
2.3.5 Horizontal Deflections .....	15

2.3.6 Optimum Locations of Outriggers .....	15
2.3.7 Introduced the Parameters .....	15
2.3.8 Performance of Outrigger Structures .....	16
2.4 Formulation of Governing Equations with Force Method (Er and Iu 2009).....	17
2.4.1 The Formulation of New Governing Equations .....	17
2.4.2 Relation Between the Conventional and New Governing Equations .....	20
CHAPTER 3 GOVERNING UNSYMMETRICAL OUTRIGGER-BRACED STRUCTURE .....	21
3.1 Governing Equation for Unsymmetrical Outrigger-braced Structures .....	21
3.1.1 Axial Forces in Column.....	22
3.1.2 Bending Moment in the Core and Deflection at Top Drift .....	35
3.1.3 Numerical Verification of the Results .....	35
3.2 Equation for Optimum Locations.....	41
3.3 Analysis for Optimum Locations of Outriggers of Unsymmetrical Structure .....	42
3.3.1 Derivation of $N_1 \sim N_6$ with Respect to $\varepsilon_1$ .....	44
3.3.2 Derivation of $N_1 \sim N_6$ with Respect to $\varepsilon_2$ .....	46
3.3.3 Derivation of $N_1 \sim N_6$ with Respect to $\varepsilon_3$ .....	48
3.3.4 Derivative of $\Delta_0$ with Respect to $x_1, x_2$ and $x_3$ , Respectively .....	50
3.4 Solution Procedure for the Optimum Locations of Outriggers of Unsymmetrical Structure .....	53
CHAPTER 4 NUMERICAL ANALYSIS.....	56
4.1 Introduction .....	56
4.2 Comparing with Different Values of $r$ .....	56
4.2.1 Summary of Comparing with Different Values of $r$ .....	58

4.3 Numerical Results for Different Values of $r$ .....	59
4.3.1 Summary of Numerical Results for Different Values of $r$ .....	62
4.4 Numerical Results for Different Values of $\beta$ .....	63
4.4.1 Summary of Numerical Results for Different Values of $\beta$ .....	69
4.5 Numerical Results for Different Values of $\alpha$ .....	70
4.5.1 Summary of Numerical Results for Different Values of $\alpha$ .....	76
CHAPTER 5 Conclusions and Final Remarks .....	77
5.1 Summary .....	77
5.2 Conclusions .....	77
5.3 Further Research .....	78
REFERENCES .....	79
APPENDIX A. DETALIS OF NUMERICAL RESULTS .....	81
APPENDIX B. COMPUTER PROGRAM .....	85



## LIST OF FIGURES

Figure 2.1 Two-outrigger structure.....	9
Figure 2.2 External moment diagram .....	9
Figure 2.3 $M_1$ diagram .....	10
Figure 2.4 $M_2$ diagram .....	10
Figure 2.5 Core resultant moment diagram .....	10
Figure 2.6 Outrigger attached to edge of core .....	11
Figure 2.7 Equivalent outrigger beam attached to centroid of core.....	11
Figure 2.8 Optimum outrigger locations for three-outrigger structure.....	16
Figure 2.9 Unknown axial forces in analyzing outrigger-braced structures.....	18
Figure 3.1 Unknown axial forces in an unsymmetrical three-story outrigger-braced structure.....	21
Figure 3.2 Moment diagram when and uniformly distributed load is applied on the structure.....	22
Figure 3.3 Moment diagram when $N_1=1$ is applied on the structure .....	23
Figure 3.4 Moment diagram when $N_2=1$ is applied on the structure .....	23
Figure 3.5 Moment diagram when $N_3=1$ is applied on the structure.....	24
Figure 3.6 Moment diagram of $N_4=1$ is applied on the structure .....	24
Figure 3.7 Moment diagram of $N_5=1$ is applied on the structure .....	25
Figure 3.8 Moment diagram of $N_6=1$ is applied on the structure .....	25
Figure 3.9 Moment equilibrium at the core wall node on third story for verification .....	39
Figure 3.10 Moment equilibrium at the core wall node on second story for verification .....	39

Figure 3.11 Moment equilibrium at the core wall node on first story for verification .....	40
Figure 3.12 Horizontal equilibrium above the first story of the structure for verification .....	40
Figure 3.13 Optimum location of three-stories unsymmetrical outrigger- braced structure .....	54
Figure 4.1 Optimum outrigger locations of three-stories unsymmetrical outrigger-braced structure comparing for $r$ being 0.9999 and 0.8, respectively .....	56
Figure 4.2 Optimum outrigger locations of three-stories unsymmetrical outrigger-braced structure comparing for $r$ being 0.9999 and 0.6, respectively .....	57
Figure 4.3 Optimum outrigger locations of three-stories unsymmetrical outrigger-braced structure comparing for $r$ being 0.9999 and 0.4, respectively .....	57
Figure 4.4 Optimum outrigger locations of the <b>third</b> story in three-stories unsymmetrical outrigger-braced structure for different values of $r$ shown in $\omega$ vs $\varepsilon_1$ .....	59
Figure 4.5 Amplification of Fig 4.4 .....	59
Figure 4.6 Optimum outrigger locations of the <b>second</b> story in three- stories unsymmetrical outrigger-braced structure for different values of $r$ shown in $\omega$ vs $\varepsilon_2$ .....	60
Figure 4.7 Amplification of Fig 4.6 .....	60

Figure 4.8 Optimum outrigger locations of the <b>first</b> story in three-stories unsymmetrical outrigger-braced structure for different values of $r$ shown in $\omega$ vs $\varepsilon_3$ .....	61
Figure 4.9 Amplification of Fig 4.8 .....	61
Figure 4.10 Optimum outrigger locations of the <b>third</b> story in three- stories unsymmetrical outrigger-braced structure for different values of $\beta$ shown in $\omega$ vs $\varepsilon_1$ when $r=0.7$ .....	63
Figure 4.11 Amplification of Fig 4.10 .....	63
Figure 4.12 Optimum outrigger locations of the <b>second</b> story in three- stories unsymmetrical outrigger-braced structure for different values of $\beta$ shown in $\omega$ vs $\varepsilon_1$ when $r=0.7$ .....	64
Figure 4.13 Amplification of Fig 4.12 .....	64
Figure 4.14 Optimum outrigger locations of the <b>first</b> story in three-stories unsymmetrical outrigger-braced structure for different values of $\beta$ shown in $\omega$ vs $\varepsilon_1$ when $r=0.7$ .....	65
Figure 4.15 Amplification of Fig 4.14 .....	65
Figure 4.16 Optimum outrigger locations of the <b>third</b> story in three- stories unsymmetrical outrigger-braced structure for different values of $\beta$ shown in $\omega$ vs $\varepsilon_1$ when $r=0.5$ .....	66
Figure 4.17 Amplification of Fig 4.16 .....	66
Figure 4.18 Optimum outrigger locations of the <b>second</b> story in three- stories unsymmetrical outrigger-braced structure for different values of $\beta$ shown in $\omega$ vs $\varepsilon_1$ when $r=0.5$ .....	67
Figure 4.19 Amplification of Fig 4.18 .....	67

Figure 4.20 Optimum outrigger locations of the <b>first</b> story in three-stories unsymmetrical outrigger-braced structure for different values of $\beta$ shown in $\omega$ vs $\varepsilon_1$ when $r=0.5$ .....	68
Figure 4.21 Amplification of Fig 4.20 .....	68
Figure 4.0.22 Optimum outrigger locations of the <b>third</b> story in three- stories unsymmetrical outrigger-braced structure for different values of $\alpha$ shown in $\omega$ vs $\varepsilon_1$ when $r=0.7$ .....	70
Figure 4.23 Amplification of Fig 4.22 .....	70
Figure 4.24 Optimum outrigger locations of the <b>second</b> story in three- stories unsymmetrical outrigger-braced structure for different values of $\alpha$ shown in $\omega$ vs $\varepsilon_1$ when $r=0.7$ .....	71
Figure 4.25 Amplification of Fig 4.24 .....	71
Figure 4.26 Optimum outrigger locations of the <b>first</b> story in three-stories unsymmetrical outrigger-braced structure for different values of $\alpha$ shown in $\omega$ vs $\varepsilon_1$ when $r=0.7$ .....	72
Figure 4.27 Amplification of Fig 4.26.....	72
Figure 4.28 Optimum outrigger locations of the <b>third</b> story in three- stories unsymmetrical outrigger-braced structure for different values of $\alpha$ shown in $\omega$ vs $\varepsilon_1$ when $r=0.5$ .....	73
Figure 4.29 Amplification of Fig 4.28 .....	73
Figure 4.30 Optimum outrigger locations of the <b>second</b> story in three- stories unsymmetrical outrigger-braced structure for different values of $\alpha$ shown in $\omega$ vs $\varepsilon_1$ when $r=0.5$ .....	74
Figure 4.31 Amplification of Fig 4.30 .....	74

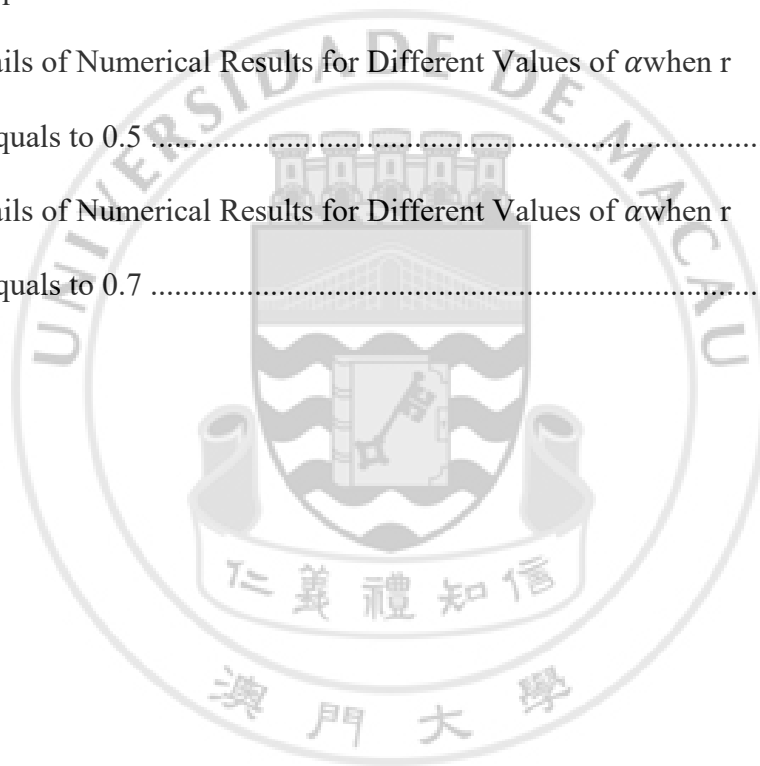


Figure 4.32 Optimum outrigger locations of the <b>first</b> story in three-stories unsymmetrical outrigger-braced structure for different values of $\alpha$ shown in $\omega$ vs $\varepsilon_1$ when $r=0.5$ .....	75
Figure 4.33 Amplification of Fig 4.32 .....	75



## LIST OF TABLES

Table 1 Details of Numerical Results for Different Values of $r$ .....	81
Table 2 Details of Numerical Results for Different Values of $\beta$ when $r$ Equals to 0.5 .....	82
Table 3 Details of Numerical Results for Different Values of $\beta$ when $r$ Equals to 0.7 .....	82
Table 4 Details of Numerical Results for Different Values of $\alpha$ when $r$ Equals to 0.5 .....	83
Table 5 Details of Numerical Results for Different Values of $\alpha$ when $r$ Equals to 0.7 .....	84





# CHAPTER 1 INTRODUCTION

## *1.1 History and Classification of Tall Building Structures*

With the society development, there is not enough space for people to live in. As the population grows, the tall building structures are needed. This demand is more serious in international cities, such as New York, London and Hong Kong. With the tall building, more space can be provided. In this way, the life condition of citizens and the development of cities can become better.

The Home Insurance Building, the first tall building, was built in Chicago in 1884. This building was considered as a modern skyscraper in that century. It's because it was mainly built by steel framing technology.

After the first tall building was built, a new era of skyscraper has come. Many tall buildings spring up in United State, followed by Europe, Asia. According to Mir M. Ail and Kyoung Sun Moon (2007), the classifications of different architectural styles are interior structural system and exterior structural system.

### *1.1.1 Interior Structural System*

According to Mir M. Ail and Kyoung Sun Moon (2007), the two basic types of lateral load-resisting systems in the category of interior structures are the moment-resisting frames and shear trusses/ shear wall. Also, to be more specific, rigid frames, shear wall frame interaction system, braced hinged frame, shear wall and outrigger braced structures are included in the interior structural systems.

In all these interior structure systems, braced hinged frame is the smallest efficient height limit system. It is only around 10 stories high. Shear truss member is used to resist the lateral loads.

Rigid frames are the second in the ranking of efficient height limit system and it can be around 30 floors with structural flexibility. Both steel and concrete can be the material of rigid frames and both of them has the advantages of providing the flexibility in floor planning.

The third ranking is the shear wall structure, which can be up to 70 floors. The advantages of the shear wall structure are that it can effectively resists lateral shear by concrete shear wall or the provided shear truss/wall. This technology was successfully used in the 311m South Wacker Drive in Chicago, which was built in 75 floors height.

Outrigger-braced structure is the structure system that has the largest efficient height limit.

### ***1.1.2 Exterior Structural System***

There are different combinations and subcategories for exterior structural system, such as tube, diagrid, super frames and exo-skeleton space truss structures.

Tube is one of the most typical exterior structures, which can be defined as a three-dimensional structural system utilizing the entire building perimeter to resist lateral loads according to Mir M. Ail and Kyoung Sun Moon (2007). Tube system was raised by Fazlur Khan in 1961 (Ail,2001) and then the tube in tube system, framed tube system, bundled tube and braced tube system structure were created in the following development of tall building system. The building of this system could be built up to 150 floors or higher. The John Hancock Center and Sears tower in Chicago are the example of its application.

With their structural efficiency as a varied version of the tubular systems, diagrid structures have been emerging as a new aesthetic trend for tall buildings in the era of pluralistic styles which according to Mir M. Ail and Kyoung Sun Moon (2007). However, the efficient height limit of diagrid structures varies for different material. For steel, the structure can be up to 100 floors. On the other hand, it reduces to 60 floors when the material is concrete.

In addition, the diagrid structures can block some outdoor view. Therefore, the diagrid structures are generally designed within the building cores.

Other types of exterior structural system are super frames, space truss structure and exo-skeleton space truss, which have been occasionally used for tall building. Some structures, like super frames structure can be built up to 160 floors. Others are little lower, but they still can be up to 100 floors. The Chicago World Trade Center, which is 168 stories, is one of the examples in the application of super frames structure.

### ***1.2 Background of Outrigger-braced Structures***

Back to the old times, outrigger system has been used in ship design to resist the wind forces in their sails, in order to make the tall masts stable and strong. The outrigger system reduces the overturn moment in the core and transfers the reduced moment to the outer columns. Hence, outrigger-braced structure benefits for resisting lateral loading.

In addition, the exterior column spacing of outrigger system can easily meet aesthetic and functional requirements. For super tall buildings, connecting the outriggers with exterior mega columns opens up the façade system for flexible aesthetic.

However, outriggers system interferes with rentable space and lack of repetitive structural framing. It results in a negative impact on the erection process.

### ***1.3 Objective of the Research***

Most of the researches of the outrigger-braced structure are about the symmetrical outrigger-braced structure. In reality, unsymmetrical outrigger-braced structure can have a better aesthetic impact and flexible interior space arrangement. This project is about the study of structural parameters that influence the optimum height of unsymmetrical three-story outrigger- braced structure. The method proposed by Er and Iu will be adopted in deriving the governing equations and analysis.

### ***1.4 Outline of This Thesis***

Chapter 2 is about the introduction of the research history. Discussion and analysis about the symmetrical outrigger braced structure are reviewed.

Chapter 3 is about the derivation and analysis of the governing equation for an unsymmetrical two-stories outrigger-braced structure.

Chapter 4 is about the comparisons and discussions for different combination of structural parameters.

Chapter 5 gives some conclusions and recommendation.

## CHAPTER 2 LITERATURE REVIEW

### *2.1 Research History*

The research for outrigger braced structure began in the mid of 1970s. Taranath (1974) assumed that the outrigger can reduce the sway of structure and introduced a simple method of analysis. It was found out that the optimum locations of outrigger is 0.445 of the structure's height from the top of it. Afterwards, McNabb et al (1975) expanded the study from the structure with one outrigger to the structure with two outriggers and confirmed the result of Taranath's research about optimum outrigger location. In addition, it was concluded that the optimum locations of the two outriggers are 0.312 and 0.685, respectively, of the height from the top of the structure.

A general solution for optimum locations of outriggers of multi-story structure were proposed by Stafford and Nwaka (1980). Meanwhile, Salim (1980) discovered that the flexibility of outriggers has an influence on the total drift and core moment for maximum reduction in drift. After one year, Smith and Salim (1981) improved their study and introduced a non-dimensional characteristic parameter  $\omega$ . This parameter is related to bending and racking shear stiffness of the braced frame and outriggers. Later, Boggs and Casparini (1983) found out that the optimum locations of outriggers change towards the top in the situation that non-prismatic columns and walls are used. In 1987, Rutenberg investigated the performance of the drift reduction in uniform and non-uniform belted structures with the rigid outriggers under several lateral load distributions. Chan and Kuang (1989) were the first people who carried out the studies on the effect of intermediate stiffening beam at an arbitrary level along the height of the structure. They revealed that the specific position of this stiffening beam can significantly influence the behavior of the structure.



In 1991, Ding discussed the effects of stiffness ratios of core outrigger and core columns on the optimum locations of an outrigger-braced structures as well as the reduction of top drift. Afterward, Stafford Smith et al. (1996) did the research about the influence of a façade rigger on the behavior in a structure. Taranath (1998) discussed the optimum locations of two outrigger system. He mentioned that core in a tall building may have double side outriggers or it may only have one side outriggers. This leads to an unsymmetrical outrigger braced structure.

The studies about outrigger-braced structures continues in the 21<sup>st</sup> century. Hoenderkamp and Snijder (2000) suggested that façade rigger braced high rise structures only need one additional parameter – the racking shear stiffness of the façade rigger. In 2003, Wu and Li claimed that the optimum location of an outrigger under triangularly horizontal distribution load can have four to five percent higher locations than those under the uniform load. Later, Lee et al. (2008) focused his research on deriving the governing equations for the wall frame structures under the lateral loads. He built a model to analyze the lateral drift of the wall frame structures with outriggers. Hoenderkamp (2008) presented a simple method to study the preliminary design of the outrigger-braced high-rise shear walls. Afterward, Er and Iu (2009) proposed a new method to formulate the governing equations based on the compatibility of columns axial deformation and the deformation and the solution procedure is more comprehensible and easier for analyzing the outrigger-braced structures.

## ***2.2 Assumptions for Analysis***

According to Smith and Coull (1911), the assumptions for analyzing the outrigger-braced structures are as follows.

1. The structure is linearly elastic.
2. Only axial forces are induced in columns.
3. Outriggers are rigidly attached to core and core is rigidly attached to foundation.
4. Sectional properties of the core, columns and outriggers are uniform throughout the height of structure.

## ***2.3 Theory of Analyzing Outrigger-braced Structures (Adapted from Smith and Coull 1911)***

Smith and Coull (1911) raised the governing equation about the symmetric outrigger-braced structures by using moment area method. With the moment area method, the rotational compatibility at the junctions of the core and the outrigger is considered.

### ***2.3.1 Compatibility Analysis of a Two-outrigger Structure***

The model for analysis is the two-outrigger structure shown in Fig. 2.1, subjected to a uniformly distributed horizontal load.

The bending moment diagram for the core, shown in Fig. 2.5, consists of the external load moment diagram, which, shown in Fig. 2.2, is induced by the outrigger restraining moments that, for each outrigger, are introduced at the outrigger level and

extend uniformly down to the base, as shown in Fig. 2.3 and Fig. 2.4. From the moment-area method which is shown in Fig. 2.1, the core rotations at levels 1 and 2 are, respectively,

$$\theta_1 = \frac{1}{EI} \int_{x_1}^{x_2} \left( \frac{qx^2}{2} - M_1 \right) dx + \frac{1}{EI} \int_{x_2}^H \left( \frac{qx^2}{2} - M_1 - M_2 \right) dx \quad (2.1)$$

$$\theta_2 = \frac{1}{EI} \int_{x_2}^H \left( \frac{qx^2}{2} - M_1 - M_2 \right) dx \quad (2.2)$$

where  $EI$  and  $H$  are the flexural rigidity and total height of the core,  $q$  is the intensity of horizontal loading,  $x_1$  and  $x_2$  are the respective heights of outriggers 1 and 2 from the top of the core, and  $M_1$  and  $M_2$  are their respective restraining moments on the core.

Expressions for the rotations of the outriggers at the points where they are connected to the core (i.e., at the ‘inboard’ ends) will be developed in the following. Each rotation consists of two components: one allowed by the differential axial deformations of the columns, and the other by the outriggers bending under the action of the column forces at their ‘outboard’ ends.

The rotation of the ‘inboard’ ends of the outrigger at level 1 is

$$\theta_1 = \frac{2M_1(H - x_1)}{d^2(EA)_c} + \frac{2M_2(H - x_2)}{d^2(EA)_c} + \frac{M_1 d}{12(EI)_o} \quad (2.3)$$

For the outrigger at level 2,

$$\theta_1 = \frac{2(M_1 + M_2)(H - x_2)}{d^2(EA)_c} + \frac{M_2 d}{12(EI)_o} \quad (2.4)$$

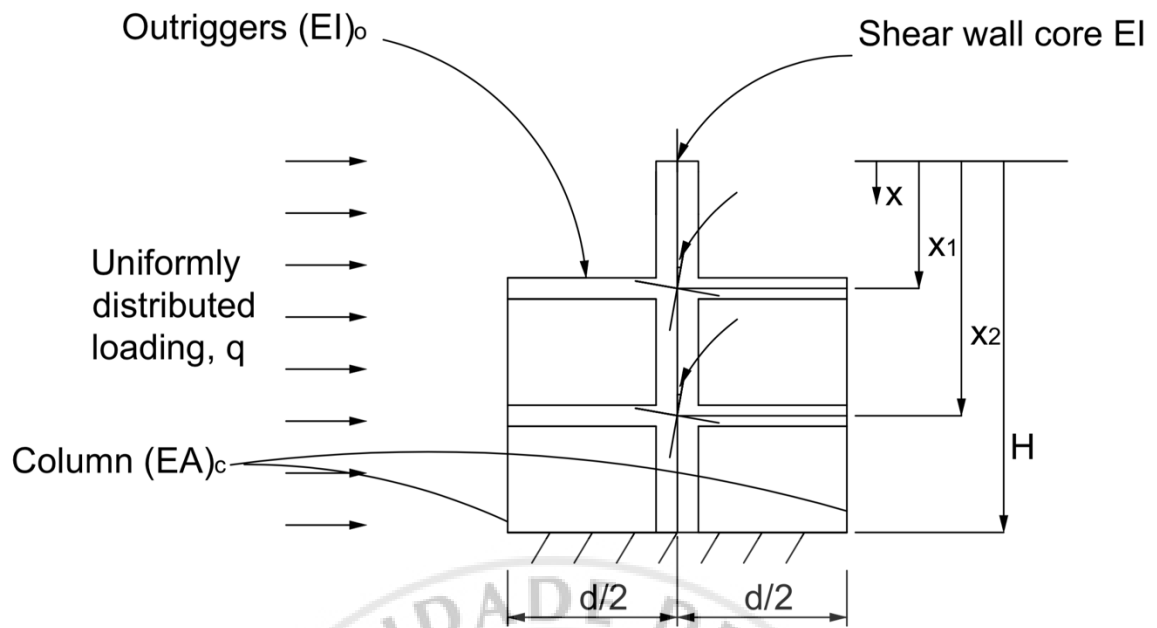


Figure 2.1 Two-outrigger structure

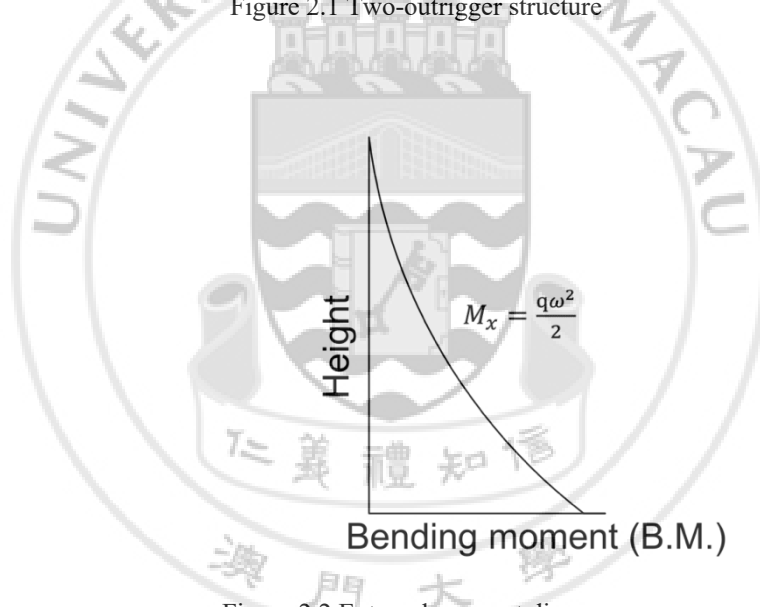


Figure 2.2 External moment diagram

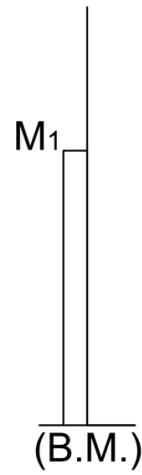


Figure 2.3  $M_1$  diagram



Figure 2.4  $M_2$  diagram

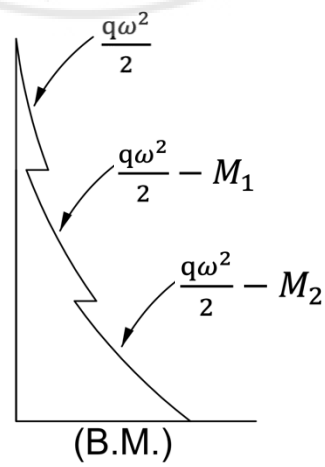


Figure 2.5 Core resultant moment diagram

where  $(EA)_c$  is the axial rigidity of the column and  $\frac{d}{2}$  is its horizontal distance from the centroid of the core.  $(EI)_o$  is the effective flexural rigidity of the outrigger, which is shown in Fig. 2.7, allowing for the wide-column effect of the core. It can be obtained from the actual flexural rigidity of the outrigger  $(EI')_o$  as

$$(EI)_o = \left(1 + \frac{a}{b}\right)^3 (EI')_o \quad (2.5)$$

as shown in Fig. 2.6.

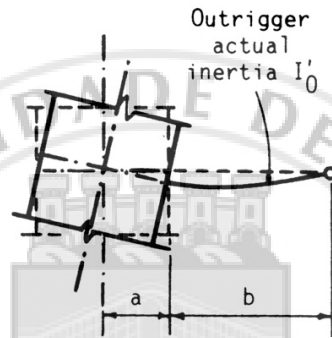


Figure 2.6 Outrigger attached to edge of core

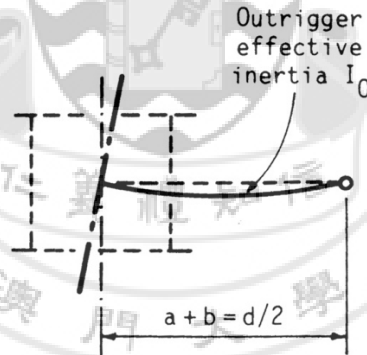


Figure 2.7 Equivalent outrigger beam attached to centroid of core

Equating the rotations of the core and outrigger at level 1 with Eqs. (2.1) and Eqs. (2.3), it gives

$$\begin{aligned} & \frac{2M_1(H - x_1)}{d^2(EA)_c} + \frac{2M_2(H - x_2)}{d^2(EA)_c} + \frac{M_1 d}{12(EI)_o} \\ &= \frac{1}{EI} \int_{x_1}^{x_2} \left( \frac{qx^2}{2} - M_1 \right) dx + \frac{1}{EI} \int_{x_2}^H \left( \frac{qx^2}{2} - M_1 - M_2 \right) dx \end{aligned} \quad (2.6)$$

Similarly, for the rotations at level 2, equating Eqs. (2.2) and Eqs. (2.4) gives

$$\frac{2(M_1 + M_2)(H - x_2)}{d^2(EA)_c} + \frac{M_2 d}{12(EI)_o} = \frac{1}{EI} \int_{x_2}^H \left( \frac{qx^2}{2} - M_1 - M_2 \right) dx \quad (2.7)$$

Rewriting Eqs. (14.6) and Eqs. (14.7) gives

$$M_1[S_1 + S(H - x_1)] + M_2 S(H - x_2) = \frac{q}{6EI} (H^3 - x_1^3) \quad (2.8)$$

And

$$M_1 S(H - x_2) + M_2[S_1 + S(H - x_2)] = \frac{q}{6EI} (H^3 - x_2^3) \quad (2.9)$$

where  $S$  and  $S_1$  are

$$S = \frac{1}{EI} + \frac{2}{d^2(EA)_c} \quad (2.10)$$

$$S_1 = \frac{d}{12(EI)_o} \quad (2.11)$$

### 2.3.2 Analysis of Force

The solution of Eqs. (2.8) and Eqs. (2.9) gives the restraining moment applied to the core by the outrigger at level 1

$$M_1 = \frac{q}{6EI} \left[ \frac{S_1(H^3 - x_1^3) + S(H - x_2)(x_2^3 - x_1^3)}{S_1^2 + S_1 S(2H - x_1 - x_2) + S^2(H - x_2)(x_2 - x_1)} \right] \quad (2.12)$$

and the moment applied to the core by the outrigger at level 2

$$M_2 = \frac{q}{6EI} \left[ \frac{S_1(H^3 - x_2^3) + S(H - x_1)(H^3 - x_2^3) - (H - x_2)(H^3 - x_1^3)}{S_1^2 + S_1 S(2H - x_1 - x_2) + S^2(H - x_2)(x_2 - x_1)} \right] \quad (2.13)$$

Having the outrigger restraining moments  $M_1$  and  $M_2$ , the resulting moment in the core, which is shown in Fig. 2.5, can be expressed generally by

$$M_1 = \frac{qx^2}{2} - M_1 - M_2 \quad (2.14)$$

In which  $M_1$  is included only for  $x > x_1$ , and  $M_2$  is included only for  $x > x_2$ .

The forces in the columns due to the outrigger action are  $\pm \frac{M_1}{d}$  for  $x_1 < x < x_2$  and  $\frac{(M_1+M_2)}{d}$  for  $x \geq x_2$ .

The maximum moment in the outriggers is then  $\frac{M_1 b}{d}$  for level 1 and  $\frac{M_2 b}{d}$  for level 2, where  $b$  is the net length of the outrigger, which is shown in Fig. 2.1.

### 2.3.3 Analysis of Horizontal Deflections

The horizontal deflections of the structure may be determined from the resulting bending moment diagram for the core by using the moment-area method. A general expression for deflections throughout the height could be written; it would, however, be very complicated. Concentrating, therefore, on the top drift only, this may be expressed as

$$\Delta_0 = \frac{1}{EI} \left[ \frac{q}{8} H^4 - \frac{1}{2} M_1 (H^2 - x_1^2) - \frac{1}{2} M_2 (H^2 - x_2^2) \right] \quad (2.15)$$

where the first term on the right-hand side represents the top drift of the core acting as a free vertical cantilever subjected to the full external loading, while the two parts of the second term represent the reductions in the top drift due to the outrigger restraining moments  $M_1$  and  $M_2$ .



### 2.3.4 Restraining Moments

The restraining moments for a uniform structure subjected to uniformly distributed loading may be expressed concisely in matrix form for simultaneous solution by computer as:

$$\begin{Bmatrix} M_1 \\ M_2 \\ \vdots \\ M_i \\ \vdots \\ M_n \end{Bmatrix} = \frac{q}{6EI} \begin{Bmatrix} S_1 + S(X - X_1) & S(H - X_2) & \cdots & S(H - X_i) & \cdots & S(H - X_n) \\ S(H - X_2) & S_1 + S(X - X_1) & \cdots & S(H - X_i) & \cdots & S(H - X_n) \\ \vdots & \vdots & \ddots & \vdots & \ddots & \vdots \\ S(H - X_i) & S(H - X_i) & \cdots & S_1 + S(X - X_1) & \cdots & S(H - X_n) \\ \vdots & \vdots & \ddots & \vdots & \ddots & \vdots \\ S(H - X_n) & S(H - X_n) & \cdots & S(H - X_n) & \cdots & S_1 + S(X - X_1) \end{Bmatrix}^{-1} \begin{Bmatrix} H^3 - X_1^3 \\ H^3 - X_2^3 \\ \vdots \\ H^3 - X_i^3 \\ \vdots \\ H^3 - X_n^3 \end{Bmatrix} \quad (2.16)$$

in which  $n$  is the number of levels of outriggers. Eqs. (2.16) requires that the properties of the structure, the levels of the outriggers, and the magnitude of loading be specified.

A general expression for the moment in the core between outriggers  $j$  and  $j + 1$  is then

$$M_x = \frac{qx^2}{2} - \sum_{n=1}^j M_i \quad (2.17)$$

In the region between the top of the structure and the first outrigger from the top, the second term on the right-hand side of Eq. (2.17) equals zero.

### 2.3.5 Horizontal Deflections

Substitution the restraining moments  $M_1$  to  $M_n$ , from the solution of Eq. (2.16) into Eq. (14.18) gives the resultant deflection at the top of the structure as

$$\Delta_0 = \frac{qH^4}{8EI} - \frac{1}{2EI} \sum_{i=1}^n M_i (H^2 - x_i^2) \quad (2.18)$$

### 2.3.6 Optimum Locations of Outriggers

The optimum levels of the outriggers are determined by minimizing the top drift. The derivative of the right-hand side of Eq. (2.18) with respect first to  $x_j$  being equal to zero gives the following governing equation for determining the optimum levels of the outriggers:

$$\frac{\partial \Delta_0}{\partial x_1} = (H^2 - x_1^2) \frac{\partial M_1}{\partial x_1} + (H^2 - x_2^2) \frac{\partial M_2}{\partial x_1} - 2x_1 M_1 = 0 \quad (2.19)$$

and

$$\frac{\partial \Delta_0}{\partial x_2} = (H^2 - x_1^2) \frac{\partial M_1}{\partial x_2} + (H^2 - x_2^2) \frac{\partial M_2}{\partial x_2} - 2x_2 M_2 = 0 \quad (2.20)$$

### 2.3.7 Introduced the Parameters

In order to simplifying and generalize the expressions, parameters  $\varepsilon_1$ , and  $\varepsilon_2$  are introduced as the ratio between the total height of the structure and the location of each story. The parameters  $\alpha$ ,  $\beta$  and  $\omega$  can reduce the complexity of the governing equations.

Ratio of outrigger locations of second story and total height:  $\varepsilon_1 = \frac{x_1}{H}$

Ratio of outrigger locations of first story and total height:  $\varepsilon_2 = \frac{x_2}{H}$

Flexural rigidity ratio of core to column (non-dimensional):  $\alpha = \frac{EI}{(EA)_c \frac{d^2}{2}}$

Flexural rigidity ratio of core to outrigger (non-dimensional):  $\beta = \frac{EI}{(EI)_o} \frac{d}{H}$

Relative rigidity between core column system and outriggers (non-dimensional):

$$\omega = \frac{\beta}{12(1 + \alpha)}$$

The parameter  $\omega$ , which is non-dimensional, is the characteristic structural parameter for a uniform structure with flexible outriggers. It is useful in that it allows various aspects of the behavior of outrigger structures to be expressed in a very concise form.

### 2.3.8 Performance of Outrigger Structures

The analysis for uniform structures presented earlier is useful in estimating the forces and drift for preliminary design. It is of further value in providing general information about the most efficient arrangement of the structure. The optimum locations are shown in the following Fig. 2.8:

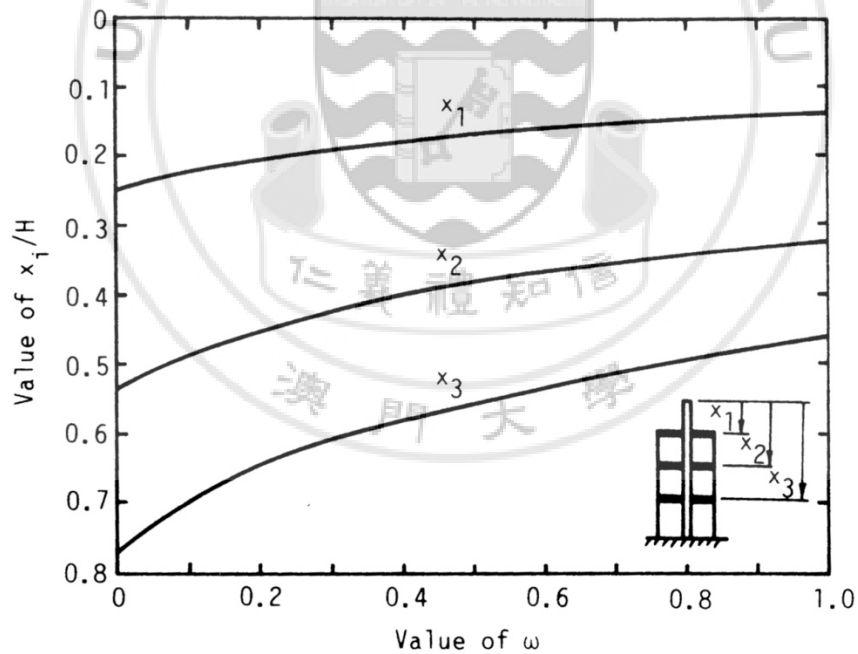


Figure 2.8 Optimum outrigger locations for three-outrigger structure

## ***2.4 Formulation of Governing Equations with Force Method (Er and Iu 2009)***

The new governing equations proposed by Er and Iu (2009) are more adaptable. The new method sets the internal forces in columns as unknown and solves them with force method. The new governing equation can be extended for analyzing more complicated outrigger braced structures.

### ***2.4.1 The Formulation of New Governing Equations***

Considering the structure with two outriggers and acted by uniformly distributed lateral load as shown in Fig. 2.9. In order to analyze the internal forces of the structure, the axial forces in the columns are taken as unknowns in the structural analysis. Denote the axial force in the columns between  $i$ th outrigger and  $(i+1)$ th outrigger as  $N_i$ . Cut each column at a cross section of the column and hence each column is separated into two parts. Each part of the column is applied by an axial force as shown in Fig. 2.9 then the compatibility equations can be formulated by the fact that there is no relative axial displacement on the cut cross sections. The following compatibility equations can be formulated in terms of the axial forces in the columns with force method.

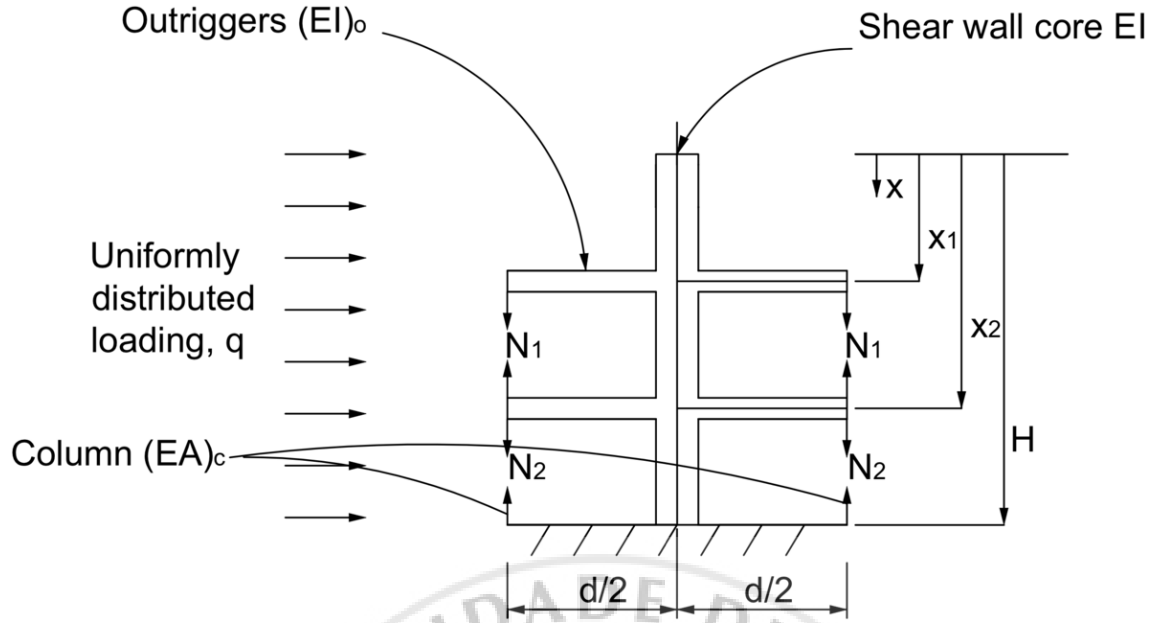


Figure 2.9 Unknown axial forces in analyzing outrigger-braced structures

$$[s(x_2 - x_1) + 2s_1]dN_1 - s_1dN_2 = \frac{q(x_2^3 - x_1^3)}{6EI} \quad (2.21)$$

$$-s_1dN_1 + [s(H - x_2) + s_1]dN_2 = \frac{q(H - x_2^3)}{6EI} \quad (2.22)$$

or

$$N_1 = \frac{q}{6EId} \frac{s_1(H^3 - x_1^3) + s(H - x_2)(x_2^3 - x_1^3)}{s_1^2 + s_1s(2H - x_1 - x_2) + s^2(H - x_2)(x_2 - x_1)} \quad (2.23)$$

$$N_2 = \frac{q}{6EId} \frac{s_1(2H - x_2^3 - x_1^3) + s(x_2 - x_1)(H^3 - x_2^3)}{s_1^2 + s_1s(2H - x_1 - x_2) + s^2(H - x_2)(x_2 - x_1)} \quad (2.24)$$

The maximum bending moments in the outriggers 1 and 2 are, respectively,

$$M_{max1} = N_1 b \quad (2.25)$$

$$M_{max2} = (N_2 - N_1)b \quad (2.26)$$

where b is the net length of outrigger.

Between outrigger  $i$  and outrigger  $i+1$ , the bending moment in the core is

$$m_i(x) = \frac{1}{2}qx^2 - N_i d \quad (i = 0,1,2) \quad (2.27)$$

The top drift is

$$\Delta_0 = \frac{1}{EI} \left[ \frac{q}{8} H^4 - \frac{1}{2} N_1 d (x_2^2 - x_1^2) - \frac{1}{2} N_2 d (H^2 - x_2^2) \right] \quad (2.28)$$

For the structure with  $n$  outriggers:

$$\begin{aligned} & \begin{pmatrix} N_1 \\ N_2 \\ \vdots \\ N_{n-1} \\ N_n \end{pmatrix} = \frac{q}{6EI d} \\ & \begin{pmatrix} s(x_2 - x_1) + 2s_1 & -s_1 & 0 & \cdots & 0 \\ -s_1 & s(x_3 - x_2) + 2s_1 & -s_1 & \cdots & 0 \\ \vdots & \vdots & \vdots & \ddots & \vdots \\ 0 & \cdots & -s_1 & s(x_n - x_{n-1}) + 2s_1 & -s_1 \\ 0 & \cdots & 0 & -s_1 & s(H - x_n) + 2s_1 \end{pmatrix}^{-1} \\ & \begin{pmatrix} x_2^3 - x_1^3 \\ x_3^3 - x_2^3 \\ \vdots \\ x_n^3 - x_{n-1}^3 \\ H^3 - x_n^3 \end{pmatrix} \end{pmatrix} \quad (2.29)$$

Between  $i$  th outrigger and  $(i+1)$ th outrigger or ground, the bending moment in core is

$$m_i(x) = \frac{1}{2} q x^2 - N_i d \quad (i = 0, 1, 2, \dots, n) \quad (2.31)$$

The top drift is

$$\Delta_0 = \frac{qH^4}{8EI} - \frac{d}{2EI} \sum_{i=1}^n (x_{i+1}^2 - x_i^2) N_i \quad (2.32)$$

where  $x_{n+1} = H$ .

The optimum levels of the outriggers are also determined by minimizing the top drift. The derivative of the right-hand side of Eq. (2.32) with respect to  $x_j$  being equal to

zero gives the following governing equations for determining the optimum levels of the outriggers

$$\sum_{i=1}^n (x_{i+1}^2 - x_i^2) \frac{\partial N_i}{\partial x_j} - 2x_j(N_j - N_{j-1}) = 0 \quad (i = 0, 1, 2, \dots, n) \quad (2.33)$$

where  $x_{n+1} = H$  and  $N_0 = 0$

#### ***2.4.2 Relation Between the Conventional and New Governing Equations***

It is evident that the restraining moment  $M_i$  is related to the axial forces in the columns by

$$M_i = (N_i - N_{i-1})d. \quad (i = 0, 1, 2, \dots, n) \quad (2.34)$$

where  $N_0 = 0$

Eq. (2.34) can be verified with the expressions of  $M_i$  and the expressions of the axial forced in the columns. Numerical analysis with the above derived equations also verified the relation expressed by Eq. (2.34).

## CHAPTER 3 GOVERNING UNSYMMETRICAL OUTRIGGER-BRACED STRUCTURE

### 3.1 Governing Equation for Unsymmetrical Outrigger-braced Structures

In this project, the method proposed by Er and Iu will be used in formulating the governing equations for analyzing an unsymmetrical outrigger braced structure with three stories. A three-stories unsymmetrical outrigger-braced structure is used to demonstrate the analysis as shown in Fig. 3.1.

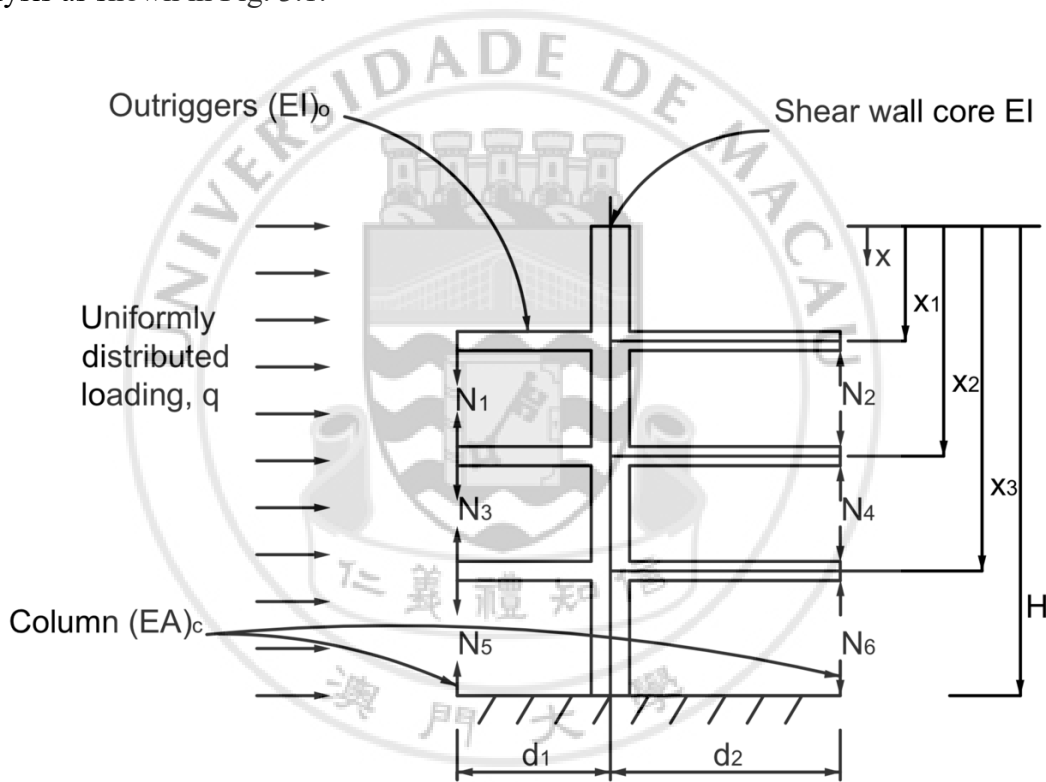


Figure 3.1 Unknown axial forces in an unsymmetrical three-story outrigger-braced structure



### 3.1.1 Axial Forces in Column

The structure with two outriggers and acted by uniformly distributed lateral load are shown in Fig. 3.2. In order to analyze the internal forces of this structure, the axial forces in the columns are taken as unknowns in the structural analysis.

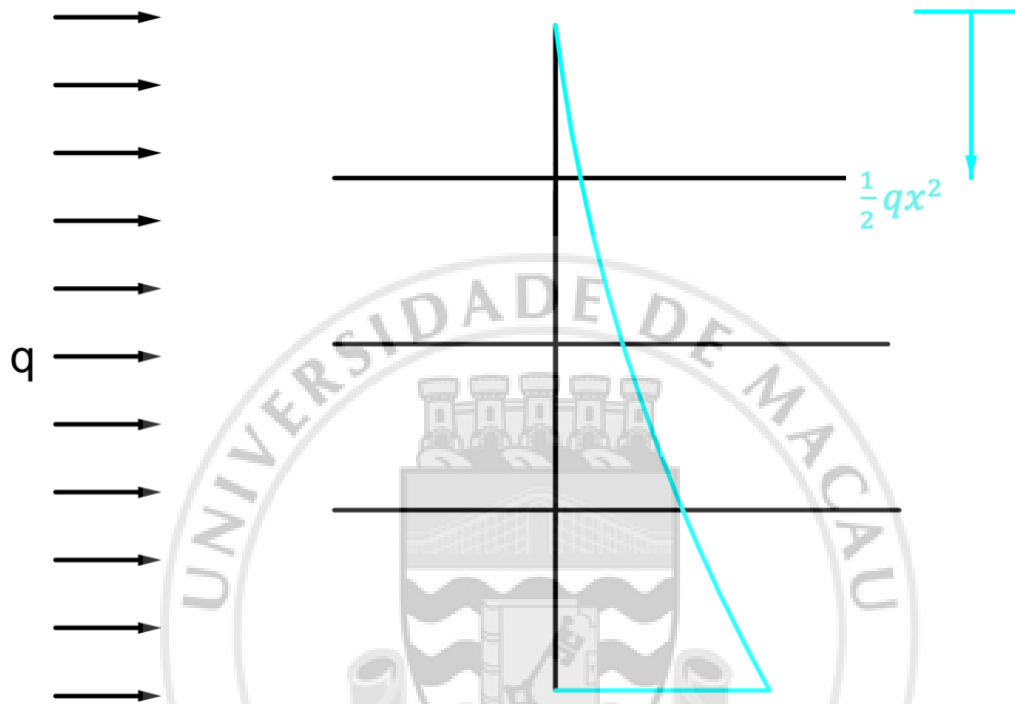


Figure 3.2 Moment diagram when and uniformly distributed load is applied on the structure

With the force method, it is assumed that the unknown axial force equals to 1. The bending moment diagrams due to the unit axial force pairs are shown in Fig. 3.3 to Fig.3.6.

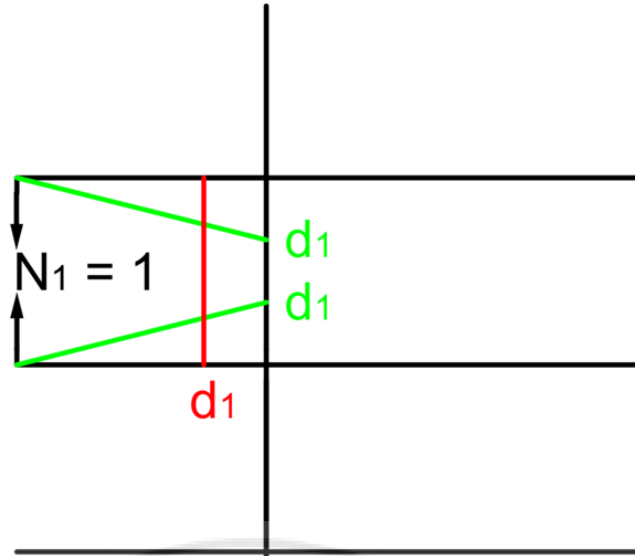


Figure 3.3 Moment diagram when  $N_1=1$  is applied on the structure

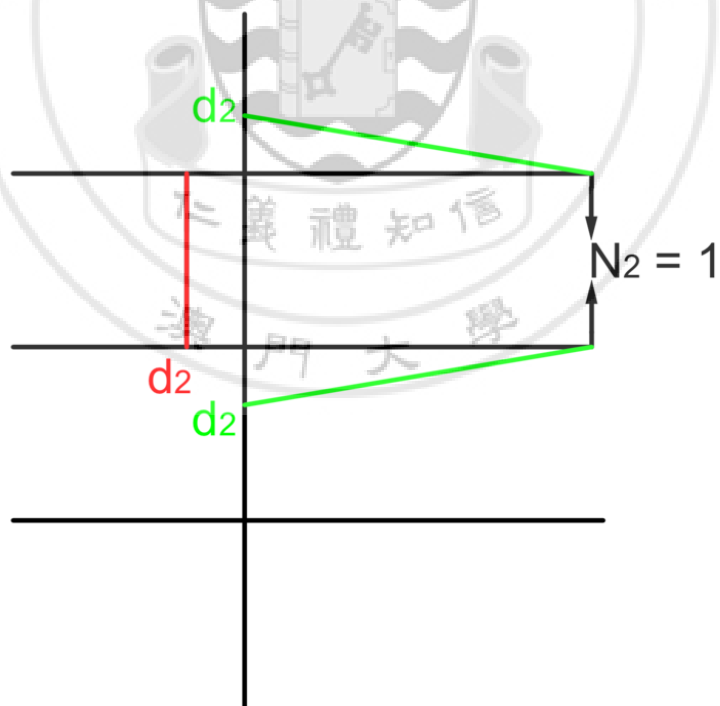


Figure 3.4 Moment diagram when  $N_2=1$  is applied on the structure

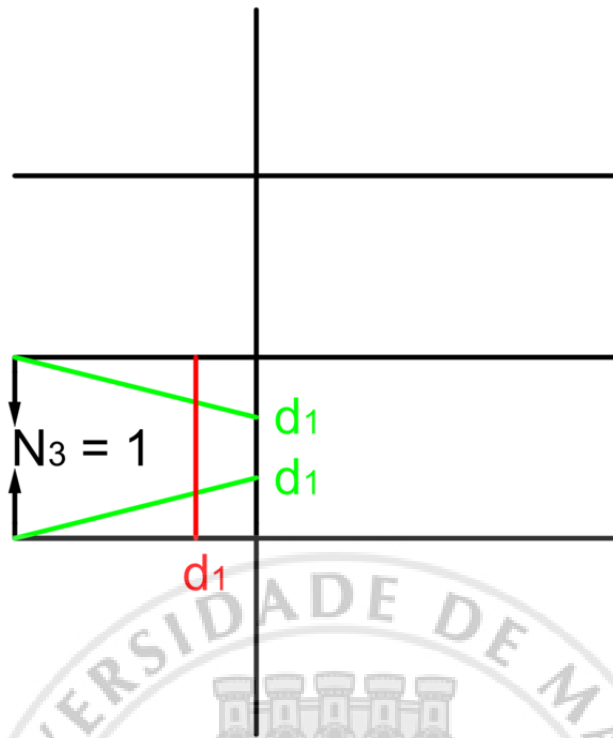


Figure 3.5 Moment diagram when  $N_3=1$  is applied on the structure

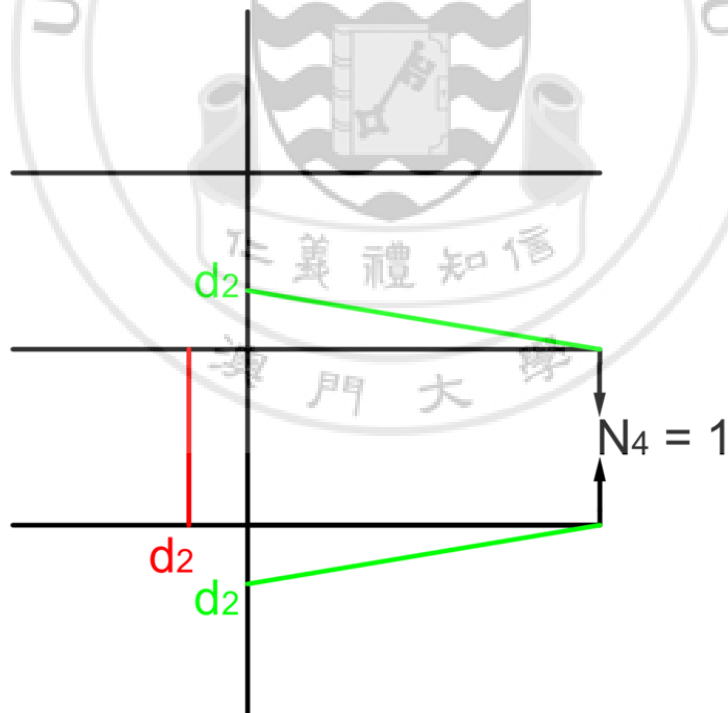


Figure 3.6 Moment diagram of  $N_4=1$  is applied on the structure

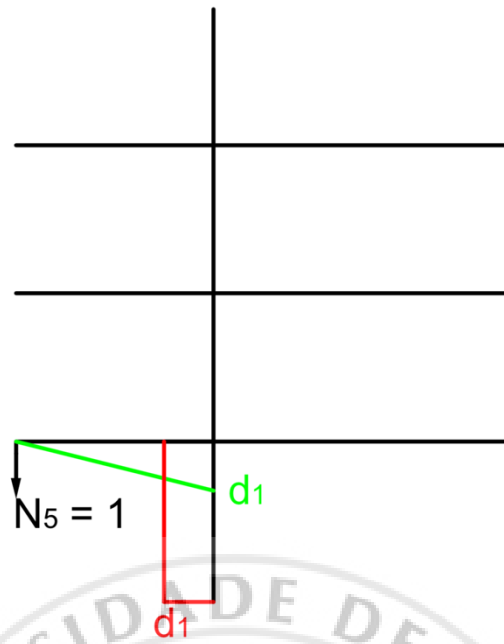


Figure 3.7 Moment diagram of  $N_5=1$  is applied on the structure

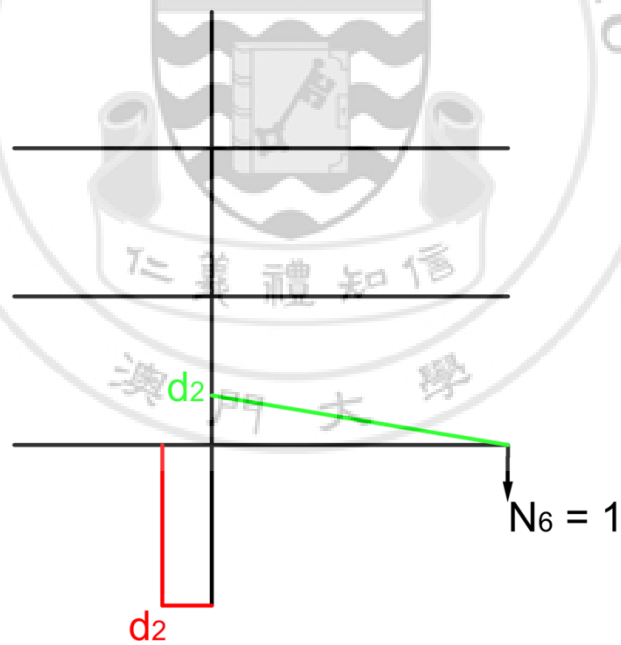


Figure 3.8 Moment diagram of  $N_6=1$  is applied on the structure

With force method, the relative displacement at the cuts are given in the following.

$$\begin{aligned}
 \Delta_1 &= \Delta_{10} + \Delta_{11} + \Delta_{12} + \Delta_{13} + \Delta_{14} + \Delta_{15} + \Delta_{16} \\
 &= \Delta_{10} + f_{11}N_1 + f_{12}N_2 + f_{13}N_3 + f_{14}N_4 + f_{15}N_5 + f_{16}N_6 \\
 \Delta_2 &= \Delta_{20} + \Delta_{21} + \Delta_{22} + \Delta_{23} + \Delta_{24} + \Delta_{25} + \Delta_{26} \\
 &= \Delta_{20} + f_{21}N_1 + f_{22}N_2 + f_{23}N_3 + f_{24}N_4 + f_{25}N_5 + f_{26}N_6 \\
 \Delta_3 &= \Delta_{30} + \Delta_{31} + \Delta_{32} + \Delta_{33} + \Delta_{34} + \Delta_{35} + \Delta_{36} \\
 &= \Delta_{30} + f_{31}N_1 + f_{32}N_2 + f_{33}N_3 + f_{34}N_4 + f_{35}N_5 + f_{36}N_6 \\
 \Delta_4 &= \Delta_{40} + \Delta_{41} + \Delta_{42} + \Delta_{43} + \Delta_{44} + \Delta_{45} + \Delta_{46} \\
 &= \Delta_{40} + f_{41}N_1 + f_{42}N_2 + f_{43}N_3 + f_{44}N_4 + f_{45}N_5 + f_{46}N_6 \\
 \Delta_5 &= \Delta_{50} + \Delta_{51} + \Delta_{52} + \Delta_{53} + \Delta_{54} + \Delta_{55} + \Delta_{56} \\
 &= \Delta_{50} + f_{51}N_1 + f_{52}N_2 + f_{53}N_3 + f_{54}N_4 + f_{55}N_5 + f_{56}N_6 \\
 \Delta_6 &= \Delta_{60} + \Delta_{61} + \Delta_{62} + \Delta_{63} + \Delta_{64} + \Delta_{65} + \Delta_{66} \\
 &= \Delta_{60} + f_{61}N_1 + f_{62}N_2 + f_{63}N_3 + f_{64}N_4 + f_{65}N_5 + f_{66}N_6
 \end{aligned}$$

The relative displacement of the cross section at the cut 1 due to the uniformly distributed loading q is

$$\Delta_{10} = -\frac{qd_1}{6EI}(x_2^3 - x_1^3) \quad (3.1)$$

The relative displacement of the cross section at the cut 2 due to the uniformly distributed loading q is

$$\Delta_{20} = -\frac{qd_2}{6EI}(x_2^3 - x_1^3) \quad (3.2)$$

The relative displacement of the cross section at the cut 3 due to the uniformly distributed loading  $q$  is

$$\Delta_{30} = -\frac{qd_1}{6EI}(x_3^3 - x_2^3) \quad (3.3)$$

The relative displacement of the cross section at the cut 4 due to the uniformly distributed loading  $q$  is

$$\Delta_{40} = -\frac{qd_2}{6EI}(x_3^3 - x_2^3) \quad (3.4)$$

The relative displacement of the cross section at the cut 5 due to the uniformly distributed loading  $q$  is

$$\Delta_{50} = -\frac{qd_1}{6EI}(H^3 - x_3^3) \quad (3.5)$$

The relative displacement of the cross section at the cut 6 due to the uniformly distributed loading  $q$  is

$$\Delta_{60} = -\frac{qd_2}{6EI}(H^3 - x_3^3) \quad (3.6)$$

The relative displacement of the cross section at the cut 1 due to the unit axial force  $N_1=1$  is

$$f_{11} = \frac{2d_1^3}{3(EI)_o} + \frac{d_1^2}{EI}(x_2 - x_1) + \frac{1}{(EA)_c}(x_2 - x_1) \quad (3.7)$$

The relative displacement of the cross section at the cut 2 due to the unit axial force  $N_1=1$  is

$$f_{12} = f_{21} = \frac{d_1 d_2}{EI} (x_2 - x_1) \quad (3.8)$$

The relative displacement of the cross section at the cut 3 due to the unit axial force  $N_1=1$  is

$$f_{13} = f_{31} = -\frac{d_1^3}{3(EI)_o} \quad (3.9)$$

The relative displacement of the cross section at the cut 4 due to the unit axial force  $N_1=1$  is

$$f_{14} = f_{41} = 0 \quad (3.10)$$

The relative displacement of the cross section at the cut 5 due to the unit axial force  $N_1=1$  is

$$f_{15} = f_{51} = 0 \quad (3.11)$$

The relative displacement of the cross section at the cut 6 due to the unit axial force  $N_1=1$  is

$$f_{16} = f_{61} = 0 \quad (3.12)$$

The relative displacement of the cross section at the cut 2 due to the unit axial force  $N_2=1$  is

$$f_{22} = \frac{2d_2^3}{3(EI)_o} + \frac{d_2^2}{EI}(x_2 - x_1) + \frac{1}{(EA)_c}(x_2 - x_1) \quad (3.13)$$

The relative displacement of the cross section at the cut 3 due to the unit axial force  $N_2=1$  is

$$f_{23} = f_{32} = 0 \quad (3.14)$$

The relative displacement of the cross section at the cut 4 due to the unit axial force  $N_2=1$  is

$$f_{24} = f_{42} = -\frac{d_2^3}{3(EI)_o} \quad (3.15)$$

The relative displacement of the cross section at the cut 5 due to the unit axial force  $N_2=1$  is

$$f_{25} = f_{52} = 0 \quad (3.16)$$

The relative displacement of the cross section at the cut 6 due to the unit axial force  $N_2=1$  is

$$f_{26} = f_{62} = 0 \quad (3.17)$$



The relative displacement of the cross section at the cut 3 due to the unit axial force  $N_3=1$  is

$$f_{33} = \frac{2d_1^3}{3(EI)_o} + \frac{d_1^2}{EI}(x_3 - x_2) + \frac{1}{(EA)_c}(x_3 - x_2) \quad (3.18)$$

The relative displacement of the cross section at the cut 4 due to the unit axial force  $N_3=1$  is

$$f_{34} = f_{43} = \frac{d_1 d_2}{EI}(x_3 - x_2) \quad (3.19)$$

The relative displacement of the cross section at the cut 5 due to the unit axial force  $N_3=1$  is

$$f_{35} = f_{53} = -\frac{d_1^3}{3(EI)_o} \quad (3.20)$$

The relative displacement of the cross section at the cut 6 due to the unit axial force  $N_3=1$  is

$$f_{36} = f_{63} = 0 \quad (3.21)$$

The relative displacement of the cross section at the cut 4 due to the unit axial force  $N_4=1$  is

$$f_{44} = \frac{2d_2^3}{3(EI)_o} + \frac{d_2^2}{EI}(x_3 - x_2) + \frac{1}{(EA)_c}(x_3 - x_2) \quad (3.22)$$

The relative displacement of the cross section at the cut 5 due to the unit axial force  $N_4=1$  is

$$f_{45} = f_{54} = 0 \quad (3.23)$$

The relative displacement of the cross section at the cut 6 due to the unit axial force  $N_4=1$  is

$$f_{46} = f_{64} = -\frac{d_2^3}{3(EI)_o} \quad (3.24)$$

The relative displacement of the cross section at the cut 5 due to the unit axial force  $N_5=1$  is

$$f_{55} = \frac{d_1^3}{3(EI)_o} + \frac{d_1^2}{EI}(H - x_3) + \frac{1}{(EA)_c}(H - x_3) \quad (3.25)$$

The relative displacement of the cross section at the cut 6 due to the unit axial force  $N_5=1$  is

$$f_{56} = f_{65} = \frac{d_1 d_2}{EI}(H - x_3) \quad (3.26)$$

The relative displacement of the cross section at the cut 6 due to the unit axial force  $N_6=1$  is

$$f_{66} = \frac{d_2^3}{3(EI)_o} + \frac{d_2^2}{EI}(H - x_3) + \frac{1}{(EA)_c}(H - x_3) \quad (3.27)$$

For the force method, there is no relative displacement at a cut, hence:

$$\therefore \Delta_1 = \Delta_2 = \Delta_3 = \Delta_4 = \Delta_5 = \Delta_6 = 0 \quad (3.28)$$

$$\therefore \Delta_{10} + f_{11}N_1 + f_{12}N_2 + f_{13}N_3 + f_{14}N_4 + f_{15}N_5 + f_{16}N_6 \quad (3.29)$$

$$\Delta_{20} + f_{21}N_1 + f_{22}N_2 + f_{23}N_3 + f_{24}N_4 + f_{25}N_5 + f_{26}N_6 \quad (3.30)$$

$$\Delta_{30} + f_{31}N_1 + f_{32}N_2 + f_{33}N_3 + f_{34}N_4 + f_{35}N_5 + f_{36}N_6 \quad (3.31)$$

$$\Delta_{40} + f_{41}N_1 + f_{42}N_2 + f_{43}N_3 + f_{44}N_4 + f_{45}N_5 + f_{46}N_6 \quad (3.32)$$

$$\Delta_{50} + f_{51}N_1 + f_{52}N_2 + f_{53}N_3 + f_{54}N_4 + f_{55}N_5 + f_{56}N_6 \quad (3.33)$$

$$\Delta_{60} + f_{61}N_1 + f_{62}N_2 + f_{63}N_3 + f_{64}N_4 + f_{65}N_5 + f_{66}N_6 \quad (3.34)$$

or

$$-\frac{qd_1}{6EI}(x_2^3 - x_1^3) + \left[ \frac{2d_1^3}{3(EI)_o} + \frac{d_1^2}{EI}(x_2 - x_1) + \frac{1}{(EA)_c}(x_2 - x_1) \right] N_1 + \left[ \frac{d_1 d_2}{EI}(x_2 - x_1) \right] N_2 - \left[ \frac{d_1^3}{3(EI)_o} \right] N_3 = 0 \quad (3.35)$$

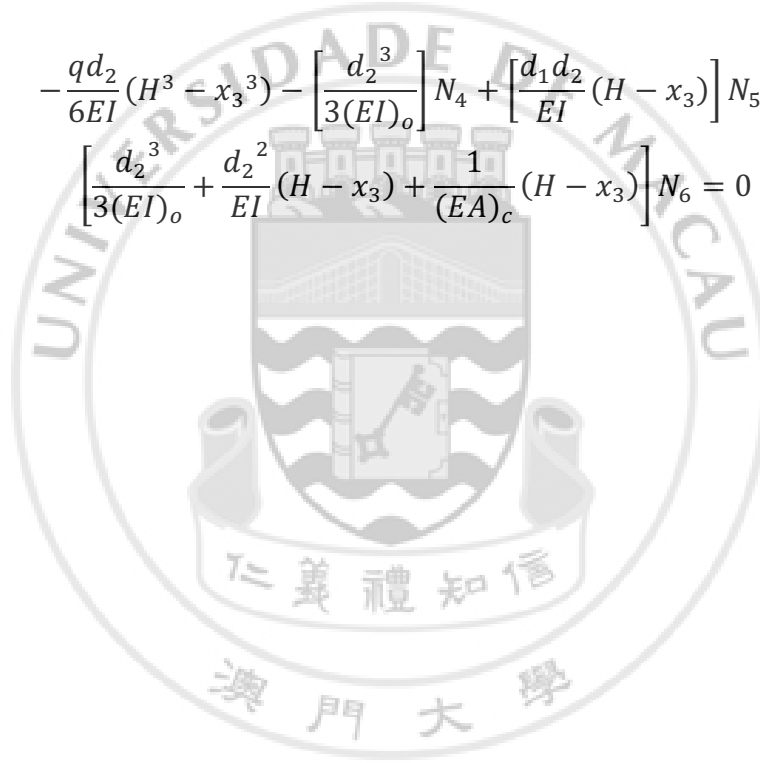
$$-\frac{qd_2}{6EI}(x_2^3 - x_1^3) + \left[ \frac{d_1 d_2}{EI}(x_2 - x_1) \right] N_1 + \left[ \frac{2d_2^3}{3(EI)_o} + \frac{d_2^2}{EI}(x_2 - x_1) + \frac{1}{(EA)_c}(x_2 - x_1) \right] N_2 - \left[ \frac{d_2^3}{3(EI)_o} \right] N_4 = 0 \quad (3.36)$$

$$-\frac{qd_1}{6EI}(x_3^3 - x_2^3) - \left[ \frac{d_1^3}{3(EI)_o} \right] N_1 + \left[ \frac{2d_1^3}{3(EI)_o} + \frac{d_1^2}{EI}(x_3 - x_2) + \frac{1}{(EA)_c}(x_3 - x_2) \right] N_3 + \left[ \frac{d_1 d_2}{EI}(x_3 - x_2) \right] N_4 - \left[ \frac{d_1^3}{3(EI)_o} \right] N_5 = 0 \quad (3.37)$$

$$\begin{aligned}
& -\frac{qd_2}{6EI}(x_3^3 - x_2^3) - \left[ \frac{d_2^3}{3(EI)_o} \right] N_2 + \left[ \frac{d_1 d_2}{EI}(x_3 - x_2) \right] N_3 + \\
& \left[ \frac{2d_2^3}{3(EI)_o} + \frac{d_2^2}{EI}(x_3 - x_2) + \frac{1}{(EA)_c}(x_3 - x_2) \right] N_4 - \left[ \frac{d_2^3}{3(EI)_o} \right] N_6 = 0
\end{aligned} \quad (3.38)$$

$$\begin{aligned}
& -\frac{qd_1}{6EI}(H^3 - x_3^3) - \left[ \frac{d_1^3}{3(EI)_o} \right] N_3 + \\
& \left[ \frac{d_1^3}{3(EI)_o} + \frac{d_1^2}{EI}(H - x_3) + \frac{1}{(EA)_c}(H - x_3) \right] N_5 + \left[ \frac{d_1 d_2}{EI}(H - x_3) \right] N_6 = 0
\end{aligned} \quad (3.39)$$

$$\begin{aligned}
& -\frac{qd_2}{6EI}(H^3 - x_3^3) - \left[ \frac{d_2^3}{3(EI)_o} \right] N_4 + \left[ \frac{d_1 d_2}{EI}(H - x_3) \right] N_5 + \\
& \left[ \frac{d_2^3}{3(EI)_o} + \frac{d_2^2}{EI}(H - x_3) + \frac{1}{(EA)_c}(H - x_3) \right] N_6 = 0
\end{aligned} \quad (3.40)$$



From Eqs. (3.35) to Eqs. (3.40),  $N_1$  to  $N_6$  can be calculated as

$$\begin{aligned}
 & \begin{Bmatrix} N_1 \\ N_2 \\ N_3 \\ N_4 \\ N_5 \\ N_6 \end{Bmatrix} = \\
 & \left\{ \begin{array}{ccc} \frac{2d_1^3}{3(EI)_o} + \frac{d_1^2}{EI}(x_2 - x_1) + \frac{1}{(EA)_c}(x_2 - x_1) & \frac{d_1 d_2}{EI}(x_2 - x_1) & -\frac{d_1^3}{3(EI)_o} \\ \frac{d_1 d_2}{EI}(x_2 - x_1) & \frac{2d_2^3}{3(EI)_o} + \frac{d_2^2}{EI}(x_2 - x_1) + \frac{1}{(EA)_c}(x_2 - x_1) & \frac{2d_1^3}{3(EI)_o} + \frac{d_1^2}{EI}(x_3 - x_2) + \frac{1}{(EA)_c}(x_3 - x_2) \\ -\frac{d_1^3}{3(EI)_o} & 0 & \frac{d_1 d_2}{EI}(x_3 - x_2) \\ 0 & -\frac{d_2^3}{3(EI)_o} & -\frac{d_1^3}{3(EI)_o} \\ 0 & 0 & 0 \\ 0 & 0 & 0 \end{array} \right\}^{-1} \\
 & \left\{ \begin{array}{ccc} 0 & 0 & 0 \\ -\frac{d_2^3}{3(EI)_o} & 0 & 0 \\ \frac{d_1 d_2}{EI}(x_3 - x_2) & -\frac{d_1^3}{3(EI)_o} & -\frac{d_2^3}{3(EI)_o} \\ \frac{2d_2^3}{3(EI)_o} + \frac{d_2^2}{EI}(x_3 - x_2) + \frac{1}{(EA)_c}(x_3 - x_2) & \frac{d_1^3}{3(EI)_o} + \frac{d_1^2}{EI}(H - x_3) + \frac{1}{(EA)_c}(H - x_3) & \frac{d_1 d_2}{EI}(H - x_3) \\ 0 & \frac{d_1 d_2}{EI}(H - x_3) & \frac{d_2^3}{3(EI)_o} + \frac{d_2^2}{EI}(H - x_3) + \frac{1}{(EA)_c}(H - x_3) \\ -\frac{d_2^3}{3(EI)_o} & 0 & 0 \end{array} \right\} \\
 & \begin{Bmatrix} \frac{q d_1}{6EI}(x_2^3 - x_1^3) \\ \frac{q d_2}{6EI}(x_2^3 - x_1^3) \\ \frac{q d_1}{6EI}(x_3^3 - x_2^3) \\ \frac{q d_2}{6EI}(x_3^3 - x_2^3) \\ \frac{q d_1}{6EI}(H^3 - x_3^3) \\ \frac{q d_2}{6EI}(H^3 - x_3^3) \end{Bmatrix} \quad (3.41)
 \end{aligned}$$

### 3.1.2 Bending Moment in the Core and Deflection at Top Drift

Between building top and outrigger 1:

$$m_0 = \frac{1}{2}qx^2 \quad (3.42)$$

Between building outrigger 1 and outrigger 2:

$$m_1 = \frac{1}{2}qx^2 - N_1d_1 - N_2d_2 \quad (3.43)$$

Between building outrigger 2 and outrigger 3:

$$m_2 = \frac{1}{2}qx^2 - N_3d_1 - N_4d_2 \quad (3.44)$$

Between building outrigger 3 and building bottom:

$$m_3 = \frac{1}{2}qx^2 - N_5d_1 - N_6d_2 \quad (3.45)$$

The top drift is

$$\Delta_0 = \frac{1}{EI} \left\{ \frac{q}{8}H^4 - \frac{d_1}{2} [N_1(x_2^2 - x_1^2) + N_3(x_3^2 - x_2^2) + N_5(H^2 - x_3^2)] - \frac{d_2}{2} [N_2(x_2^2 - x_1^2) + N_4(x_3^2 - x_2^2) + N_6(H^2 - x_3^2)] \right\} \quad (3.46)$$

### 3.1.3 Numerical Verification of the Results

In this part, numerical values of the structural parameters are given in order to verify the results obtained by the equations of unknown axial forces. Moment equilibrium at the nodes of the shear wall core for each story and the total lateral equilibrium are provided in the following.

The structural parameters in the equations are given as follows.

$$d_1=5,$$

$$d_2=10,$$

$$(EI)_o=100,$$

$$EI=1000,$$

$$(EA)_c=300,$$

$$x_1=3,$$

$$x_2=6,$$

$$x_3=9,$$

$$H=12,$$

$$q=100$$

Then the axial forces for  $N_s$  are obtained by

$$\begin{Bmatrix} N_1 \\ N_2 \\ N_3 \\ N_4 \\ N_5 \\ N_6 \end{Bmatrix} = \begin{Bmatrix} 551/600 & 3/20 & -5/12 & 0 & 0 & 0 \\ 3/20 & 2093/300 & 0 & -10/3 & 0 & 0 \\ -5/12 & 0 & 551/600 & 3/20 & -5/12 & 0 \\ 0 & -10/3 & 3/20 & 2093/300 & 0 & -10/3 \\ 0 & 0 & -5/12 & 0 & 551/600 & 3/20 \\ 0 & 0 & 0 & -10/3 & 3/20 & 2093/300 \end{Bmatrix}^{-1} \begin{Bmatrix} 63/4 \\ 63/2 \\ 171/4 \\ 171/2 \\ 333/4 \\ 333/2 \end{Bmatrix}$$

which gives

$$\begin{Bmatrix} N_1 \\ N_2 \\ N_3 \\ N_4 \\ N_5 \\ N_6 \end{Bmatrix} = \begin{Bmatrix} 79.29252343 \\ 20.70633777 \\ 144.4150032 \\ 37.45652851 \\ 149.882494 \\ 38.53885154 \end{Bmatrix}$$

The bending moments of the top and bottom at the core wall node on the third story are got, respectively, as

$$m_{III,top} = \frac{1}{2} * 100 * 3^2 = 450$$

$$m_{III,bottom} = \frac{1}{2} * 100 * 3^2 - 79.29252343 * 5 - 20.70633777 * 10 = -153.5259948$$

The bending moments of the top and bottom at the core wall node on the second story are got , respectively, as

$$m_{II,top} = \frac{1}{2} * 100 * 6^2 - 79.29252343 * 5 - 20.70633777 * 10 = 1196.474005$$

$$m_{II,bottom} = \frac{1}{2} * 100 * 6^2 - 144.4150032 * 5 - 37.45652851 * 10 = 703.3596989$$

The bending moments of the top and bottom at the core wall node on the first story are got, respectively, as

$$m_{I,top} = \frac{1}{2} * 100 * 9^2 - 144.4150032 * 5 - 37.45652851 * 10 = 2953.359699$$

$$m_{I,bottom} = \frac{1}{2} * 100 * 9^2 - 149.882494 * 5 - 38.53885154 * 10 = 2915.199015$$

The bending moments of the left side and right side at the core wall node on the third story are got, respectively, as

$$m_{III,left} = N_1 d_1 = 79.29252343 * 5 = 396.4626171$$

$$m_{III,right} = N_2 d_2 = 20.70633777 * 10 = 207.0633777$$



The bending moment of the left side and right side at the core wall node on the second story are got, respectively, as

$$m_{II,left}=(N_3 - N_1)d_1 = (144.4150032 - 79.29252343) * 5 = 325.6123989$$

$$m_{II,right}=(N_4 - N_2)d_2 = (37.45652851 - 20.70633777) * 10 = 167.5019074$$

The bending moment of the left side and right side at the core wall node on the first story are got, respectively, as

$$m_{I,left}=(N_5 - N_3)d_1 = (149.882494 - 144.4150032) * 5 = 27.337454$$

$$m_{I,right}=(N_6 - N_4)d_2 = (38.53885154 - 37.45652851) * 10 = 10.8232303$$

Taking derivative of m with respect to x, the shear force equation can be obtained as

$$V(x) = m'(x) = qx$$

Then the shear force at the bottom of the shear wall is

$$V(H) = V(12) = 100 * 12 = 1200$$

The lateral load applied on the structure is

$$F = q * H = 100 * 12 = 1200$$

The moment equilibrium at the core wall node on the third story is checked by

$$\begin{aligned} \sum m_{III} &= m_{III,top} - m_{III,bottom} - m_{III,left} - m_{III,right} \\ &= 450 - (-153.5259948) - 396.4626171 - 207.0633777 = 0 \end{aligned}$$

The moment equilibrium at the core wall node on the second story is checked by

$$\begin{aligned}\sum m_{II} &= m_{II,top} - m_{II,bottom} - m_{II,left} - m_{II,right} \\ &= 1196.474005 - 703.3596989 - 325.6123989 - 167.5019074 = 0\end{aligned}$$

The moment equilibrium at the core wall node on the first story is checked by

$$\begin{aligned}\sum m_I &= m_{I,top} - m_{I,bottom} - m_{I,left} - m_{I,right} \\ &= 2953.359699 - 2915.199015 - 27.337454 - 10.8232303 = 0\end{aligned}$$

The total horizontal equilibrium above the first story is checked by

$$\sum F_x = F - V(H) = 1200 - 1200 = 0$$

The moments applied at each node are the lateral forces applied on the structure for equilibrium equations are shown in the following figures.

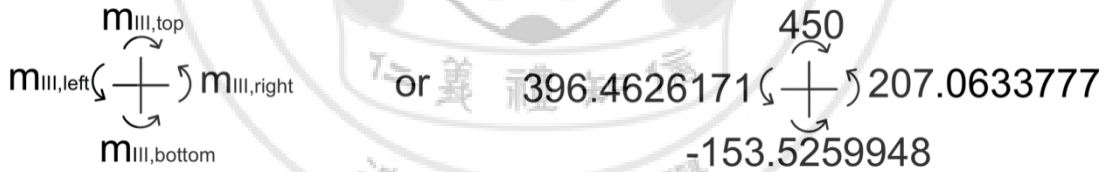


Figure 3.9 Moment equilibrium at the core wall node on third story for verification

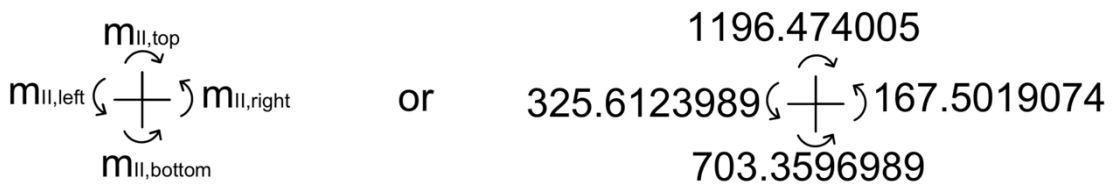


Figure 3.10 Moment equilibrium at the core wall node on second story for verification

$$\begin{array}{ccc}
 \begin{array}{c} m_{l,top} \\ \curvearrowright \\ m_{l,left} \left( \begin{array}{c} \text{---} \\ | \\ \text{---} \end{array} \right) m_{l,right} \\ \curvearrowleft \\ m_{l,bottom} \end{array} & \text{or} & \begin{array}{c} 2953.359699 \\ \curvearrowright \\ 27.337454 \left( \begin{array}{c} \text{---} \\ | \\ \text{---} \end{array} \right) 10.8232303 \\ \curvearrowleft \\ 2915.199015 \end{array}
 \end{array}$$

Figure 3.11 Moment equilibrium at the core wall node on first story for verification

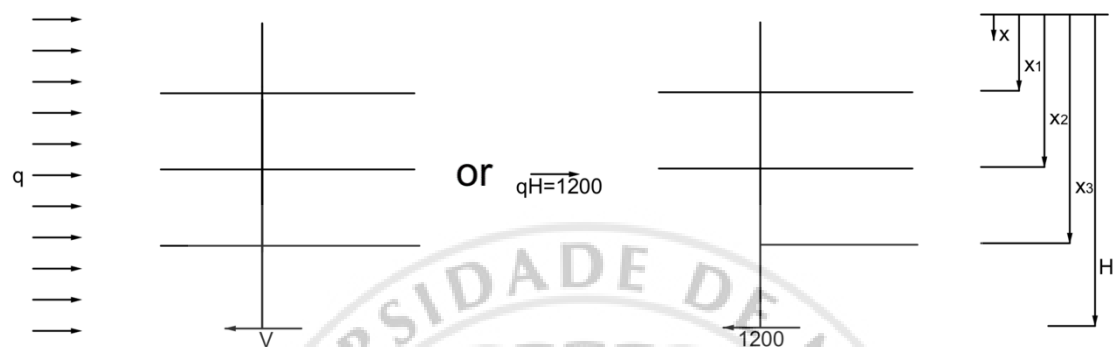


Figure 3.12 Horizontal equilibrium above the first story of the structure for verification

From the above verification, it is seen that all the equilibriums are satisfied. It means that the equations of  $N_s$  and  $m$  are correct.

### 3.2 Equation for Optimum Locations

The optimum locations of the outriggers can be got by minimizing the top drift. Taking derivation of  $\Delta_0$  with respect to  $x_1$  and  $x_2$  and  $x_3$ , it gives

$$\begin{aligned} \frac{\partial \Delta_0}{\partial x_1} = & -\frac{d_1}{2EI} \left[ (x_2^2 - x_1^2) \frac{\partial N_1}{\partial x_1} - 2x_1 N_1 + (x_3^2 - x_2^2) \frac{\partial N_3}{\partial x_1} + (H^2 - x_3^2) \frac{\partial N_5}{\partial x_1} \right] - \\ & \frac{d_2}{2EI} \left[ (x_2^2 - x_1^2) \frac{\partial N_2}{\partial x_1} - 2x_1 N_2 + (x_3^2 - x_2^2) \frac{\partial N_4}{\partial x_1} + (H^2 - x_3^2) \frac{\partial N_6}{\partial x_1} \right] = 0 \end{aligned} \quad (3.47)$$

$$\begin{aligned} \frac{\partial \Delta_0}{\partial x_2} = & -\frac{d_1}{2EI} \left[ (x_2^2 - x_1^2) \frac{\partial N_1}{\partial x_2} + 2x_2 N_1 + \right. \\ & \left. (x_3^2 - x_2^2) \frac{\partial N_3}{\partial x_2} - 2x_2 N_3 + (H^2 - x_3^2) \frac{\partial N_5}{\partial x_2} \right] - \\ & \frac{d_2}{2EI} \left[ (x_2^2 - x_1^2) \frac{\partial N_2}{\partial x_2} + 2x_2 N_2 + (x_3^2 - x_2^2) \frac{\partial N_4}{\partial x_2} - \right. \\ & \left. 2x_2 N_4 + (H^2 - x_3^2) \frac{\partial N_6}{\partial x_2} \right] = 0 \end{aligned} \quad (3.48)$$

$$\begin{aligned} \frac{\partial \Delta_0}{\partial x_3} = & -\frac{d_1}{2EI} \left[ (x_2^2 - x_1^2) \frac{\partial N_1}{\partial x_3} + (x_3^2 - x_2^2) \frac{\partial N_3}{\partial x_3} + \right. \\ & \left. 2x_2 N_3 + (H^2 - x_3^2) \frac{\partial N_5}{\partial x_3} - 2x_3 N_5 \right] - \\ & \frac{d_2}{2EI} \left[ (x_2^2 - x_1^2) \frac{\partial N_2}{\partial x_3} + (x_3^2 - x_2^2) \frac{\partial N_4}{\partial x_3} + \right. \\ & \left. 2x_3 N_4 + (H^2 - x_3^2) \frac{\partial N_6}{\partial x_3} - 2x_1 N_6 \right] = 0 \end{aligned} \quad (3.49)$$

### 3.3 Analysis for Optimum Locations of Outriggers of Unsymmetrical Structure

In order to make the results from numerical analysis represent more general cases, the un-dimensional parameters  $\varepsilon_1$ ,  $\varepsilon_2$  and  $\varepsilon_3$  are introduced as the ratio of the total height of the structure and the location of each story. The un-dimensional parameter  $r$  is introduced to reflect the un-symmetry of the structure. The un-dimensional parameters  $\alpha$ ,  $\beta$  and  $\omega$  are also introduced for more general analysis

Introduce the parameters  $\varepsilon_1 = \frac{x_1}{H}$ ,  $\varepsilon_2 = \frac{x_2}{H}$ ,  $\varepsilon_3 = \frac{x_3}{H}$  and  $r = \frac{d_2}{d_1}$

Flexural rigidity ratio of core to column (non-dimensional):  $\alpha = \frac{EI}{2(EA)_c d^2}$

Flexural rigidity ratio of core to outrigger (non-dimensional):  $\beta = \frac{2EI}{(EI)_o} \frac{d}{H}$

Then the relative rigidity between core column system and outriggers (non-dimensional) is got to be:

$$\omega = \frac{\beta}{12(1 + \alpha)}$$

The parameter  $\omega$  is the characteristic structural parameter for a uniform structure with flexible outriggers. It is useful in that it allows various aspects of the behavior of outrigger structures to be expressed in a very concise form.

Then equations (3.35) – (3.40) can be rewritten as:

Both sides of the equations are multiplied by  $\frac{EI}{Hd_1^2}$

$$-\frac{qH^2}{6d_1}(\varepsilon_2^3 - \varepsilon_1^3) + \left[ \frac{\beta}{3} + (\varepsilon_2 - \varepsilon_1) + 2\alpha(\varepsilon_2 - \varepsilon_1) \right] N_1 + [r(\varepsilon_2 - \varepsilon_1)]N_2 - \left[ \frac{\beta}{6} \right] N_3 = 0 \quad (3.50)$$

$$\begin{aligned}
& -\frac{rqH^2}{6d_1}(\varepsilon_2^3 - \varepsilon_1^3) + [r(\varepsilon_2 - \varepsilon_1)]N_1 + \\
& \left[ \frac{r^3\beta}{3} + r^3(\varepsilon_2 - \varepsilon_1) + 2\alpha(\varepsilon_2 - \varepsilon_1) \right] N_2 - \left[ \frac{r^3\beta}{6} \right] N_4 = 0
\end{aligned} \tag{3.51}$$

$$\begin{aligned}
& -\frac{qH^2}{6d_1}(\varepsilon_3^3 - \varepsilon_2^3) - \left[ \frac{\beta}{6} \right] N_1 + \left[ \frac{\beta}{3} + (\varepsilon_3 - \varepsilon_2) + 2\alpha(\varepsilon_3 - \varepsilon_2) \right] N_3 + \\
& [r(\varepsilon_3 - \varepsilon_2)]N_4 - \left[ \frac{\beta}{6} \right] N_5 = 0
\end{aligned} \tag{3.52}$$

$$\begin{aligned}
& -\frac{rqH^2}{6d_1}(\varepsilon_3^3 - \varepsilon_2^3) - \left[ \frac{r^3\beta}{6} \right] N_2 + [r(\varepsilon_3 - \varepsilon_2)]N_3 + \\
& \left[ \frac{r^3\beta}{3} + r^2(\varepsilon_3 - \varepsilon_2) + 2\alpha(\varepsilon_3 - \varepsilon_2) \right] N_4 - \left[ \frac{r^3\beta}{6} \right] N_6 = 0
\end{aligned} \tag{3.53}$$

$$\begin{aligned}
& -\frac{qH^2}{6d_1}(1 - \varepsilon_3^3) - \left[ \frac{\beta}{6} \right] N_3 + \left[ \frac{\beta}{3} + (1 - \varepsilon_3) + 2\alpha(1 - \varepsilon_3) \right] N_5 + \\
& [r(1 - \varepsilon_3)]N_6 = 0
\end{aligned} \tag{3.54}$$

$$\begin{aligned}
& -\frac{rqH^2}{6d_1}(1 - \varepsilon_3^3) - \left[ \frac{r^3\beta}{6} \right] N_4 + [r(1 - \varepsilon_3)]N_5 + \\
& \left[ \frac{r^3\beta}{3} + r^2(1 - \varepsilon_3) + 2\alpha(1 - \varepsilon_3) \right] N_6 = 0
\end{aligned} \tag{3.55}$$

As the expressions of  $N_1, N_2, N_3, N_4, N_5$  and  $N_6$  are very complicate, it is difficult to get the derivatives of  $N_1, N_2, N_3, N_4, N_5$  and  $N_6$  with respect to  $\varepsilon_1, \varepsilon_2$  and  $\varepsilon_3$ . Therefore, the equation  $\{f\}\{N\} = \{P\}$  is used in getting the derivatives.

### 3.3.1 Derivation of $N_1 \sim N_6$ with Respect to $\varepsilon_1$

$$-\frac{qH^2}{6d_1}(\varepsilon_2^3 - \varepsilon_1^3) + \left[\frac{\beta}{3} + (\varepsilon_2 - \varepsilon_1) + 2\alpha(\varepsilon_2 - \varepsilon_1)\right]N_1 + [r(\varepsilon_2 - \varepsilon_1)]N_2 - \left[\frac{\beta}{6}\right]N_3 = 0 \quad (3.50)$$

gives

$$\frac{qH^2}{2d_1}\varepsilon_1^2 - [1 + 2\alpha]N_1 - [r]N_2 + \mathfrak{f}_{11}\frac{\partial N_1}{\partial \varepsilon_1} + \mathfrak{f}_{12}\frac{\partial N_2}{\partial \varepsilon_1} + \mathfrak{f}_{13}\frac{\partial N_3}{\partial \varepsilon_1} = 0 \quad (3.56)$$

$$-\frac{rqH^2}{6d_1}(\varepsilon_2^3 - \varepsilon_1^3) + [r(\varepsilon_2 - \varepsilon_1)]N_1 + \left[\frac{r^3\beta}{3} + r^3(\varepsilon_2 - \varepsilon_1) + 2\alpha(\varepsilon_2 - \varepsilon_1)\right]N_2 - \left[\frac{r^3\beta}{6}\right]N_4 = 0 \quad (3.51)$$

gives

$$\frac{rqH^2}{2d_1}\varepsilon_1^2 - [r]N_1 - [r^2 + 2\alpha]N_2 + \mathfrak{f}_{21}\frac{\partial N_1}{\partial \varepsilon_1} + \mathfrak{f}_{22}\frac{\partial N_2}{\partial \varepsilon_1} + \mathfrak{f}_{24}\frac{\partial N_4}{\partial \varepsilon_1} = 0 \quad (3.57)$$

$$-\frac{qH^2}{6d_1}(\varepsilon_3^3 - \varepsilon_2^3) - \left[\frac{\beta}{6}\right]N_1 + \left[\frac{\beta}{3} + (\varepsilon_3 - \varepsilon_2) + 2\alpha(\varepsilon_3 - \varepsilon_2)\right]N_3 + [r(\varepsilon_3 - \varepsilon_2)]N_4 - \left[\frac{\beta}{6}\right]N_5 = 0 \quad (3.52)$$

gives

$$\mathfrak{f}_{31}\frac{\partial N_1}{\partial \varepsilon_1} + \mathfrak{f}_{33}\frac{\partial N_3}{\partial \varepsilon_1} + \mathfrak{f}_{34}\frac{\partial N_4}{\partial \varepsilon_1} + \mathfrak{f}_{35}\frac{\partial N_5}{\partial \varepsilon_1} = 0 \quad (3.58)$$

$$\begin{aligned}
& -\frac{rqH^2}{6d_1}(\varepsilon_3^3 - \varepsilon_2^3) - \left[\frac{r^3\beta}{6}\right]N_2 + [r(\varepsilon_3 - \varepsilon_2)]N_3 + \\
& \left[\frac{r^3\beta}{3} + r^2(\varepsilon_3 - \varepsilon_2) + 2\alpha(\varepsilon_3 - \varepsilon_2)\right]N_4 - \left[\frac{r^3\beta}{6}\right]N_6 = 0
\end{aligned} \tag{3.53}$$

gives

$$\mathfrak{f}_{42} \frac{\partial N_2}{\partial \varepsilon_1} + \mathfrak{f}_{43} \frac{\partial N_3}{\partial \varepsilon_1} + \mathfrak{f}_{44} \frac{\partial N_4}{\partial \varepsilon_1} + \mathfrak{f}_{46} \frac{\partial N_6}{\partial \varepsilon_1} = 0 \tag{3.59}$$

$$\begin{aligned}
& -\frac{qH^2}{6d_1}(1 - \varepsilon_3^3) - \left[\frac{\beta}{6}\right]N_3 + \\
& \left[\frac{\beta}{3} + (1 - \varepsilon_3) + 2\alpha(1 - \varepsilon_3)\right]N_5 + [r(1 - \varepsilon_3)]N_6 = 0
\end{aligned} \tag{3.54}$$

gives

$$\mathfrak{f}_{53} \frac{\partial N_3}{\partial \varepsilon_1} + \mathfrak{f}_{55} \frac{\partial N_5}{\partial \varepsilon_1} + \mathfrak{f}_{56} \frac{\partial N_6}{\partial \varepsilon_1} = 0 \tag{3.60}$$

$$\begin{aligned}
& -\frac{rqH^2}{6d_1}(1 - \varepsilon_3^3) - \left[\frac{r^3\beta}{6}\right]N_4 + [r(1 - \varepsilon_3)]N_5 + \\
& \left[\frac{r^3\beta}{3} + r^2(1 - \varepsilon_3) + 2\alpha(1 - \varepsilon_3)\right]N_6 = 0
\end{aligned} \tag{3.55}$$

gives

$$\mathfrak{f}_{64} \frac{\partial N_4}{\partial \varepsilon_1} + \mathfrak{f}_{65} \frac{\partial N_5}{\partial \varepsilon_1} + \mathfrak{f}_{66} \frac{\partial N_6}{\partial \varepsilon_1} = 0 \tag{3.61}$$



### 3.3.2 Derivation of $N_1 \sim N_6$ with Respect to $\varepsilon_2$

$$-\frac{qH^2}{6d_1}(\varepsilon_2^3 - \varepsilon_1^3) + \left[\frac{\beta}{3} + (\varepsilon_2 - \varepsilon_1) + 2\alpha(\varepsilon_2 - \varepsilon_1)\right]N_1 + [r(\varepsilon_2 - \varepsilon_1)]N_2 - \left[\frac{\beta}{6}\right]N_3 = 0 \quad (3.50)$$

gives

$$-\frac{qH^2}{2d_1}\varepsilon_2^2 + [1 + 2\alpha]N_1 + [r]N_2 + \mathfrak{f}_{11}\frac{\partial N_1}{\partial \varepsilon_2} + \mathfrak{f}_{12}\frac{\partial N_2}{\partial \varepsilon_2} + \mathfrak{f}_{13}\frac{\partial N_3}{\partial \varepsilon_2} = 0 \quad (3.62)$$

$$-\frac{rqH^2}{6d_1}(\varepsilon_2^3 - \varepsilon_1^3) + [r(\varepsilon_2 - \varepsilon_1)]N_1 + \left[\frac{r^3\beta}{3} + r^3(\varepsilon_2 - \varepsilon_1) + 2\alpha(\varepsilon_2 - \varepsilon_1)\right]N_2 - \left[\frac{r^3\beta}{6}\right]N_4 = 0 \quad (3.51)$$

gives

$$-\frac{rqH^2}{2d_1}\varepsilon_2^2 + [r]N_1 + [r^2 + 2\alpha]N_2 + \mathfrak{f}_{21}\frac{\partial N_1}{\partial \varepsilon_2} + \mathfrak{f}_{22}\frac{\partial N_2}{\partial \varepsilon_2} + \mathfrak{f}_{24}\frac{\partial N_4}{\partial \varepsilon_2} = 0 \quad (3.63)$$

$$-\frac{qH^2}{6d_1}(\varepsilon_3^3 - \varepsilon_2^3) - \left[\frac{\beta}{6}\right]N_1 + \left[\frac{\beta}{3} + (\varepsilon_3 - \varepsilon_2) + 2\alpha(\varepsilon_3 - \varepsilon_2)\right]N_3 + [r(\varepsilon_3 - \varepsilon_2)]N_4 - \left[\frac{\beta}{6}\right]N_5 = 0 \quad (3.52)$$

gives

$$\frac{qH^2}{2d_1}\varepsilon_2^2 - [1 + 2\alpha]N_3 - [r]N_4 + \mathfrak{f}_{31}\frac{\partial N_1}{\partial \varepsilon_2} + \mathfrak{f}_{33}\frac{\partial N_3}{\partial \varepsilon_2} + \mathfrak{f}_{34}\frac{\partial N_4}{\partial \varepsilon_2} + \mathfrak{f}_{35}\frac{\partial N_5}{\partial \varepsilon_2} = 0 \quad (3.64)$$

$$\begin{aligned}
& -\frac{rqH^2}{6d_1}(\varepsilon_3^3 - \varepsilon_2^3) - \left[\frac{r^3\beta}{6}\right]N_2 + [r(\varepsilon_3 - \varepsilon_2)]N_3 + \\
& \left[\frac{r^3\beta}{3} + r^2(\varepsilon_3 - \varepsilon_2) + 2\alpha(\varepsilon_3 - \varepsilon_2)\right]N_4 - \left[\frac{r^3\beta}{6}\right]N_6 = 0
\end{aligned} \tag{3.53}$$

gives

$$\begin{aligned}
& \frac{rqH^2}{2d_1}\varepsilon_2^2 - [r]N_3 - [r^2 + 2\alpha]N_4 + \mathfrak{f}_{42} \frac{\partial N_2}{\partial \varepsilon_2} + \\
& \mathfrak{f}_{43} \frac{\partial N_3}{\partial \varepsilon_2} + \mathfrak{f}_{44} \frac{\partial N_4}{\partial \varepsilon_2} + \mathfrak{f}_{46} \frac{\partial N_6}{\partial \varepsilon_2} = 0
\end{aligned} \tag{3.65}$$

$$\begin{aligned}
& -\frac{qH^2}{6d_1}(1 - \varepsilon_3^3) - \left[\frac{\beta}{6}\right]N_3 + \left[\frac{\beta}{3} + (1 - \varepsilon_3) + 2\alpha(1 - \varepsilon_3)\right]N_5 + [r(1 - \varepsilon_3)]N_6 = 0
\end{aligned} \tag{3.54}$$

gives

$$\mathfrak{f}_{53} \frac{\partial N_3}{\partial \varepsilon_2} + \mathfrak{f}_{55} \frac{\partial N_5}{\partial \varepsilon_2} + \mathfrak{f}_{56} \frac{\partial N_6}{\partial \varepsilon_2} = 0 \tag{3.66}$$

$$\begin{aligned}
& -\frac{rqH^2}{6d_1}(1 - \varepsilon_3^3) - \left[\frac{r^3\beta}{6}\right]N_4 + [r(1 - \varepsilon_3)]N_5 + \\
& \left[\frac{r^3\beta}{3} + r^2(1 - \varepsilon_3) + 2\alpha(1 - \varepsilon_3)\right]N_6 = 0
\end{aligned} \tag{3.55}$$

gives

$$\mathfrak{f}_{64} \frac{\partial N_4}{\partial \varepsilon_2} + \mathfrak{f}_{65} \frac{\partial N_5}{\partial \varepsilon_2} + \mathfrak{f}_{66} \frac{\partial N_6}{\partial \varepsilon_2} = 0 \tag{3.67}$$

### 3.3.3 Derivation of $N_1 \sim N_6$ with Respect to $\varepsilon_3$

$$-\frac{qH^2}{6d_1}(\varepsilon_2^3 - \varepsilon_1^3) + \left[\frac{\beta}{3} + (\varepsilon_2 - \varepsilon_1) + 2\alpha(\varepsilon_2 - \varepsilon_1)\right]N_1 + [r(\varepsilon_2 - \varepsilon_1)]N_2 - \left[\frac{\beta}{6}\right]N_3 = 0 \quad (3.50)$$

gives

$$\mathfrak{f}_{11} \frac{\partial N_1}{\partial \varepsilon_3} + \mathfrak{f}_{12} \frac{\partial N_2}{\partial \varepsilon_3} + \mathfrak{f}_{13} \frac{\partial N_3}{\partial \varepsilon_3} = 0 \quad (3.68)$$

$$-\frac{rqH^2}{6d_1}(\varepsilon_2^3 - \varepsilon_1^3) + [r(\varepsilon_2 - \varepsilon_1)]N_1 + \left[\frac{r^3\beta}{3} + r^3(\varepsilon_2 - \varepsilon_1) + 2\alpha(\varepsilon_2 - \varepsilon_1)\right]N_2 - \left[\frac{r^3\beta}{6}\right]N_4 = 0 \quad (3.51)$$

gives

$$\mathfrak{f}_{21} \frac{\partial N_1}{\partial \varepsilon_3} + \mathfrak{f}_{22} \frac{\partial N_2}{\partial \varepsilon_3} + \mathfrak{f}_{24} \frac{\partial N_4}{\partial \varepsilon_3} = 0 \quad (3.69)$$

$$-\frac{qH^2}{6d_1}(\varepsilon_3^3 - \varepsilon_2^3) - \left[\frac{\beta}{6}\right]N_1 + \left[\frac{\beta}{3} + (\varepsilon_3 - \varepsilon_2) + 2\alpha(\varepsilon_3 - \varepsilon_2)\right]N_3 + [r(\varepsilon_3 - \varepsilon_2)]N_4 - \left[\frac{\beta}{6}\right]N_5 = 0 \quad (3.52)$$

gives

$$-\frac{qH^2}{2d_1}\varepsilon_3^2 + [1 + 2\alpha]N_3 + [r]N_4 + \mathfrak{f}_{31} \frac{\partial N_1}{\partial \varepsilon_3} + \mathfrak{f}_{33} \frac{\partial N_3}{\partial \varepsilon_3} + \mathfrak{f}_{34} \frac{\partial N_4}{\partial \varepsilon_3} + \mathfrak{f}_{35} \frac{\partial N_5}{\partial \varepsilon_3} = 0 \quad (3.70)$$

$$\begin{aligned}
& -\frac{rqH^2}{6d_1}(\varepsilon_3^3 - \varepsilon_2^3) - \left[\frac{r^3\beta}{6}\right]N_2 + [r(\varepsilon_3 - \varepsilon_2)]N_3 + \\
& \left[\frac{r^3\beta}{3} + r^2(\varepsilon_3 - \varepsilon_2) + 2\alpha(\varepsilon_3 - \varepsilon_2)\right]N_4 - \left[\frac{r^3\beta}{6}\right]N_6 = 0
\end{aligned} \tag{3.53}$$

gives

$$\begin{aligned}
& -\frac{rqH^2}{2d_1}\varepsilon_3^2 + [r]N_3 + [r^2 + 2\alpha]N_4 + \mathfrak{f}_{42} \frac{\partial N_2}{\partial \varepsilon_3} + \\
& \mathfrak{f}_{43} \frac{\partial N_3}{\partial \varepsilon_3} + \mathfrak{f}_{44} \frac{\partial N_4}{\partial \varepsilon_3} + \mathfrak{f}_{46} \frac{\partial N_6}{\partial \varepsilon_3} = 0
\end{aligned} \tag{3.71}$$

$$\begin{aligned}
& -\frac{qH^2}{6d_1}(1 - \varepsilon_3^3) - \left[\frac{\beta}{6}\right]N_3 + \\
& \left[\frac{\beta}{3} + (1 - \varepsilon_3) + 2\alpha(1 - \varepsilon_3)\right]N_5 + [r(1 - \varepsilon_3)]N_6 = 0
\end{aligned} \tag{3.54}$$

gives

$$\frac{qH^2}{2d_1}\varepsilon_3^2 - [1 + 2\alpha]N_5 - [r]N_6 + \mathfrak{f}_{53} \frac{\partial N_3}{\partial \varepsilon_3} + \mathfrak{f}_{55} \frac{\partial N_5}{\partial \varepsilon_3} + \mathfrak{f}_{56} \frac{\partial N_6}{\partial \varepsilon_3} = 0 \tag{3.72}$$

$$\begin{aligned}
& -\frac{rqH^2}{6d_1}(1 - \varepsilon_3^3) - \left[\frac{r^3\beta}{6}\right]N_4 + [r(1 - \varepsilon_3)]N_5 + \\
& \left[\frac{r^3\beta}{3} + r^2(1 - \varepsilon_3) + 2\alpha(1 - \varepsilon_3)\right]N_6 = 0
\end{aligned} \tag{3.55}$$

gives

$$\frac{rqH^2}{2d_1}\varepsilon_3^2 - [r]N_5 - [r^2 + 2\alpha]N_6 + \mathfrak{f}_{64} \frac{\partial N_4}{\partial \varepsilon_3} + \mathfrak{f}_{65} \frac{\partial N_5}{\partial \varepsilon_3} + \mathfrak{f}_{66} \frac{\partial N_6}{\partial \varepsilon_3} = 0 \tag{3.73}$$

### 3.3.4 Derivative of $\Delta_0$ with Respect to $x_1, x_2$ and $x_3$ , Respectively

From the above 3 parts, the derivatives of  $N_1, N_2, N_3, N_4, N_5$  and  $N_6$  with respect to  $\varepsilon_1, \varepsilon_2$  and  $\varepsilon_3$ , respectively, are expressed as follow in matrix form.

$$\begin{pmatrix} \frac{\partial N_1}{\partial \varepsilon_1} \\ \frac{\partial N_2}{\partial \varepsilon_1} \\ \frac{\partial N_3}{\partial \varepsilon_1} \\ \frac{\partial N_4}{\partial \varepsilon_1} \\ \frac{\partial N_5}{\partial \varepsilon_1} \\ \frac{\partial N_6}{\partial \varepsilon_1} \end{pmatrix} = \{f\}^{-1} \begin{pmatrix} -\frac{qH^2}{2d_1}\varepsilon_1^2 + [1 + 2\alpha]N_1 + [r]N_2 \\ -\frac{rqH^2}{2d_1}\varepsilon_1^2 + [r]N_1 + [r^2 + 2\alpha]N_2 \\ 0 \\ 0 \\ 0 \\ 0 \end{pmatrix} \quad (3.74)$$

$$\begin{pmatrix} \frac{\partial N_1}{\partial \varepsilon_2} \\ \frac{\partial N_2}{\partial \varepsilon_2} \\ \frac{\partial N_3}{\partial \varepsilon_2} \\ \frac{\partial N_4}{\partial \varepsilon_2} \\ \frac{\partial N_5}{\partial \varepsilon_2} \\ \frac{\partial N_6}{\partial \varepsilon_2} \end{pmatrix} = \{f\}^{-1} \begin{pmatrix} \frac{qH^2}{2d_1}\varepsilon_2^2 - [1 + 2\alpha]N_1 - [r]N_2 \\ \frac{rqH^2}{2d_1}\varepsilon_2^2 - [r]N_1 - [r^2 + 2\alpha]N_2 \\ -\frac{qH^2}{2d_1}\varepsilon_2^2 + [1 + 2\alpha]N_3 + [r]N_4 \\ -\frac{rqH^2}{2d_1}\varepsilon_2^2 + [r]N_3 + [r^2 + 2\alpha]N_4 \\ 0 \\ 0 \end{pmatrix} \quad (3.75)$$

$$\begin{pmatrix} \frac{\partial N_1}{\partial \varepsilon_3} \\ \frac{\partial N_2}{\partial \varepsilon_3} \\ \frac{\partial N_3}{\partial \varepsilon_3} \\ \frac{\partial N_4}{\partial \varepsilon_3} \\ \frac{\partial N_5}{\partial \varepsilon_3} \\ \frac{\partial N_6}{\partial \varepsilon_3} \end{pmatrix} = \{f\}^{-1} \begin{pmatrix} 0 \\ 0 \\ \frac{qH^2}{2d_1} \varepsilon_3^2 - [1 + 2\alpha]N_3 - [r]N_4 \\ \frac{rqH^2}{2d_1} \varepsilon_3^2 - [r]N_3 - [r^2 + 2\alpha]N_4 \\ -\frac{qH^2}{2d_1} \varepsilon_3^2 + [1 + 2\alpha]N_5 + [r]N_6 \\ -\frac{rqH^2}{2d_1} \varepsilon_3^2 + [r]N_5 + [r^2 + 2\alpha]N_6 \end{pmatrix} \quad (3.76)$$

Introducing the flexural rigidity ratio into equations (3.47) – (3.49), the optimum locations of the outriggers can be got from the following equation.

$$\begin{aligned} \frac{\partial \Delta_0}{\partial x_1} = & -\frac{d_1}{2EI} \left[ (x_2^2 - x_1^2) \frac{\partial N_1}{\partial x_1} - 2x_1 N_1 + (x_3^2 - x_2^2) \frac{\partial N_3}{\partial x_1} + (H^2 - x_3^2) \frac{\partial N_5}{\partial x_1} \right] - \\ & \frac{d_2}{2EI} \left[ (x_2^2 - x_1^2) \frac{\partial N_2}{\partial x_1} - 2x_1 N_2 + (x_3^2 - x_2^2) \frac{\partial N_4}{\partial x_1} + (H^2 - x_3^2) \frac{\partial N_6}{\partial x_1} \right] = 0 \end{aligned} \quad (3.47)$$

which becomes

$$\begin{aligned} & \left[ (\varepsilon_2^2 - \varepsilon_1^2) \frac{\partial N_1}{\partial \varepsilon_1} - 2\varepsilon_1 N_1 + (\varepsilon_3^2 - \varepsilon_2^2) \frac{\partial N_3}{\partial \varepsilon} + (H^2 - \varepsilon_3^2) \frac{\partial N_5}{\partial \varepsilon_1} \right] + \\ & r \left[ (\varepsilon_2^2 - \varepsilon_1^2) \frac{\partial N_2}{\partial \varepsilon_1} - 2\varepsilon_1 N_2 + (\varepsilon_3^2 - \varepsilon_2^2) \frac{\partial N_4}{\partial \varepsilon_1} + (H^2 - \varepsilon_3^2) \frac{\partial N_6}{\partial \varepsilon_1} \right] = 0 \end{aligned} \quad (3.77)$$

$$\begin{aligned}
\frac{\partial \Delta_0}{\partial x_2} = & -\frac{d_1}{2EI} [(x_2^2 - x_1^2) \frac{\partial N_1}{\partial x_2} + 2x_2 N_1 + \\
& (x_3^2 - x_2^2) \frac{\partial N_3}{\partial x_2} - 2x_2 N_3 + (H^2 - x_3^2) \frac{\partial N_5}{\partial x_2}] - \\
& \frac{d_2}{2EI} [(x_2^2 - x_1^2) \frac{\partial N_2}{\partial x_2} + 2x_2 N_2 + (x_3^2 - x_2^2) \frac{\partial N_4}{\partial x_2} - \\
& 2x_2 N_4 + (H^2 - x_3^2) \frac{\partial N_6}{\partial x_2}] = 0
\end{aligned} \tag{3.48}$$

which becomes

$$\begin{aligned}
& \left[ (\varepsilon_2^2 - \varepsilon_1^2) \frac{\partial N_1}{\partial \varepsilon_2} + 2\varepsilon_2 N_1 + (\varepsilon_3^2 - \varepsilon_2^2) \frac{\partial N_3}{\partial \varepsilon_2} - 2\varepsilon_2 N_3 + (1 - \varepsilon_3^2) \frac{\partial N_5}{\partial \varepsilon_2} \right] + \\
& r \left[ (\varepsilon_2^2 - \varepsilon_1^2) \frac{\partial N_2}{\partial \varepsilon_2} + 2\varepsilon_2 N_2 + (\varepsilon_3^2 - \varepsilon_2^2) \frac{\partial N_4}{\partial \varepsilon_2} - 2\varepsilon_2 N_4 + (1 - \varepsilon_3^2) \frac{\partial N_6}{\partial \varepsilon_2} \right] = 0
\end{aligned} \tag{3.78}$$

$$\begin{aligned}
\frac{\partial \Delta_0}{\partial x_3} = & -\frac{d_1}{2EI} [(x_2^2 - x_1^2) \frac{\partial N_1}{\partial x_3} + (x_3^2 - x_2^2) \frac{\partial N_3}{\partial x_3} + \\
& 2x_2 N_3 + (H^2 - x_3^2) \frac{\partial N_5}{\partial x_3} - 2x_3 N_5] - \\
& \frac{d_2}{2EI} [(x_2^2 - x_1^2) \frac{\partial N_2}{\partial x_3} + (x_3^2 - x_2^2) \frac{\partial N_4}{\partial x_3} + 2x_3 N_4 + \\
& (H^2 - x_3^2) \frac{\partial N_6}{\partial x_3} - 2x_1 N_6] = 0
\end{aligned} \tag{3.49}$$

which becomes

$$\begin{aligned}
& \left[ (\varepsilon_2^2 - \varepsilon_1^2) \frac{\partial N_1}{\partial \varepsilon_3} + (\varepsilon_3^2 - \varepsilon_2^2) \frac{\partial N_3}{\partial \varepsilon_3} + 2\varepsilon_2 N_3 + (1 - \varepsilon_3^2) \frac{\partial N_5}{\partial \varepsilon_3} - 2\varepsilon_3 N_5 \right] + \\
& r \left[ (\varepsilon_2^2 - \varepsilon_1^2) \frac{\partial N_2}{\partial \varepsilon_3} + (\varepsilon_3^2 - \varepsilon_2^2) \frac{\partial N_4}{\partial \varepsilon_3} + 2\varepsilon_3 N_4 + (1 - \varepsilon_3^2) \frac{\partial N_6}{\partial \varepsilon_3} - 2\varepsilon_1 N_6 \right] = 0
\end{aligned} \tag{3.79}$$

### 3.4 Solution Procedure for the Optimum Locations of Outriggers of Unsymmetrical Structure

In order to obtain the numerical results of  $\varepsilon_1$ ,  $\varepsilon_2$  and  $\varepsilon_3$  from equations (3.76), (3.77) and (3.78), computer program coded in Matlab is adopted. The solution procedure is as follows.

- I. Set the initial value for  $r$ ;
- II. Calculate  $\{N\}$  values from the equation  $\{N\} = \{f\}^{-1}\{\Delta\}$ , or equations (3.35) – (3.41)
- III. Calculate  $\left\{\frac{\partial N}{\partial \varepsilon_1}\right\}$  values from the equation  $\left\{\frac{\partial N}{\partial \varepsilon_1}\right\} = \{f\}^{-1}\left\{\frac{\partial \Delta}{\partial \varepsilon_1}\right\}$  or equations (3.56) – (3.61) and (3.74)
- IV. Calculate  $\left\{\frac{\partial N}{\partial \varepsilon_2}\right\}$  values from the equation  $\left\{\frac{\partial N}{\partial \varepsilon_2}\right\} = \{f\}^{-1}\left\{\frac{\partial \Delta}{\partial \varepsilon_2}\right\}$  or equations (3.62) – (3.67) and (3.75)
- V. Calculate  $\left\{\frac{\partial N}{\partial \varepsilon_3}\right\}$  values from the equation  $\left\{\frac{\partial N}{\partial \varepsilon_3}\right\} = \{f\}^{-1}\left\{\frac{\partial \Delta}{\partial \varepsilon_3}\right\}$  or equations (3.68) – (3.73) and (3.76)
- VI. Use Newton's method to solves the equation  $\frac{\partial \Delta_0}{\partial \varepsilon_1} = 0, \frac{\partial \Delta_0}{\partial \varepsilon_2} = 0, \frac{\partial \Delta_0}{\partial \varepsilon_3} = 0$  equations (3.77) – (3.79) in order to get the values of  $\varepsilon_1$ ,  $\varepsilon_2$  and  $\varepsilon_3$  with different  $r$  values, respectively.

The codes of the computer program for optimum outrigger locations are validated when  $r = 0.9999 \approx 1$ . It's because the results of the program for analyzing the  $\varepsilon$  in three-stories unsymmetrical outrigger-braced structure all equal to the results of three-stories symmetrical outrigger-braced structure as shown in Fig. 2.8 which is adapted from Smith and Coull (1911).



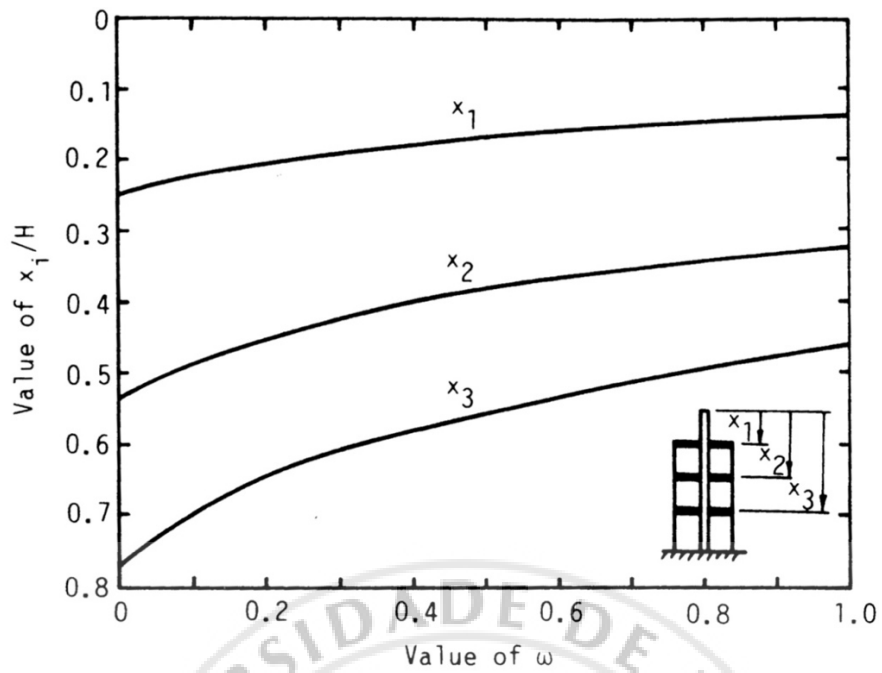


Figure 2.8 Optimum outrigger locations for three-outrigger structure

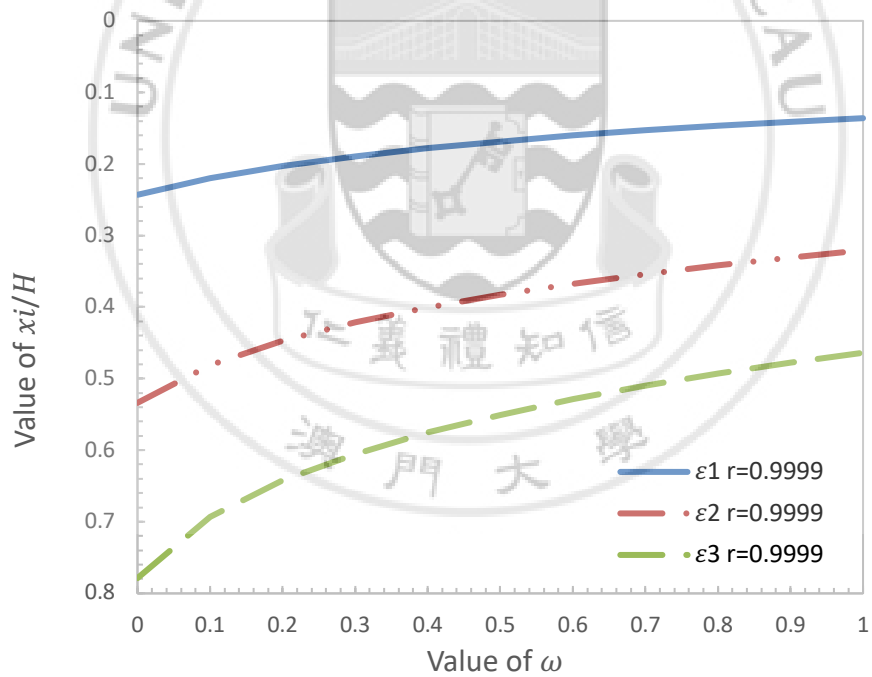


Figure 3.13 Optimum location of three-stories unsymmetrical outrigger-braced structure

( $r = 0.9999 \approx 1$ )

Comparing to Fig.2.8 and Fig.3.8, they are almost the same. Therefore, the codes of computer program are verified, and it is used for the analysis in the following. In addition, the derived equations for unsymmetrical structure can be reduced to those of symmetrical structure when  $r = 1$ .



## CHAPTER 4 NUMERICAL ANALYSIS

### 4.1 Introduction

The optimum locations can be obtained for given  $r$  and  $\omega$ . In this chapter, the numerical analysis, results comparisons and discussions are presented in the following.

### 4.2 Comparing with Different Values of $r$

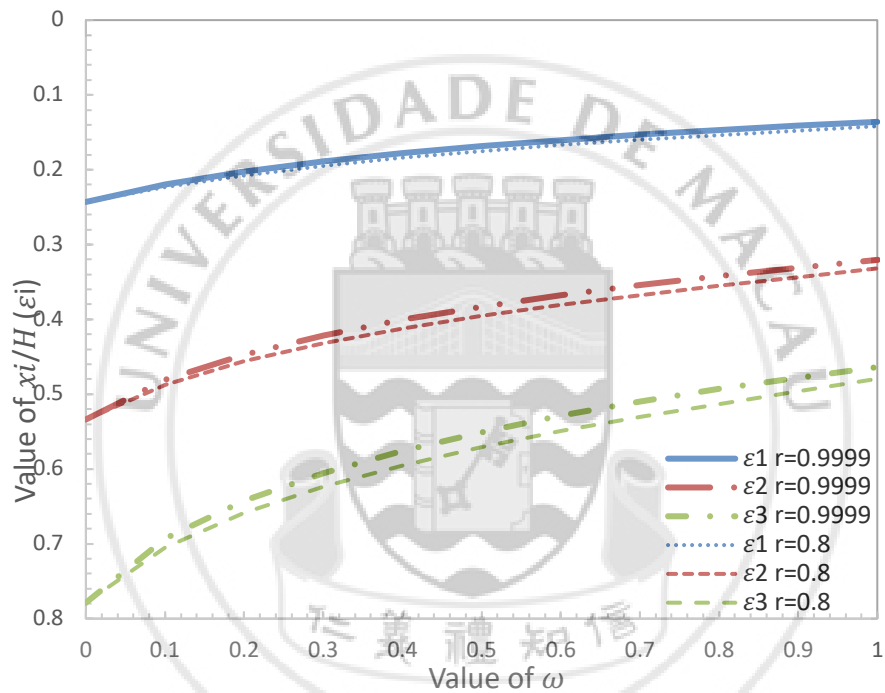


Figure 4.1 Optimum outrigger locations of three-stories unsymmetrical outrigger-braced structure comparing for  $r$  being 0.9999 and 0.8, respectively

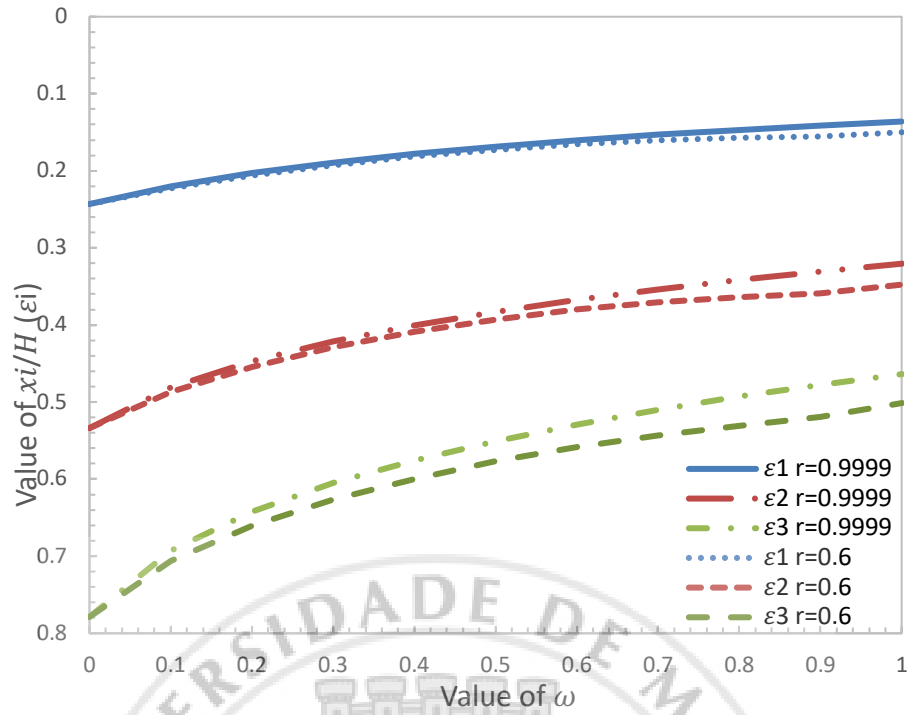


Figure 4.2 Optimum outrigger locations of three-stories unsymmetrical outrigger-braced structure comparing for  $r$  being 0.9999 and 0.6, respectively

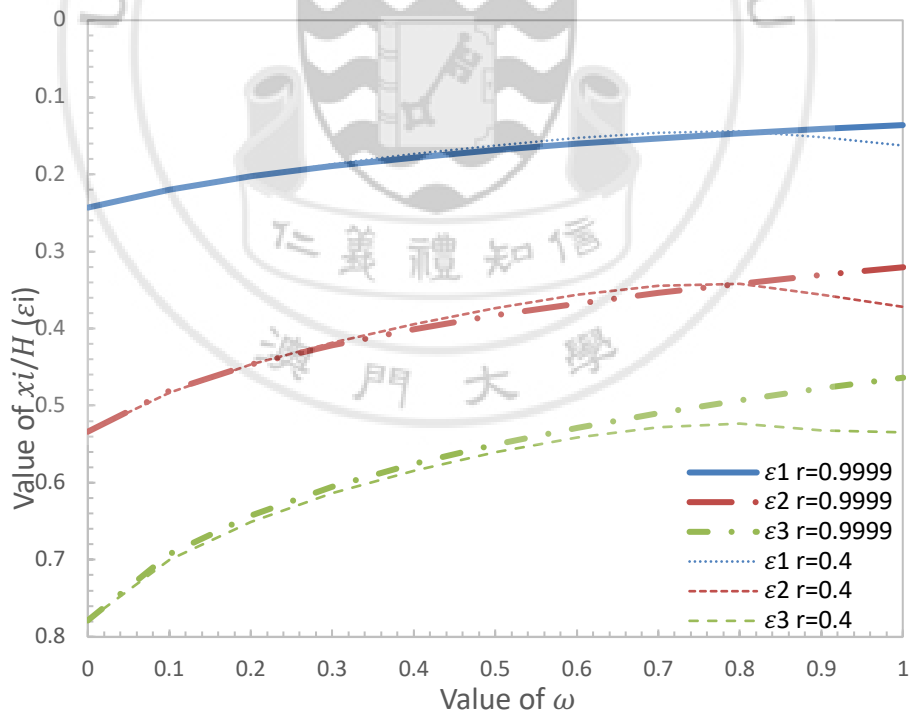


Figure 4.3 Optimum outrigger locations of three-stories unsymmetrical outrigger-braced structure comparing for  $r$  being 0.9999 and 0.4, respectively

#### ***4.2.1 Summary of Comparing with Different Values of $r$***

The aims is to compare the results with different values of  $r$ .

1. For given value of  $r=0.9999$ , the values of  $\varepsilon_1$ ,  $\varepsilon_2$  and  $\varepsilon_3$  are similar or smaller than those when  $r=0.8$  and  $r=0.6$  as shown in Fig.4.1 and Fig.4.2.
2. For given value of  $r=0.4$ , the values of  $\varepsilon_1$ ,  $\varepsilon_2$  and  $\varepsilon_3$  are smaller than those when  $r=0.4$  at some points as shown in Fig.4.3.



### 4.3 Numerical Results for Different Values of $r$

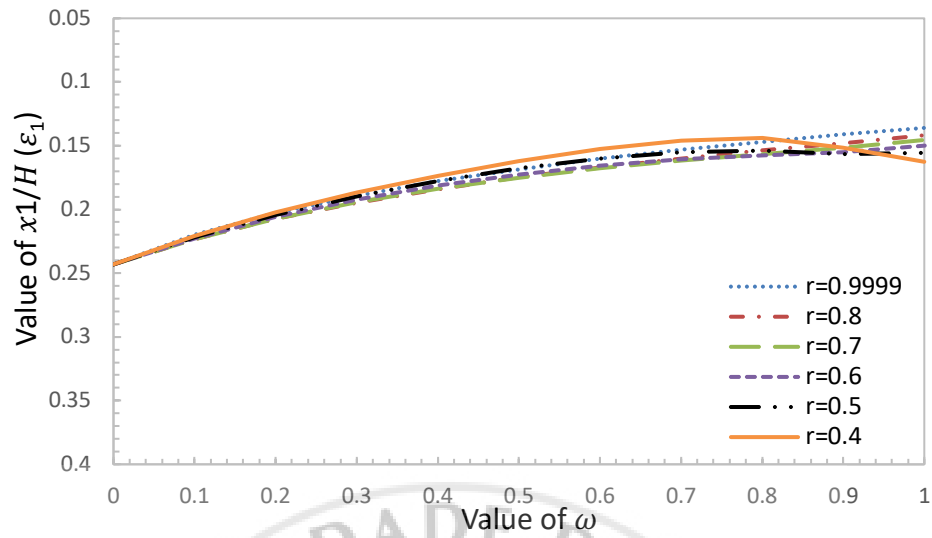


Figure 4.4 Optimum outrigger locations of the **third** story in three-stories unsymmetrical outrigger-braced structure for different values of  $r$  shown in  $\omega$  vs  $\varepsilon_1$

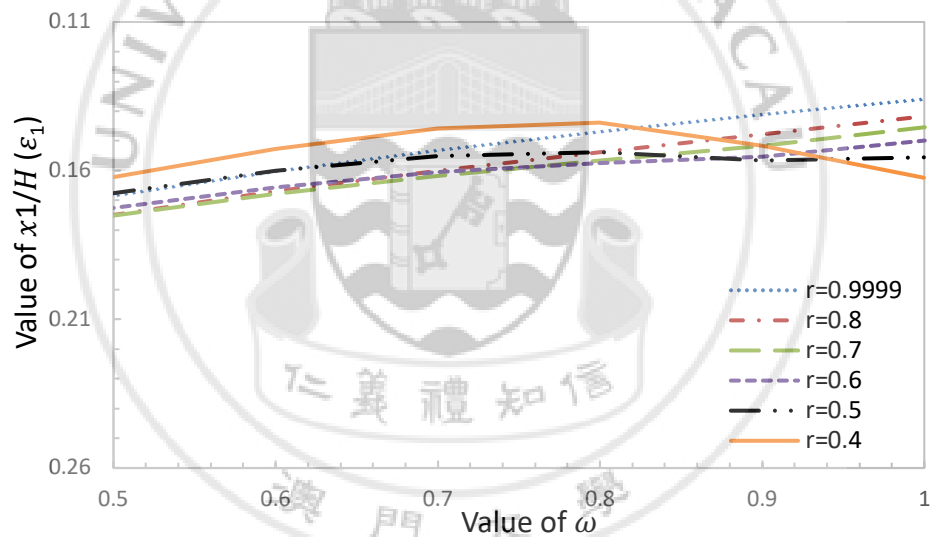


Figure 4.5 Amplification of Fig 4.4

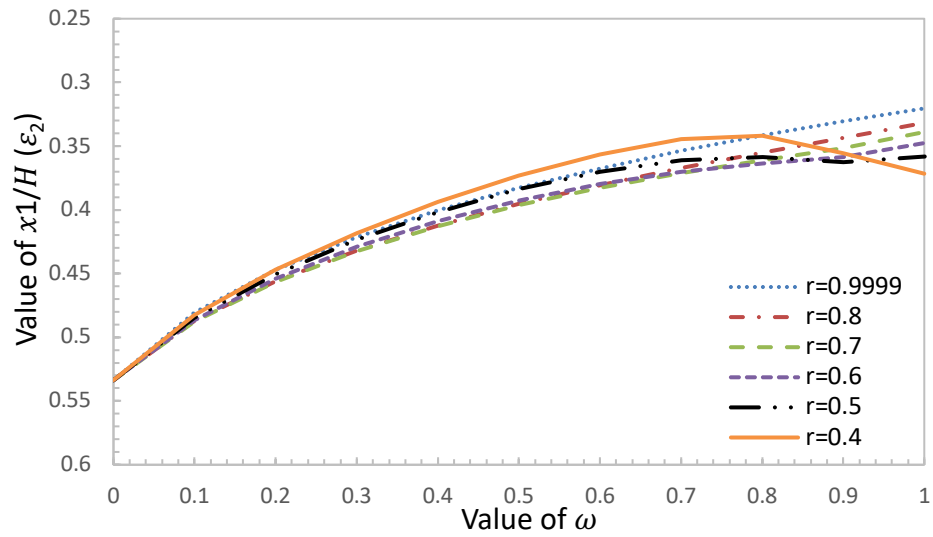


Figure 4.6 Optimum outrigger locations of the second story in three-stories unsymmetrical outrigger-braced structure for different values of  $r$  shown in  $\omega$  vs  $\varepsilon_2$

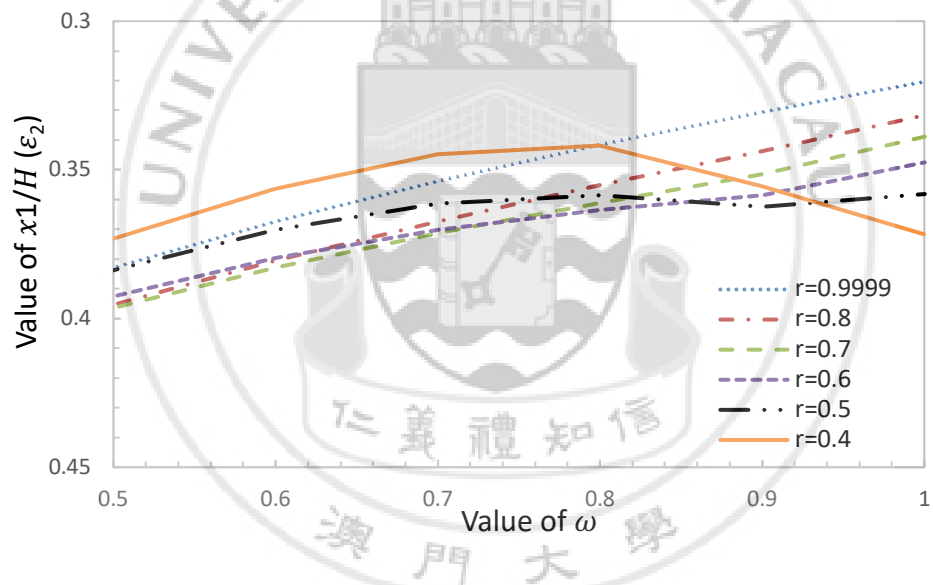


Figure 4.7 Amplification of Fig 4.6

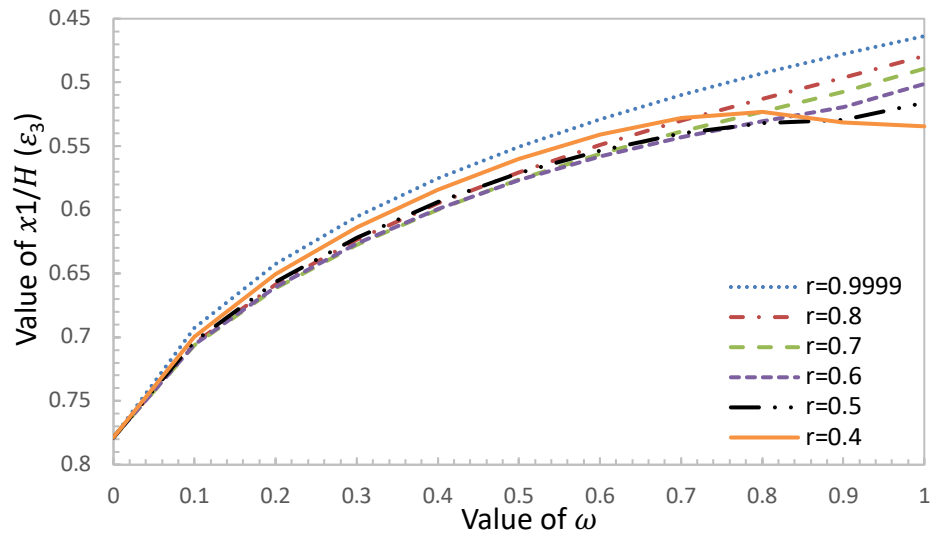


Figure 4.8 Optimum outrigger locations of the first story in three-stories unsymmetrical outrigger-braced structure for different values of  $r$  shown in  $\omega$  vs  $\varepsilon_3$

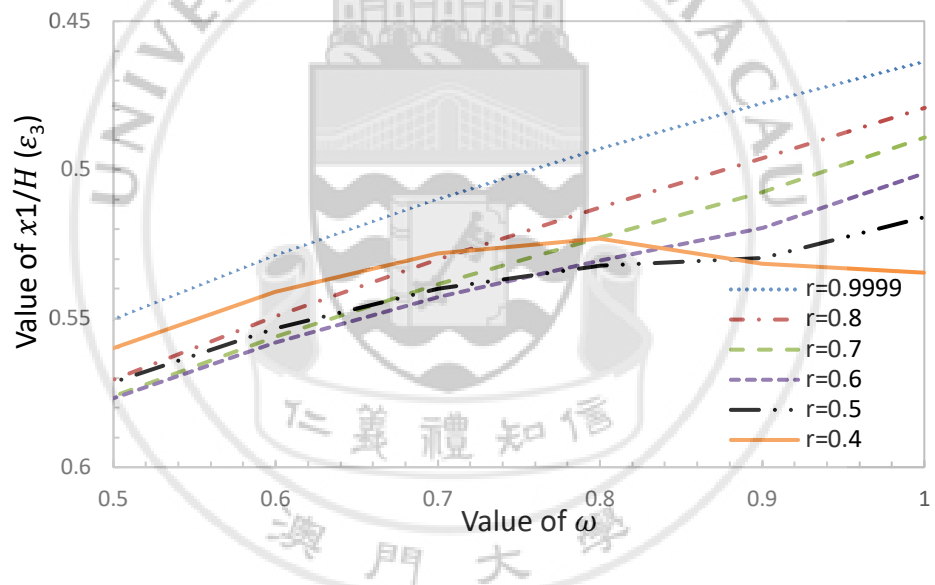


Figure 4.9 Amplification of Fig 4.8



#### 4.3.1 Summary of Numerical Results for Different Values of $r$

The aim of this part is to compare the numerical results for different values of  $r$ .

1. For given values of  $r=0.9999$ ,  $r=0.8$ , and  $r=0.7$ ,  $\varepsilon_1$ ,  $\varepsilon_2$  and  $\varepsilon_3$  decrease as  $\omega$  increases.  
Furthermore, for given values of  $r=0.6$ ,  $r=0.5$  and  $r=0.4$ ,  $\varepsilon_1$ ,  $\varepsilon_2$  and  $\varepsilon_3$  have critical values and the results are shown in Fig.4.4, Fig.4.6 and Fig.4.8.
2. Fig.4.5 shows that  $\varepsilon_1$  increases as  $r$  decreases for  $r=0.9999$ ,  $r=0.8$  and  $r=0.7$ . On the other hand,  $\varepsilon_1$  increases as  $r$  increases for  $r=0.7$ ,  $r=0.6$ ,  $r=0.5$  and  $r=0.4$  at some points. In addition, it shows that the  $\varepsilon_1$  at  $r=0.7$  and  $r=0.6$  makes the first crossing point. The performance is same for the result of  $\varepsilon_2$  as shown in Fig.4.7.
3. Fig.4.9 shows that  $\varepsilon_3$  increases as  $r$  decreases for  $r=0.9999$ ,  $r=0.8$ ,  $r=0.7$  and  $r=0.6$ . On the other hand,  $\varepsilon_3$  increases as  $r$  increases for  $r=0.6$ ,  $r=0.5$  and  $r=0.4$  at some points. In addition, it shows that the  $\varepsilon_3$  at  $r=0.6$  and  $r=0.5$  makes the first crossing point.
4. According to I, II and III, the stability increases with the value of  $r$  increases.

#### 4.4 Numerical Results for Different Values of $\beta$

The value of  $\omega$  influenced by the value of  $\beta$ , the comparisons of different results of  $r$  are shown in the following.

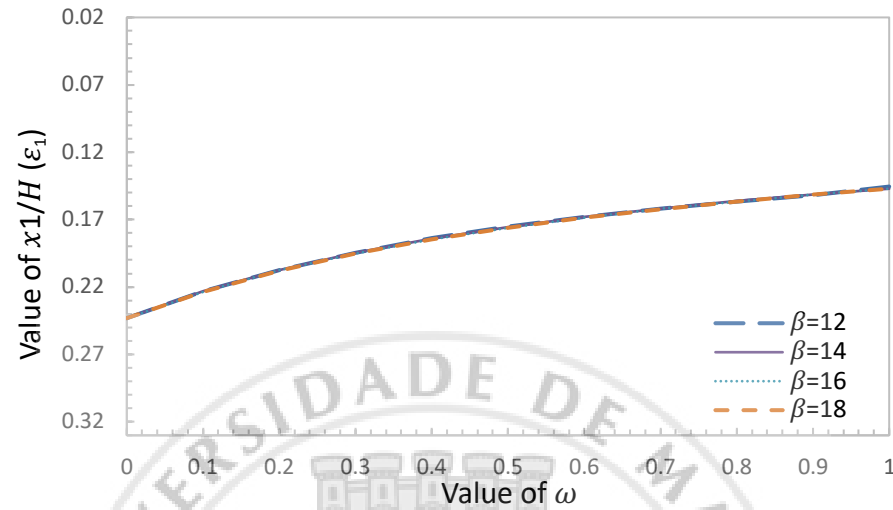


Figure 4.10 Optimum outrigger locations of the **third** story in three-stories unsymmetrical outrigger-braced structure for different values of  $\beta$  shown in  $\omega$  vs  $\epsilon_1$  when  $r=0.7$

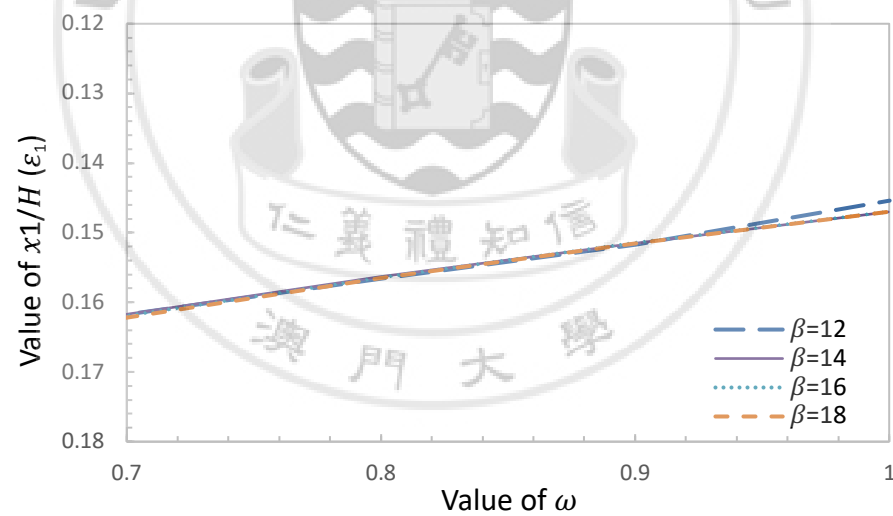


Figure 4.11 Amplification of Fig 4.10

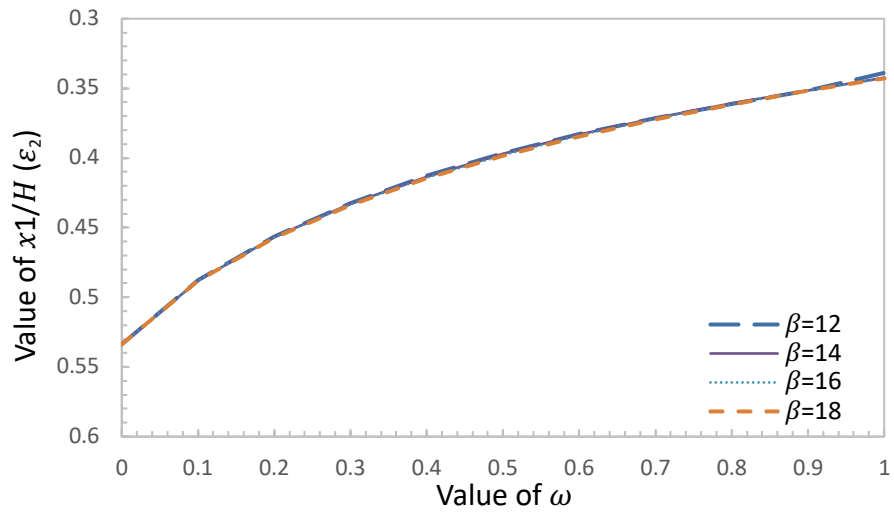


Figure 4.12 Optimum outrigger locations of the **second** story in three-stories unsymmetrical outrigger-braced structure for different values of  $\beta$  shown in  $\omega$  vs  $\epsilon_1$  when  $r=0.7$

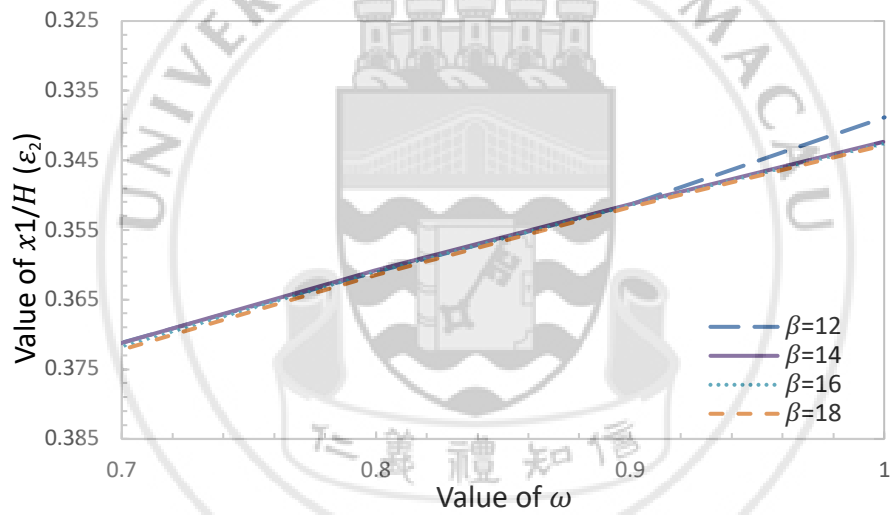


Figure 4.13 Amplification of Fig 4.12

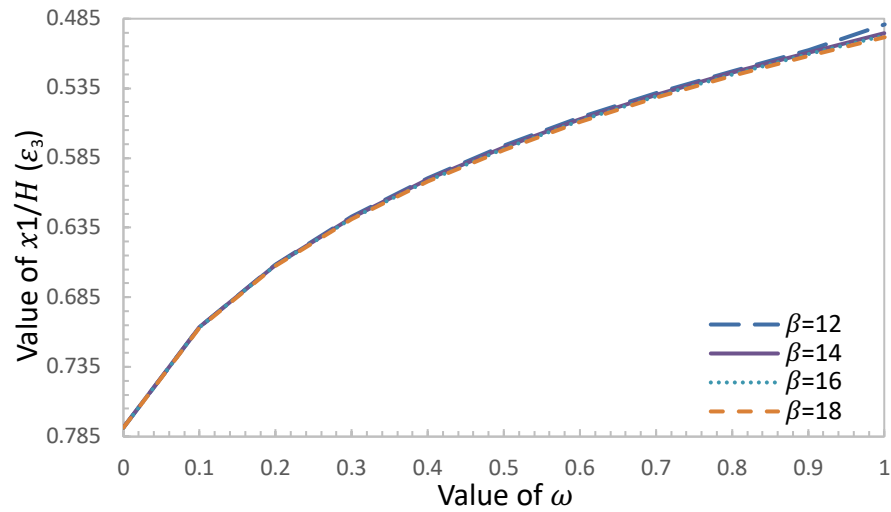


Figure 4.14 Optimum outrigger locations of the **first** story in three-stories unsymmetrical outrigger-braced structure for different values of  $\beta$  shown in  $\omega$  vs  $\varepsilon_1$  when  $r=0.7$

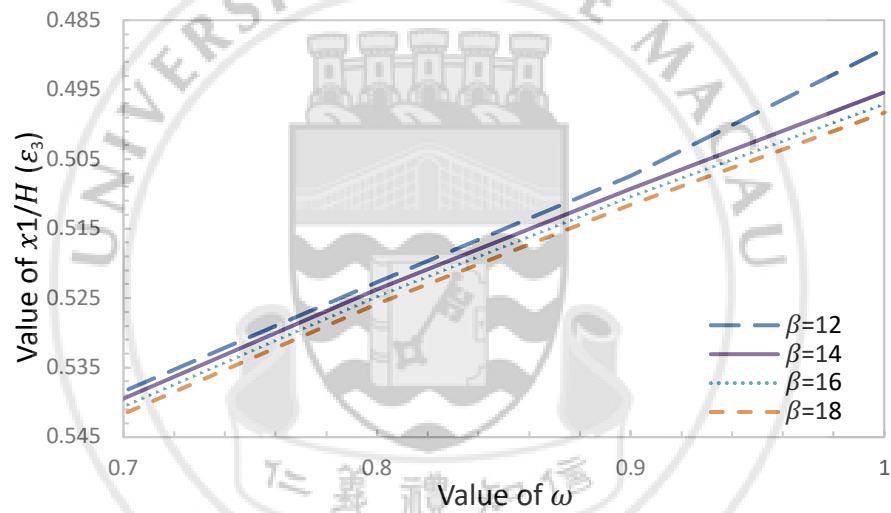


Figure 4.15 Amplification of Fig 4.14

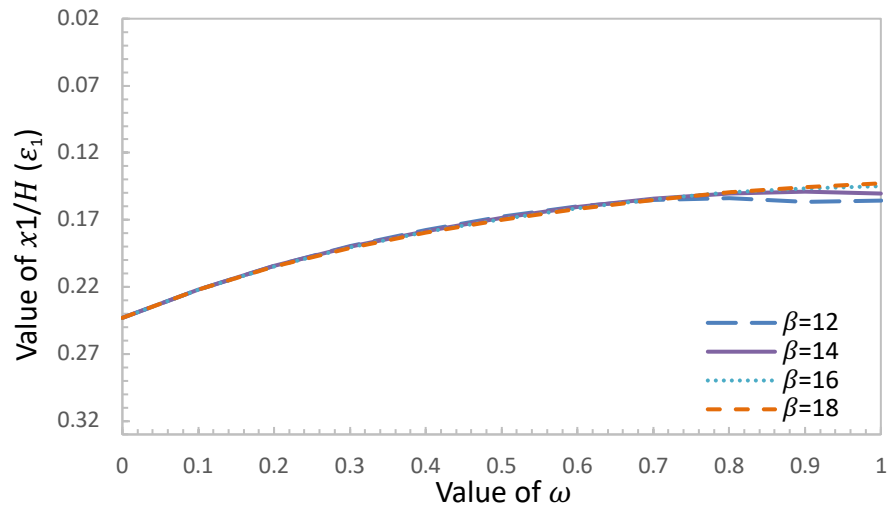


Figure 4.16 Optimum outrigger locations of the **third** story in three-stories unsymmetrical outrigger-braced structure for different values of  $\beta$  shown in  $\omega$  vs  $\varepsilon_1$  when  $r=0.5$

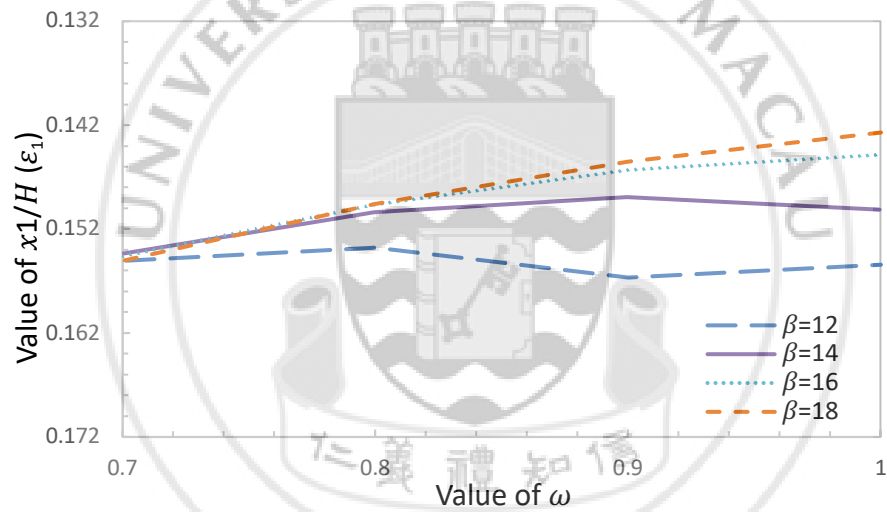


Figure 4.17 Amplification of Fig 4.16

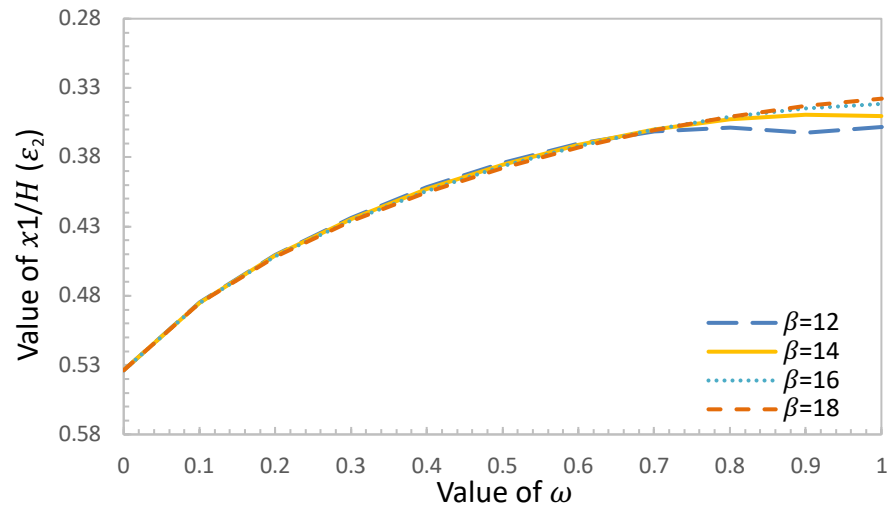


Figure 4.18 Optimum outrigger locations of the **second** story in three-stories unsymmetrical outrigger-braced structure for different values of  $\beta$  shown in  $\omega$  vs  $\epsilon_1$  when  $r=0.5$

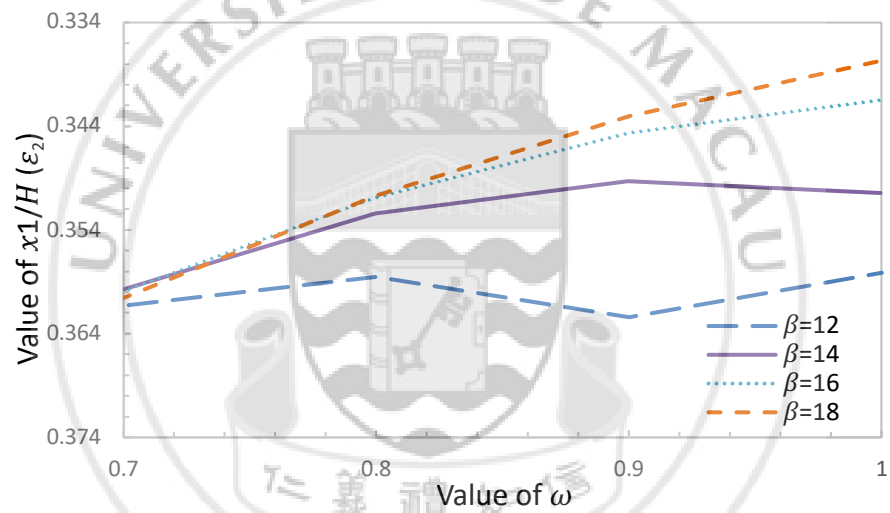


Figure 4.19 Amplification of Fig 4.18

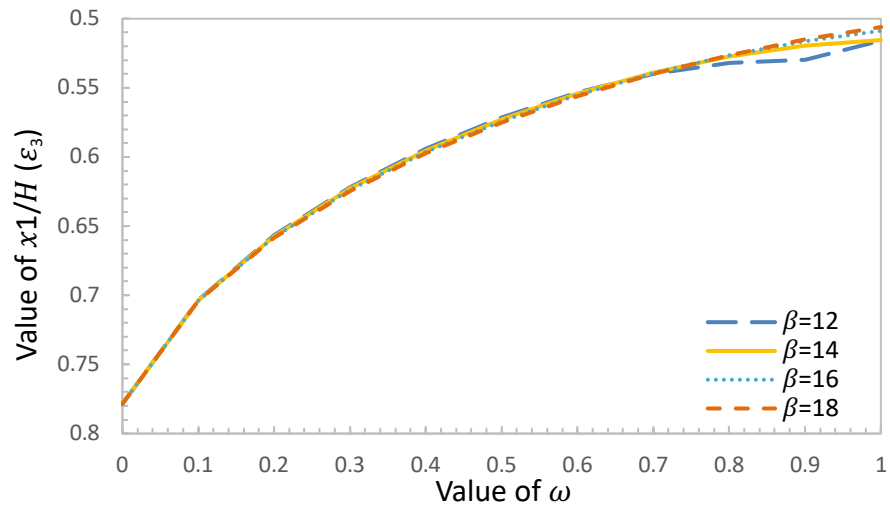


Figure 4.20 Optimum outrigger locations of the **first** story in three-stories unsymmetrical outrigger-braced structure for different values of  $\beta$  shown in  $\omega$  vs  $\epsilon_1$  when  $r=0.5$

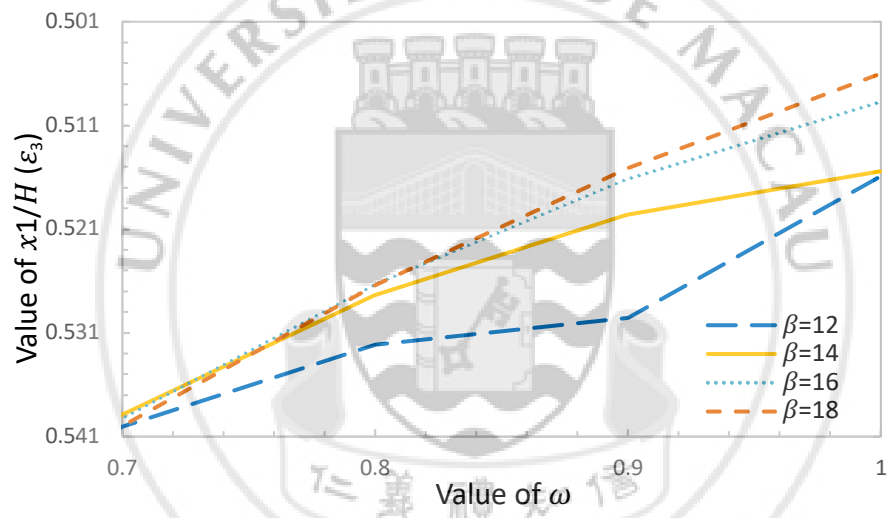
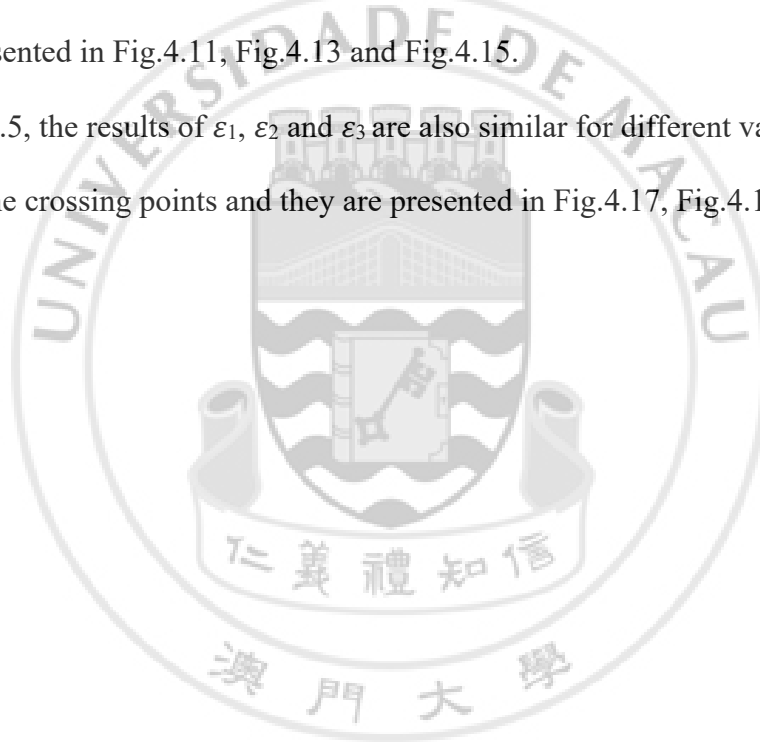


Figure 4.21 Amplification of Fig 4.20

#### 4.4.1 Summary of Numerical Results for Different Values of $\beta$

The aim of this part is to compare the numerical results for different values of  $\beta$

1. When  $r=0.7$ , for given values of  $\beta=18, \beta=16, \beta=14$  and  $\beta=12$ ,  $\varepsilon_1, \varepsilon_2$  and  $\varepsilon_3$  decrease while  $\omega$  increases. The results are shown in Fig.4.10, Fig.4.12 and Fig.4.14. On the other hand, when  $r=0.5$ , for given values of  $\beta=18$  and  $\beta=16$ ,  $\varepsilon_1, \varepsilon_2$  and  $\varepsilon_3$  decrease while  $\omega$  increases. Furthermore, for given values of  $\beta=14$  and  $\beta=12$ ,  $\varepsilon_1, \varepsilon_2$  and  $\varepsilon_3$  have critical points and the results are shown in Fig.4.16, Fig.4.18 and Fig.4.20.
2. For  $r=0.7$ , the results of  $\varepsilon_1, \varepsilon_2$  and  $\varepsilon_3$  are very similar for different values of  $\beta$ . They are presented in Fig.4.11, Fig.4.13 and Fig.4.15.
3. For  $r=0.5$ , the results of  $\varepsilon_1, \varepsilon_2$  and  $\varepsilon_3$  are also similar for different values of  $\beta$ . There are some crossing points and they are presented in Fig.4.17, Fig.4.19 and Fig.4.21.





#### 4.5 Numerical Results for Different Values of $\alpha$

The value of  $\omega$  is influenced by the value of  $\alpha$ . The comparisons of the results with different values of  $r$  are shown in the following.

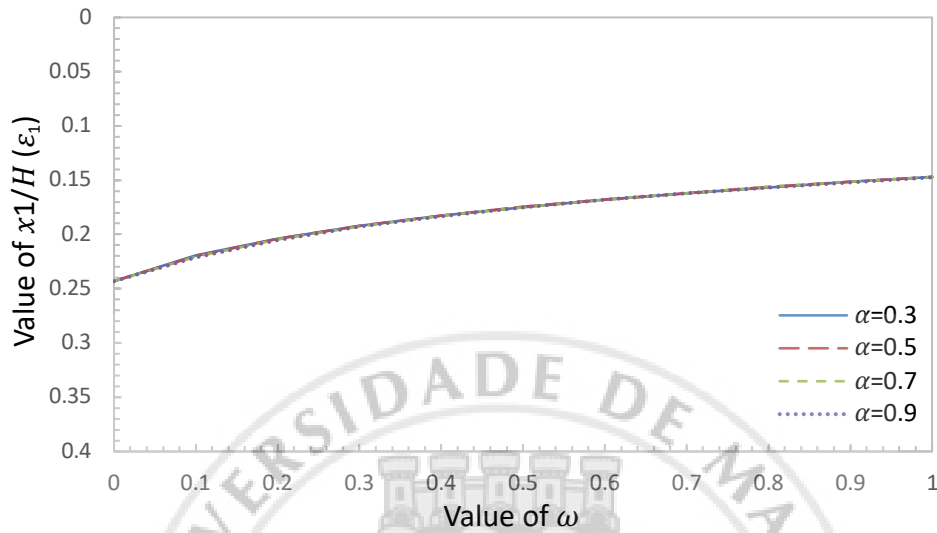


Figure 4.0.22 Optimum outrigger locations of the **third** story in three-stories unsymmetrical outrigger-braced structure for different values of  $\alpha$  shown in  $\omega$  vs  $\epsilon_1$  when  $r=0.7$

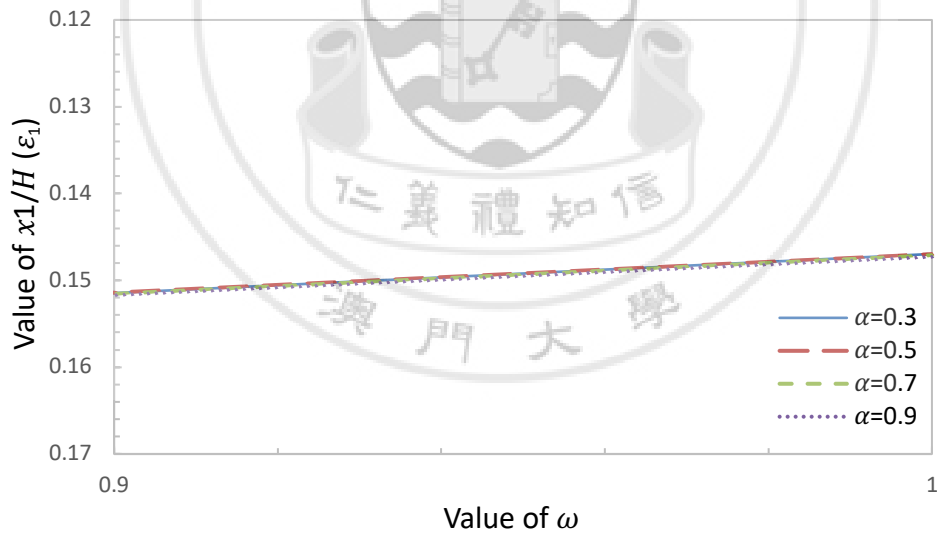


Figure 4.23 Amplification of Fig 4.22

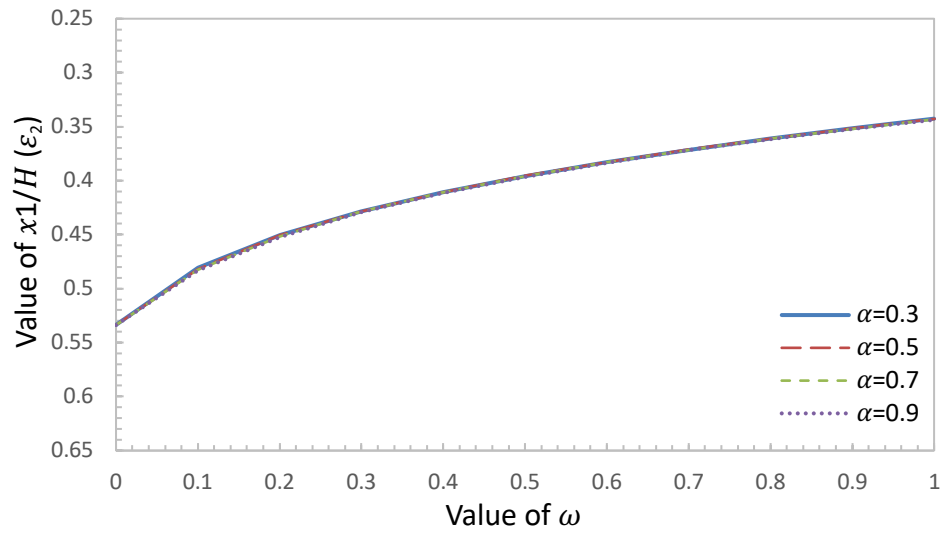


Figure 4.24 Optimum outrigger locations of the **second** story in three-stories unsymmetrical outrigger-braced structure for different values of  $\alpha$  shown in  $\omega$  vs  $\epsilon_1$  when  $r=0.7$

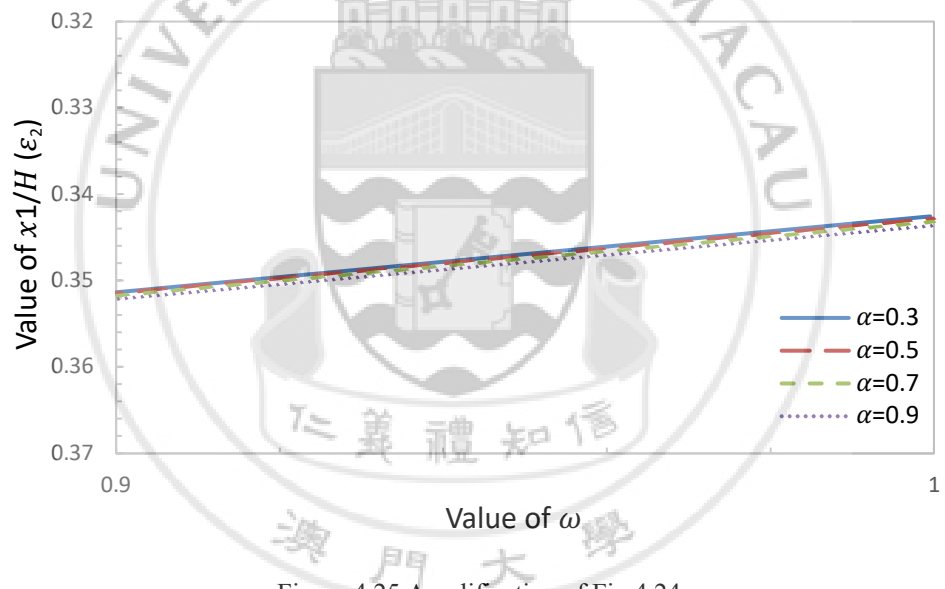


Figure 4.25 Amplification of Fig 4.24

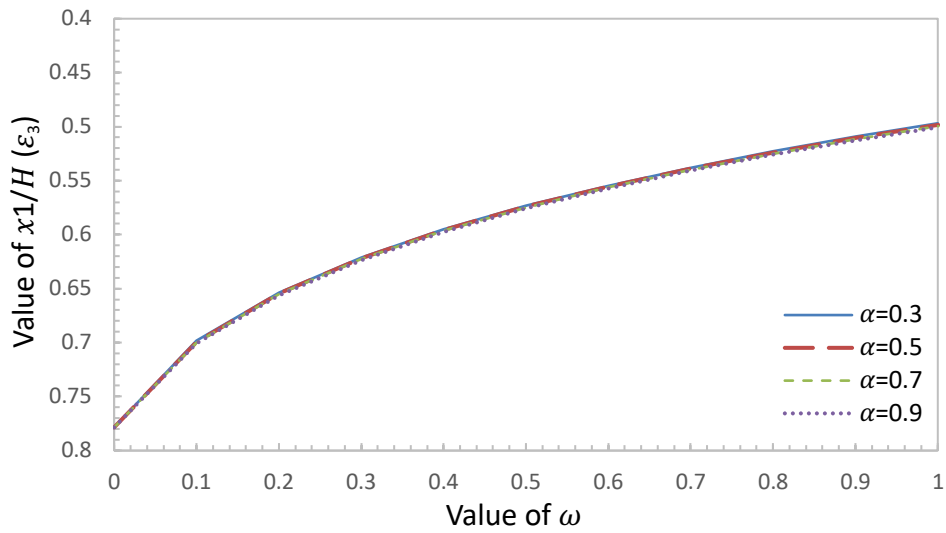


Figure 4.26 Optimum outrigger locations of the **first** story in three-stories unsymmetrical outrigger-braced structure for different values of  $\alpha$  shown in  $\omega$  vs  $\epsilon_1$  when  $r=0.7$

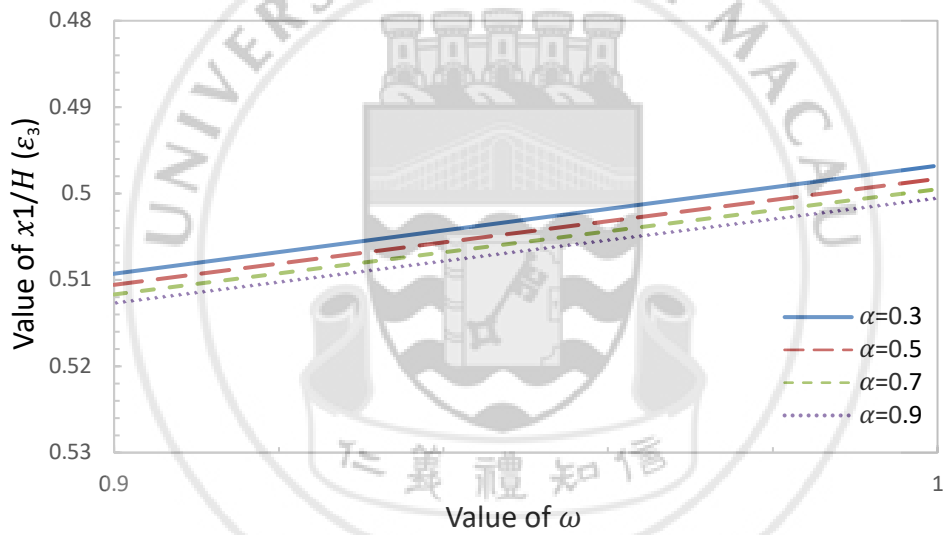


Figure 4.27 Amplification of Fig 4.26

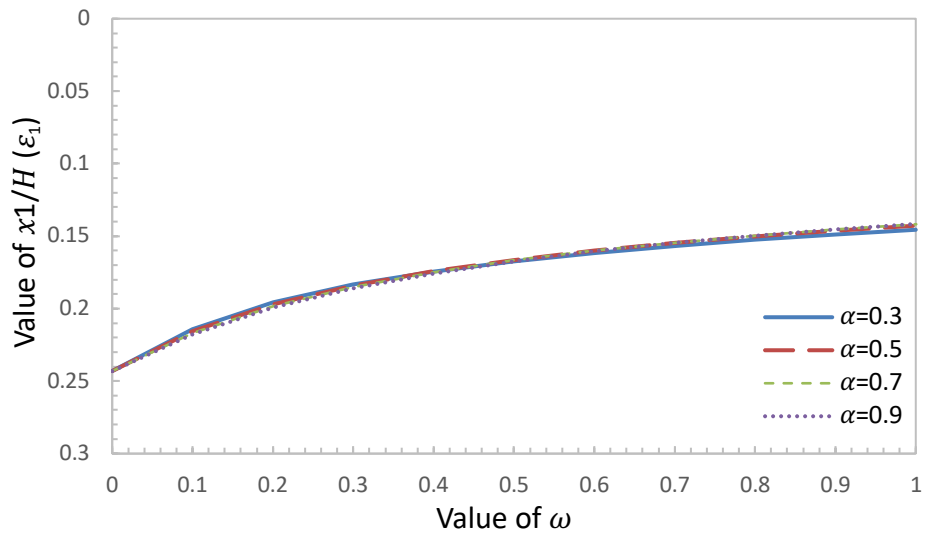


Figure 4.28 Optimum outrigger locations of the **third** story in three-stories unsymmetrical outrigger-braced structure for different values of  $\alpha$  shown in  $\omega$  vs  $\epsilon_1$  when  $r=0.5$

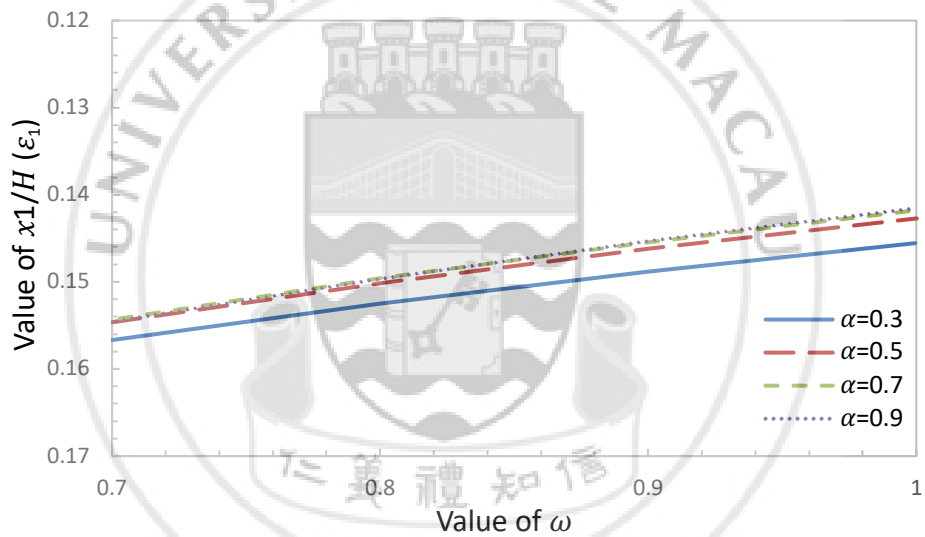


Figure 4.29 Amplification of Fig 4.28

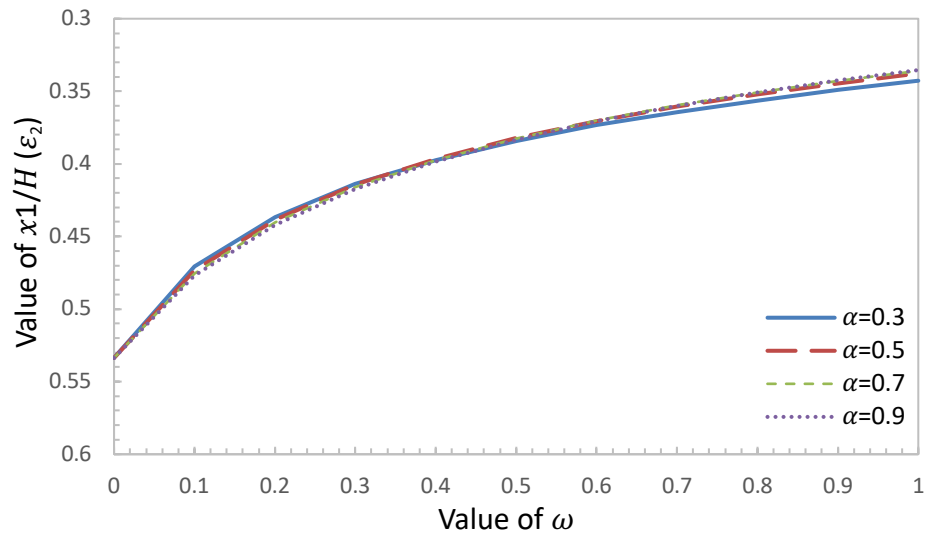


Figure 4.30 Optimum outrigger locations of the **second** story in three-stories unsymmetrical outrigger-braced structure for different values of  $\alpha$  shown in  $\omega$  vs  $\varepsilon_1$  when  $r=0.5$

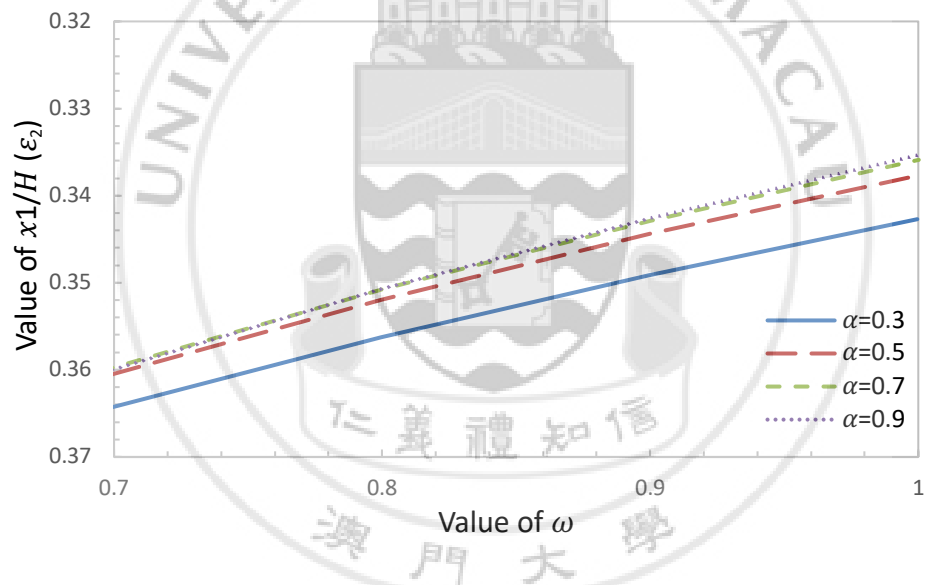


Figure 4.31 Amplification of Fig 4.30

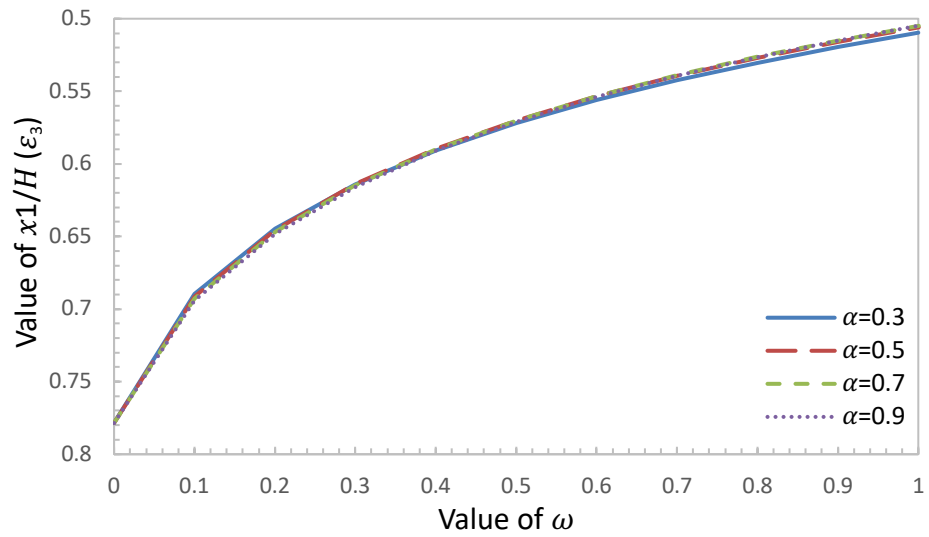


Figure 4.32 Optimum outrigger locations of the **first** story in three-stories unsymmetrical outrigger-braced structure for different values of  $\alpha$  shown in  $\omega$  vs  $\epsilon_1$  when  $r=0.5$

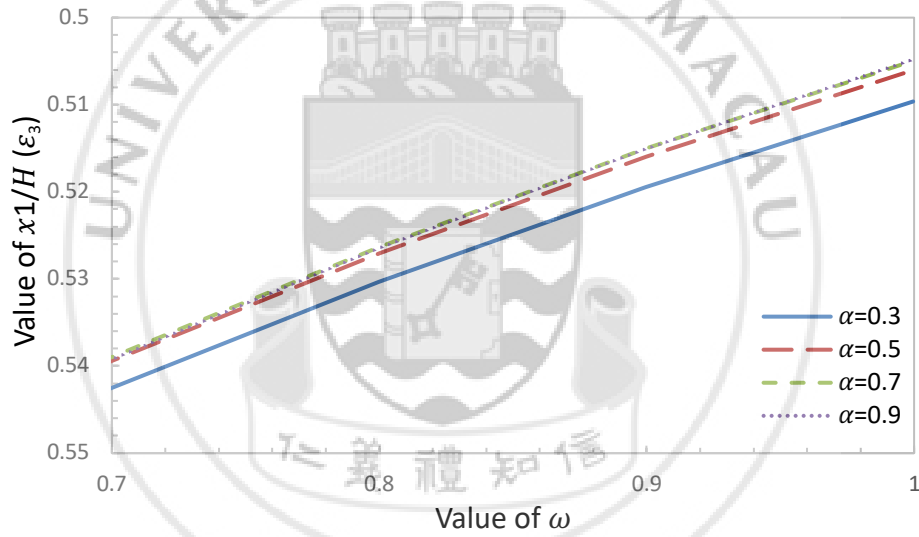
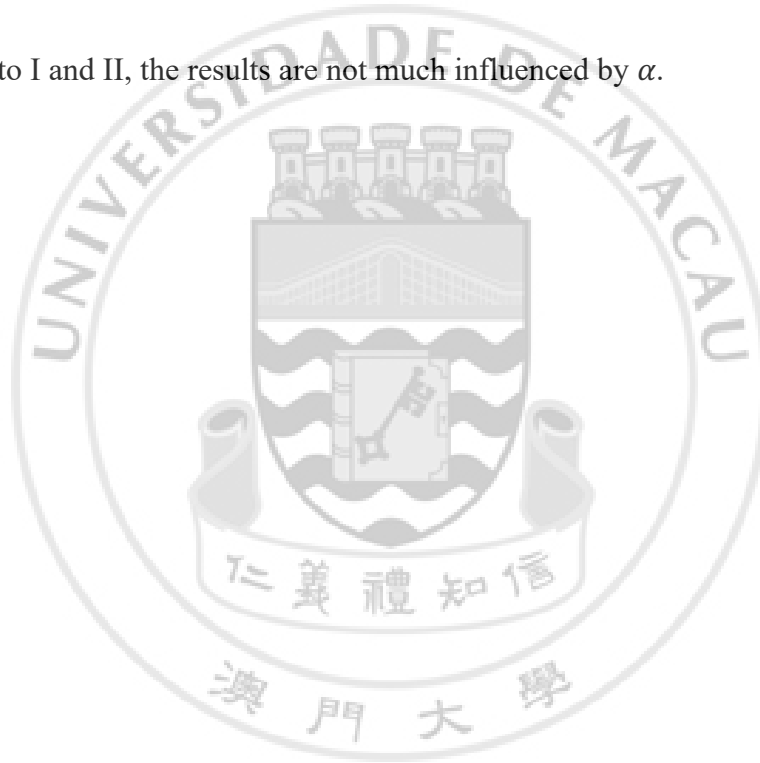


Figure 4.33 Amplification of Fig 4.32

#### 4.5.1 Summary of Numerical Results for Different Values of $\alpha$

The aim of this part is to compare the numerical results for different values of  $\alpha$ .

1. When  $r=0.7$  and  $r=0.5$ , for given values of  $\alpha=0.9$ ,  $\alpha=0.7$ ,  $\alpha=0.5$  and  $\alpha=0.3$ ,  $\varepsilon_1$ ,  $\varepsilon_2$  and  $\varepsilon_3$  decrease as  $\omega$  increases. The results are shown in Fig.4.22, Fig.4.24, Fig.4.26, Fig.4.28, Fig.4.30 and Fig.4.32.
2. For  $r=0.7$  and  $r=0.5$ , the results of  $\varepsilon_1$ ,  $\varepsilon_2$  and  $\varepsilon_3$  are very similar for different values of  $\alpha$ . They are presented in Fig.4.23, Fig.4.25, Fig.4.27, Fig.4.29, Fig.4.31 and Fig.4.33.
3. According to I and II, the results are not much influenced by  $\alpha$ .



## **CHAPTER 5 Conclusions and Final Remarks**

### **5.1 Summary**

This project aims to get the relationship between the optimum locations and the mechanical properties of the unsymmetrical three-stories outrigger-braced structure. Also, this is a topic that was not studied in the past.

There are the following three steps in the analysis.:

1. The governing equations about the compatibility of columns' axial deformation are derived based on the idea proposed by Er and Lu (2009), which is the improved version of that proposed by Smith and Coull (1991) for the symmetrical outrigger-braced structures.
2. Formulate the governing equations for the optimum locations of the unsymmetrical three-stories outrigger-braced structure. Computer program is developed for solving the nonlinear algebraic equations and parameter analysis.
3. Test the computer program by comparing the result obtained by the computer program with those obtained by Smith and Coull (1991).
4. Conduct parameter analysis.
5. Give conclusions and design guidelines through numerical analysis.

### **5.2 Conclusions**

The main conclusions of this project are:

1. The governing equations for analyzing the optimum locations of the outriggers of unsymmetrical three-stories outriggers braced structures have been formulated based on the compatibility of the columns' axial deformation.



2. The governing equations for analyzing the optimum locations of the outriggers of unsymmetrical three-stories outriggers braced structures have been formulated based on the compatibility of the columns' axial deformation.
3. The procedure of solving the nonlinear equations in using Matlab and plot figures has been developed.
4. The optimum locations of outrigger have been obtained under different conditions.
5. For various values of  $r$ ,  $\varepsilon_1 (x_1/H)$  increases as  $r$  increases when  $r$  is less or equal to 0.6. When  $r$  is greater than 0.6,  $\varepsilon_1$  decreases at some point even though  $r$  increases. The behavior of  $\varepsilon_2 (x_2/H)$  is similar.  $\varepsilon_3 (x_3/H)$ , decreases at some point as  $r$  increases.
6. As  $\beta$  increases,  $\varepsilon_1$ ,  $\varepsilon_2$  and  $\varepsilon_3$  decreases. However,  $\varepsilon$  decreases suddenly after  $\omega$  equals to 0.9 or 0.8 as  $\beta$  decreases. Meanwhile,  $\varepsilon$  decreases as  $\omega$  increases for given value of  $\beta$  normally.
7.  $\varepsilon_1$ ,  $\varepsilon_2$  and  $\varepsilon_3$  decreases as  $\alpha$  increases. In addition,  $\varepsilon$  decreases as  $\omega$  increases for given value of  $\alpha$ . Compared to  $r$  or  $\beta$ ,  $\alpha$  has less influence on the optimum outrigger locations of the structure.

### 5.3 Further Research

In this research, only the three-stories unsymmetrical outrigger-braced structure is analyzed, and also the limited parameter analyses were conducted. Therefore, the following researches related to the outrigger-braced structure can be considered in the future.

1. Analysis of the structure with more layers of outriggers;
2. Analysis of 3D outrigger-braced structures;
3. Analysis of the unsymmetrical structure under different type of distributed loads over the height of the structure.

## REFERENCES

1. Taranath, B.S. (1974). Optimum belt truss location for high-rise structures.  
*Engineering Journal, American Institute of Steel Construction, Vol. 11, pp. 18-21.*
2. Smith, B. S. and Nwaka, I. O. (1980). Behavior of Multi-outrigger Braced Tall Buildings. *America Concrete Institute Special Publication of Papers for Symposium on Reinforced Concrete Structure, sponsored by Committee 442.*
3. Smith, B. S. and Salim, I. (1981). Parameter study of outrigger-braced tall building structures. *Journal of the Structural Division, Vol. 107, Issue 10, Pg. 2001-2014.*
4. Boggs, P.C., Casparini, D.A. (1983). Lateral stiffness of core outrigger systems.  
*Engineering Journal, AISC 20: 172-180.*
5. Rutenburg, A., T.D. (1987). Lateral load response of belted tall building structures.  
*Engineering Structure. 9: 53-67.*
6. Coates, R.C. Coutie, M.G. and Kong, F. K. ( )Structural Analysis, Third Edition,  
Chapman and Hall.
7. Ding J.M. (1991). Optimum belt truss location for high-rise structures and top level drift coefficient. *Journal of Building Structures (4): 10–13.*
8. Smith, B.S. and Coull, A. (1991). Tall Building Structures. *New York : Wiley, ©1991.*
9. Ali, M.M. (2001). Art of the Skyscraper: the Genius of Fazlur Khan. *New York*
10. Wu, J.R. and Li, Q.S. (2003). Structural Performance of Multi-Outrigger-Braced Tall Buildings. *The Structural Design of Tall and Special Buildings, Volume 12, Issue 2, pages 155–176, June 2003.*
11. Ali, M.M. and Moon, K.S. (2007). Structural Developments in Tall Buildings:  
*Current Trends and Future Prospects. Architectural Science Review. Volume 50.3, pp 205-223.*

12. Hoenderkamp J.C.D. (2008). Second Outrigger at Optimum Location on High-Rise Shear Wall. *The Structural Design of Tall and Special Buildings Structure*. Design Tall Spec. Build. 17, 619–634 (2008).
13. Er, G.K. and Iu, V.P. (2009). General Procedure of Formulating the Governing Equations for Analyzing Outrigger-braced Structures. *Proceedings of 7th International Conference on Tall Buildings*, pp. 589-595, 28-30 October 2009, Hong Kong.



## APPENDIX A. DETALIS OF NUMERICAL RESULTS

Table 1 Details of Numerical Results for Different Values of  $r$

$r = 0.9999$

	0	0.1	0.2	0.3	0.4	0.5	0.6	0.7	0.8	0.9	1
$\varepsilon_1$	0.24302	0.21999	0.20269	0.18905	0.17787	0.16842	0.16027	0.15313	0.14679	0.14109	0.13594
$\varepsilon_2$	0.53361	0.48052	0.44684	0.42128	0.40044	0.38276	0.36738	0.35376	0.34153	0.33045	0.32033
$\varepsilon_3$	0.77844	0.69265	0.64217	0.60501	0.57525	0.55030	0.52876	0.50980	0.49285	0.47753	0.46356

$r = 0.8$

	0	0.1	0.2	0.3	0.4	0.5	0.6	0.7	0.8	0.9	1
$\varepsilon_1$	0.24303	0.22314	0.20734	0.19456	0.18391	0.17484	0.16697	0.16002	0.15375	0.14784	0.14169
$\varepsilon_2$	0.53363	0.48730	0.45613	0.43205	0.41222	0.39528	0.38046	0.36724	0.35516	0.34364	0.33163
$\varepsilon_3$	0.77846	0.70455	0.65838	0.62340	0.59481	0.57045	0.54912	0.53006	0.51261	0.49607	0.47916

$r = 0.7$

	0	0.1	0.2	0.3	0.4	0.5	0.6	0.7	0.8	0.9	1
$\varepsilon_1$	0.24303	0.22318	0.20717	0.19433	0.18380	0.17507	0.16780	0.16174	0.15658	0.15172	0.14539
$\varepsilon_2$	0.53363	0.48763	0.45625	0.43216	0.41266	0.39643	0.38276	0.37114	0.36102	0.35131	0.33882
$\varepsilon_3$	0.77847	0.70640	0.66126	0.62718	0.59949	0.57614	0.55603	0.53843	0.52266	0.50742	0.48911

$r = 0.6$

	0	0.1	0.2	0.3	0.4	0.5	0.6	0.7	0.8	0.9	1
$\varepsilon_1$	0.24303	0.22259	0.20584	0.19233	0.18134	0.17247	0.16555	0.16054	0.15737	0.15527	0.14986
$\varepsilon_2$	0.53363	0.48654	0.45394	0.42884	0.40871	0.39248	0.37965	0.37006	0.36349	0.35857	0.34748
$\varepsilon_3$	0.77846	0.70577	0.66046	0.62649	0.59925	0.57675	0.55807	0.54276	0.53041	0.51941	0.50109

$r = 0.5$

	0	0.1	0.2	0.3	0.4	0.5	0.6	0.7	0.8	0.9	1
$\varepsilon_1$	0.24303	0.22173	0.20403	0.18949	0.17742	0.16754	0.15993	0.15505	0.15378	0.15666	0.15541
$\varepsilon_2$	0.53363	0.48470	0.45039	0.42347	0.40153	0.38375	0.37011	0.36127	0.35851	0.36239	0.35812
$\varepsilon_3$	0.77846	0.70324	0.65652	0.62160	0.59381	0.57127	0.55331	0.54004	0.53216	0.52955	0.51587

$r = 0.4$

	0	0.1	0.2	0.3	0.4	0.5	0.6	0.7	0.8	0.9	1
$\varepsilon_1$	0.24302	0.22083	0.20235	0.18687	0.17361	0.16223	0.15276	0.14591	0.14383	0.15167	0.16248
$\varepsilon_2$	0.53362	0.48269	0.44683	0.41804	0.39376	0.37314	0.35633	0.34469	0.34182	0.35554	0.37157
$\varepsilon_3$	0.77845	0.69962	0.65056	0.61364	0.58406	0.56003	0.54112	0.52801	0.52311	0.53165	0.53461

Table 2 Details of Numerical Results for Different Values of  $\beta$  when r Equals to 0.5 $\beta=14$ 

	0	0.1	0.2	0.3	0.4	0.5	0.6	0.7	0.8	0.9	1
$\varepsilon_1$	0.24303	0.22184	0.20440	0.19015	0.17831	0.16848	0.16048	0.15437	0.15039	0.14892	0.15011
$\varepsilon_2$	0.53363	0.48492	0.45106	0.42462	0.40303	0.38523	0.37081	0.35977	0.35243	0.34929	0.35045
$\varepsilon_3$	0.77846	0.70353	0.65726	0.62279	0.59527	0.57267	0.55401	0.53892	0.52738	0.51962	0.51542

 $\beta=16$ 

	0	0.1	0.2	0.3	0.4	0.5	0.6	0.7	0.8	0.9	1
$\varepsilon_1$	0.24303	0.22192	0.20467	0.19063	0.17899	0.16924	0.16114	0.15459	0.14961	0.14632	0.14484
$\varepsilon_2$	0.53363	0.48509	0.45155	0.42547	0.40417	0.38648	0.37182	0.35995	0.35085	0.34463	0.34146
$\varepsilon_3$	0.77846	0.70374	0.65782	0.62368	0.59642	0.57390	0.55503	0.53925	0.52631	0.51612	0.50870

 $\beta=18$ 

	0	0.1	0.2	0.3	0.4	0.5	0.6	0.7	0.8	0.9	1
$\varepsilon_1$	0.24303	0.22199	0.20488	0.19101	0.17951	0.16986	0.16175	0.15502	0.14960	0.14549	0.14271
$\varepsilon_2$	0.53363	0.48522	0.45193	0.42612	0.40507	0.38751	0.37279	0.36057	0.35066	0.34303	0.33767
$\varepsilon_3$	0.77846	0.70390	0.65825	0.62438	0.59734	0.57493	0.55602	0.53996	0.52638	0.51509	0.50598

Table 3 Details of Numerical Results for Different Values of  $\beta$  when r Equals to 0.7 $\beta=14$ 

	0	0.1	0.2	0.3	0.4	0.5	0.6	0.7	0.8	0.9	1
$\varepsilon_1$	0.24303	0.22325	0.20738	0.19467	0.18421	0.17547	0.16807	0.16175	0.15631	0.15151	0.14701
$\varepsilon_2$	0.53363	0.48777	0.45663	0.43276	0.41339	0.39716	0.38330	0.37131	0.36080	0.35135	0.34234
$\varepsilon_3$	0.77847	0.70658	0.66175	0.62796	0.60052	0.57733	0.55725	0.53957	0.52376	0.50929	0.49542

 $\beta=16$ 

	0	0.1	0.2	0.3	0.4	0.5	0.6	0.7	0.8	0.9	1
$\varepsilon_1$	0.24303	0.22330	0.20754	0.19492	0.18454	0.17581	0.16837	0.16195	0.15636	0.15142	0.14696
$\varepsilon_2$	0.53363	0.48788	0.45691	0.43322	0.41397	0.39778	0.38388	0.37174	0.36102	0.35141	0.34258
$\varepsilon_3$	0.77847	0.70672	0.66211	0.62855	0.60133	0.57830	0.55832	0.54066	0.52484	0.51045	0.49710

 $\beta=18$ 

	0	0.1	0.2	0.3	0.4	0.5	0.6	0.7	0.8	0.9	1
$\varepsilon_1$	0.24303	0.22335	0.20766	0.19512	0.18480	0.17610	0.16865	0.16219	0.15652	0.15150	0.14697
$\varepsilon_2$	0.53363	0.48796	0.45714	0.43358	0.41443	0.39831	0.38441	0.37223	0.36141	0.35168	0.34280
$\varepsilon_3$	0.77847	0.70682	0.66239	0.62902	0.60196	0.57908	0.55921	0.54163	0.52585	0.51150	0.49828

Table 4 Details of Numerical Results for Different Values of  $\alpha$  when  $r$  Equals to 0.5 $\alpha=0.3$ 

	0	0.1	0.2	0.3	0.4	0.5	0.6	0.7	0.8	0.9	1
$\varepsilon_1$	0.24302	0.21398	0.19567	0.18333	0.17427	0.16722	0.16149	0.15666	0.15250	0.14883	0.14555
$\varepsilon_2$	0.53360	0.47086	0.43660	0.41395	0.39729	0.38420	0.37344	0.36427	0.35627	0.34914	0.34270
$\varepsilon_3$	0.77842	0.68968	0.64483	0.61425	0.59096	0.57211	0.55624	0.54250	0.53038	0.51950	0.50962

 $\alpha=0.5$ 

	0	0.1	0.2	0.3	0.4	0.5	0.6	0.7	0.8	0.9	1
$\varepsilon_1$	0.24302	0.21560	0.19704	0.18394	0.17407	0.16630	0.15996	0.15465	0.15012	0.14618	0.14271
$\varepsilon_2$	0.53361	0.47341	0.43846	0.41443	0.39640	0.38213	0.37039	0.36048	0.35191	0.34438	0.33767
$\varepsilon_3$	0.77842	0.69120	0.64538	0.61375	0.58956	0.56998	0.55355	0.53941	0.52700	0.51595	0.50598

 $\alpha=0.7$ 

	0	0.1	0.2	0.3	0.4	0.5	0.6	0.7	0.8	0.9	1
$\varepsilon_1$	0.24302	0.21671	0.19829	0.18497	0.17477	0.16665	0.15997	0.15437	0.14958	0.14542	0.14176
$\varepsilon_2$	0.53361	0.47530	0.44044	0.41595	0.39731	0.38243	0.37015	0.35974	0.35076	0.34289	0.33589
$\varepsilon_3$	0.77843	0.69278	0.64675	0.61471	0.59009	0.57012	0.55335	0.53892	0.52627	0.51502	0.50490

 $\alpha=0.9$ 

	0	0.1	0.2	0.3	0.4	0.5	0.6	0.7	0.8	0.9	1
$\varepsilon_1$	0.24302	0.21750	0.19929	0.18591	0.17556	0.16724	0.16037	0.15459	0.14962	0.14531	0.14151
$\varepsilon_2$	0.53361	0.47672	0.44208	0.41743	0.39850	0.38328	0.37066	0.35994	0.35068	0.34256	0.33534
$\varepsilon_3$	0.77843	0.69411	0.64812	0.61589	0.59104	0.57084	0.55386	0.53924	0.52642	0.51503	0.50478

Table 5 Details of Numerical Results for Different Values of  $\alpha$  when  $r$  Equals to 0.7 $\alpha=0.3$ 

	0	0.1	0.2	0.3	0.4	0.5	0.6	0.7	0.8	0.9	1
$\varepsilon_1$	0.24302	0.21935	0.20379	0.19221	0.18285	0.17493	0.16804	0.16195	0.15647	0.15151	0.14697
$\varepsilon_2$	0.53361	0.48072	0.45035	0.42841	0.41081	0.39592	0.38293	0.37136	0.36091	0.35135	0.34255
$\varepsilon_3$	0.77844	0.69838	0.65363	0.62113	0.59519	0.57342	0.55457	0.53790	0.52292	0.50931	0.49683

 $\alpha=0.5$ 

	0	0.1	0.2	0.3	0.4	0.5	0.6	0.7	0.8	0.9	1
$\varepsilon_1$	0.24302	0.21990	0.20398	0.19212	0.18260	0.17463	0.16776	0.16171	0.15630	0.15142	0.14697
$\varepsilon_2$	0.53362	0.48158	0.45065	0.42828	0.41047	0.39554	0.38260	0.37113	0.36082	0.35143	0.34280
$\varepsilon_3$	0.77844	0.69920	0.65424	0.62163	0.59569	0.57399	0.55527	0.53877	0.52398	0.51056	0.49828

 $\alpha=0.7$ 

	0	0.1	0.2	0.3	0.4	0.5	0.6	0.7	0.8	0.9	1
$\varepsilon_1$	0.24302	0.22039	0.20439	0.19239	0.18277	0.17473	0.16783	0.16177	0.15638	0.15152	0.14710
$\varepsilon_2$	0.53362	0.48242	0.45133	0.42875	0.41080	0.39579	0.38282	0.37136	0.36108	0.35174	0.34318
$\varepsilon_3$	0.77845	0.70007	0.65514	0.62249	0.59654	0.57486	0.55618	0.53973	0.52501	0.51168	0.49949

 $\alpha=0.9$ 

	0	0.1	0.2	0.3	0.4	0.5	0.6	0.7	0.8	0.9	1
$\varepsilon_1$	0.24302	0.22077	0.20479	0.19272	0.18303	0.17495	0.16802	0.16195	0.15655	0.15169	0.14727
$\varepsilon_2$	0.53362	0.48310	0.45201	0.42933	0.41128	0.39621	0.38320	0.37174	0.36146	0.35214	0.34361
$\varepsilon_3$	0.77845	0.70083	0.65599	0.62335	0.59740	0.57573	0.55707	0.54064	0.52596	0.51267	0.50052

## APPENDIX B. COMPUTER PROGRAM

```
%set the initial value of parameters
syms q h d1 d2 e1 e2 e3 r alp beta omi
q=1
d1=1
h=1
omi=0:10:1
alp=0.3
beta=omi*12*(1+alp)
r=0.9999

%matric {P}
p1=q*h^2*(e2^3-e1^3)/(6*d1)
p2=q*h^2*r*(e2^3-e1^3)/(6*d1)
p3=q*h^2*(e3^3-e2^3)/(6*d1)
p4=q*h^2*r*(e3^3-e2^3)/(6*d1)
p5=q*h^2*(1-e3^3)/(6*d1)
p6=q*h^2*r*(1-e3^3)/(6*d1)
P=[p1;p2;p3;p4;p5;p6]

%matric {delta}
d11=(e2-e1)+beta/3+2*alp*(e2-e1)
d12=r*(e2-e1)
d13=-beta/6
d14=0
d15=0
d16=0

d21=d12
d22=r^2*(e2-e1)+r^3*beta/3+2*alp*(e2-e1)
d23=0
d24=-beta*r^3/6
d25=0
d26=0

d31=d13
d32=d23
d33=(e3-e2)+beta/3+2*alp*(e3-e2)
d34=r*(e3-e2)
d35=-beta/6
d36=0

d41=d14
d42=d24
d43=d34
d44=r^2*(e3-e2)+r^3*beta/3+2*alp*(e3-e2)
d45=0
d46=-beta*r^3/6
```



```

d51=d15
d52=d25
d53=d35
d54=d45
d55=(1-e3)+beta/6+2*alp*(1-e3)
d56=r*(1-e3)

d61=d16
d62=d26
d63=d36
d64=d46
d65=d56
d66=r^2*(1-e3)+r^3*beta/6+2*alp*(1-e3)
D=[d11 d12 d13 d14 d15 d16;d21 d22 d23 d24 d25 d26;d31 d32 d33 d34 d35 d36;d41
d42 d43 d44 d45 d46;d51 d52 d53 d54 d55 d56;d61 d62 d63 d64 d65 d66]

```

```

%matric {N}
N=D\p

```

```

%Take derivatives with respect to e1 on equation {delta}*{N}={P}

```

```

dp11=-q*h^2*e1^2/(2*d1)-(-1-2*alp)*N(1)-(-r)*N(2)
dp12=-r*q*h^2*e1^2/(2*d1)-(-r)*N(1)-(-r^2-2*alp)*N(2)
dp13=0
dp14=0
dp15=0
dp16=0

```

```

%Take derivatives with respect to e2 on equation {delta}*{N}={P}

```

```

dp21=q*h^2*e2^2/(2*d1)-(1+2*alp)*N(1)-(-r)*N(2)
dp22=r*q*h^2*e2^2/(2*d1)-(-r)*N(1)-(-r^2+2*alp)*N(2)
dp23=-q*h^2*e2^2/(2*d1)-(-1-2*alp)*N(3)-(-r)*N(4)
dp24=-r*q*h^2*e2^2/(2*d1)-(-r)*N(3)-(-r^2-2*alp)*N(4)
dp25=0
dp26=0

```

```

%Take derivatives with respect to e3 on equation {delta}*{N}={P}

```

```

dp31=0
dp32=0
dp33=q*h^2*e3^2/(2*d1)-(1+2*alp)*N(3)-(-r)*N(4)
dp34=r*q*h^2*e3^2/(2*d1)-(-r)*N(3)-(-r^2+2*alp)*N(4)
dp35=-q*h^2*e3^2/(2*d1)-(-1-2*alp)*N(5)-(-r)*N(6)
dp36=-r*q*h^2*e3^2/(2*d1)-(-r)*N(5)-(-r^2-2*alp)*N(6)

```

```

%matric of derivatives with respect to e1, e2 and e3 on equation {delta}*{N}={P}

```

```

Dp1=[dp11;dp12;dp13;dp14;dp15;dp16]
Dp2=[dp21;dp22;dp23;dp24;dp25;dp26]
Dp3=[dp31;dp32;dp33;dp34;dp35;dp36]

```

```

% derivatives of N with respect to e1, e2 and e3

```

```

Nd1=D\Dp1

```

Nd2=D\Dp2

Nd3=D\Dp3

%final equations to get the optimum locations

```
E1=(N(1)*(-2*e1)+Nd1(1)*(e2^2-e1^2)+Nd1(3)*(e3^2-e2^2)+Nd1(5)*(1-  
e3^2))+r*(N(2)*(-2*e1)+Nd1(2)*(e2^2-e1^2)+Nd1(4)*(e3^2-e2^2)+Nd1(6)*(1-e3^2))  
E2=(N(1)*(2*e2)+Nd2(1)*(e2^2-e1^2)+ N(3)*(-2*e2)+Nd2(3)*(e3^2-e2^2)+Nd2(5)*(1-  
e3^2))+r*(N(2)*(2*e2)+Nd2(2)*(e2^2-e1^2)+N(4)*(-2*e2)+Nd2(4)*(e3^2-  
e2^2)+Nd2(6)*(1-e3^2))  
E3=(N(3)*(2*e3)+Nd3(1)*(e2^2-e1^2)+ N(5)*(-2*e3)+Nd3(3)*(e3^2-e2^2)+Nd3(5)*(1-  
e3^2))+r*(N(4)*(2*e3)+Nd3(2)*(e2^2-e1^2)+N(6)*(-2*e3)+Nd3(4)*(e3^2-  
e2^2)+Nd3(6)*(1-e3^2))
```

%solving E1, E2 and E3 in Newtons method

```
fun=inline(' [E1;E2;E3]','e1','e2','e3')  
[e1,fval,iter,exieflag]=Newtons(fun,[0.5;0.5;0.5])
```

